

# **Texas 2000 Air Quality Study – Phase II**

## **Analysis of NOAA Data**



## **Final Report**

**NOAA Aeronomy Laboratory  
March 2003**



## Table of Contents

<b>Introduction</b>	2
Analysis of NOAA data	3
<b>Task C-1: Data Analysis and Evaluation</b>	4
Background	4
Initial VOC reactivity in the Houston area	6
Ozone formation rate and yield	7
Findings	11
Particle production	12
<b>Task D-1: Improvement of Inventories</b>	14
(Alkene/NO <sub>x</sub> ) emission ratios	14
Sensitivity of model estimates to emission inputs	17
Finding	20
<b>References</b>	21
<b>Appendix (attached preprints)</b>	
Signatures of Terminal Alkene Oxidation in Airborne Formaldehyde Measurements During TexAQS 2000, Wert et al	
Particle growth in urban and industrial plumes in Texas, Brock et al.	
Effect of petrochemical industrial emissions of reactive alkenes and NO <sub>x</sub> on tropospheric ozone formation in Houston, TX, Ryerson et al.	

## Introduction

The metropolitan area of Houston, Texas is home to more than 3 million people and the largest grouping of petrochemical industrial plants in the United States. During the summer, sources of nitrogen oxides ( $\text{NO}_x$ ) and volatile organic compounds (VOCs), in combination with intense solar radiation and stagnant meteorological conditions, lead to the highest ozone mixing ratios routinely encountered in the continental U.S. in the present day. The Houston metropolitan area is also at risk of exceeding the proposed standards for the concentration of the dry mass of aerosol particles with diameters  $<2.5 \mu\text{m}$  ( $\text{PM}_{2.5}$ ). As a result, photochemical ozone and aerosol production in the Houston area was the focus of the Texas Air Quality Study 2000 field project [Brock *et al.*, 2002; Kleinman *et al.*, 2002; Neuman *et al.*, 2002; Wert *et al.*, 2002].

Like most U. S. cities, emissions from on- and off-road vehicles, power plants, and forests contribute to ozone formation in Houston. What makes Houston unique is the extensive petrochemical industry that contributes both reactive VOCs and  $\text{NO}_x$  to the pollutant mix and ultimately to ozone formation in the region. The sources of  $\text{PM}_{2.5}$  in the Houston area are believed to include the gas-phase photooxidation of  $\text{SO}_2$  and reactive organic compounds, followed by condensation of the lower-vapor-pressure oxidation products. Other sources of  $\text{PM}_{2.5}$  in the Houston area include combustion, roadways, and sea-spray. A quantitative understanding of the relationship between emissions of particles and precursor gases such as  $\text{SO}_2$  and downwind aerosol properties is needed for mitigation efforts.



**Figure 1.** Downtown Houston from the Williams Tower

The primary goal of the Texas 2000 Air Quality Study (TexAQS 2000) was to improve understanding of the chemical and meteorological causes of ozone exceedance episodes in the Houston-Galveston and Dallas metropolitan areas. A further goal of the study was to investigate the sources and characteristics of aerosol particles in the study region in anticipation of expected regulation of  $\text{PM}_{2.5}$  sources. Airborne and surface observations, as well as modeling and forecasting tools, were used to achieve these program goals.

From 16 August to 13 September 2000, measurements of particulate and gas-phase pollutants and tracer species were made on the Lockheed Electra aircraft, operated by the National Center for Atmospheric Research (NCAR), in a variety of power plant, petrochemical, and urban plumes in eastern Texas and Oklahoma (Figure 2). These flights, and those of other research aircraft, were supported by a network of Houston-area ground-based sites measuring photochemically active compounds and meteorological

conditions, a network of microwave wind profilers, and two sites with a large variety of instruments for measuring gas-phase concentrations and the microphysical, optical, and chemical properties of aerosol particles. Meteorological and chemical modeling and emissions inventory efforts were also integral components of the TexAQS 2000 program.

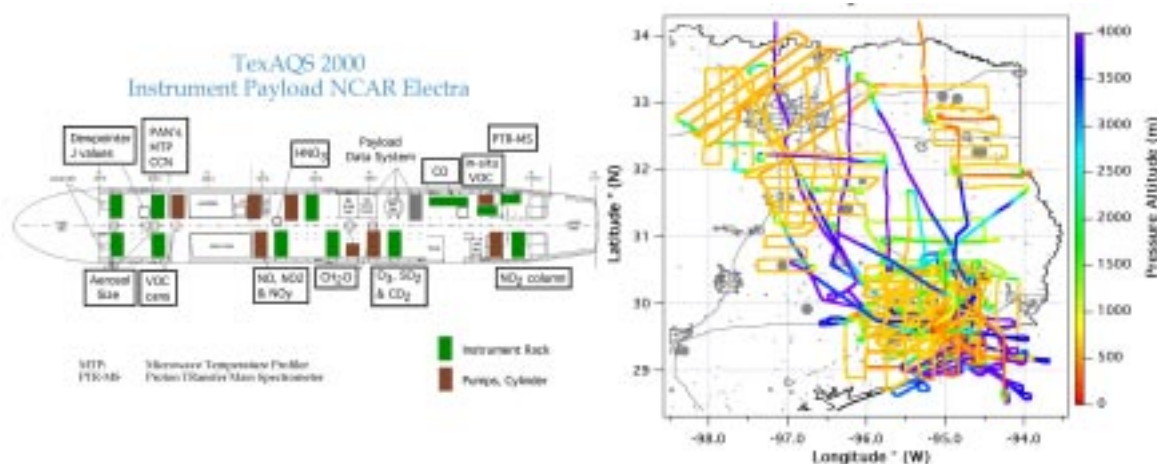


**Figure 2.** The instrument payload (left) and flight tracks (right) for the NCAR Electra aircraft during TexAQS 2000.

### Analysis of NOAA data

The Texas Commission on Environmental Quality (TCEQ) provided support to NOAA's Aeronomy Laboratory for the analysis of data collected during the TexAQS 2000 field study. Two data analysis tasks were performed:

1. *Task C-1: Data analysis and evaluation* – The aim of this task was to analyze data taken during the TexAQS 2000 field study to determine the efficiency of production of ozone and fine particles from urban and industrial plumes in the Houston area.
2. *Task D-1: Improvement of inventories* – The aim of this task was to collaborate with TCEQ to develop improved emission inventories for the Houston area.

The analyses conducted under these tasks produced significant new insights into the emission sources and atmospheric processes that control the formation and distribution of ozone and fine particles in the Houston area. In this report we describe the work conducted under these tasks and highlight the major scientific findings that resulted.

## Task C-1: Data Analysis and Evaluation

### Background

Ozone ( $O_3$ ) is formed in the troposphere by photochemical reactions involving the oxides of nitrogen  $NO$  and  $NO_2$  (summed as  $NO_x$ ) and reactive volatile organic compounds (VOCs). Model studies have shown that ozone formation rates and yields are dependent upon both the absolute concentrations of  $NO_x$  and VOCs and upon the ratios of these species (e.g., [Liu *et al.*, 1987; Sillman, 2000]). Results from ambient measurements have confirmed that substantial differences in the rate and magnitude of ozone production consistently occur in plumes downwind of different anthropogenic source types, characterized by different  $NO_x$  and VOC emissions rates and the VOC/ $NO_x$  ratios that result (e.g., [Neuman *et al.*, 2002; Ryerson *et al.*, 1998; Ryerson *et al.*, 2001]).

Three anthropogenic source types with contrasting emissions rates and VOC/ $NO_x$  ratios are fossil-fueled electric power plants, the transportation sources typical of urban areas, and the petrochemical industry. The first two combined account for approximately 75% of total U.S. anthropogenic  $NO_x$  emissions annually [EPA, 2001]. Fossil-fueled electric power plants are very concentrated point sources of  $NO_x$  but do not emit appreciable amounts of VOCs. Thus, ozone production observed in plumes downwind of isolated, rural power plants in the U.S. occurs as a result of mixing plume  $NO_x$  with primarily biogenic reactive VOCs, especially with isoprene [Trainer *et al.*, 1987a; Trainer *et al.*, 1987b], over time during plume transport. Measurements confirm the strong dependence of ozone production on  $NO_x$  concentration [Ryerson *et al.*, 1998] and on ambient VOC concentration and reactivity [Ryerson *et al.*, 2001].

Power plant plume VOC/ $NO_x$  ratios can be sufficiently low that ozone formation is initially suppressed in favor of efficient nitric acid ( $HNO_3$ ) production, removing  $NO_x$  from further participation in ozone formation cycles [Neuman *et al.*, 2002; Ryerson *et al.*, 2001]. In contrast, the tailpipe emissions that dominate urban areas are sources of both  $NO_x$  and VOCs. The many small individual sources contributing to urban emissions are usually considered together as an area source dispersed over tens to hundreds of square kilometers. As a result, urban plumes are relatively dilute, with total  $NO_x$  emissions rates comparable to those from power plants but dispersed over a much larger area. Co-emission in this manner results in initial VOC/ $NO_x$  ratios that favor ozone formation immediately upon emission, typically leading to faster ozone production rates and higher yields in urban plumes than in concentrated power plant plumes.

The fastest rates of ozone formation, and the highest yields per  $NO_x$  molecule emitted, are predicted for conditions where strongly elevated concentrations of  $NO_x$  and reactive VOCs are simultaneously present. These conditions can be routinely found in the  $NO_x$ - and VOC-rich plumes from petrochemical industrial. Petrochemical  $NO_x$  emissions are a byproduct of fossil-fuel combustion for electric power generation, for heat generation, and from flaring of unwanted volatile materials;  $NO_x$  emission from a large

petrochemical facility can approach that from a large electric utility power plant. While a given facility may have hundreds of combustion sources, spread over many square kilometers, the majority of petrochemical  $\text{NO}_x$  emissions typically come from only a few of the largest sources. Thus, concentrations of  $\text{NO}_x$  in plumes from large petrochemical facilities are typically much higher than in those from urban areas. Sources of VOC emissions from a petrochemical industrial facility are thought to be much more numerous than sources of  $\text{NO}_x$ . VOCs can be emitted via continuous emissions from stacks, episodic emissions specific to individual processes, and leaks from pipes and valving. The wide variety of VOC compounds typically emitted from petrochemical facilities, with differing reactivities toward the hydroxyl radical (OH), must be considered to understand the ozone-forming potential of these sources.

Measurements taken from an instrumented aircraft during that project to were used to evaluate the effects of petrochemical industrial emissions on tropospheric ozone formation. In the study, ozone production in spatially-resolved plumes from the geographically isolated complexes at Sweeny, Freeport, and Chocolate Bayou (Figure 3) were analyzed. This analysis was extended to include data from coalesced plumes downwind of multiple petrochemical complexes in the heavily industrialized Houston Ship Channel and Texas City areas. Finally, ozone production in petrochemical industrial plumes was compared to that observed downwind of urban areas and rural, fossil-fueled electric utility power plants.

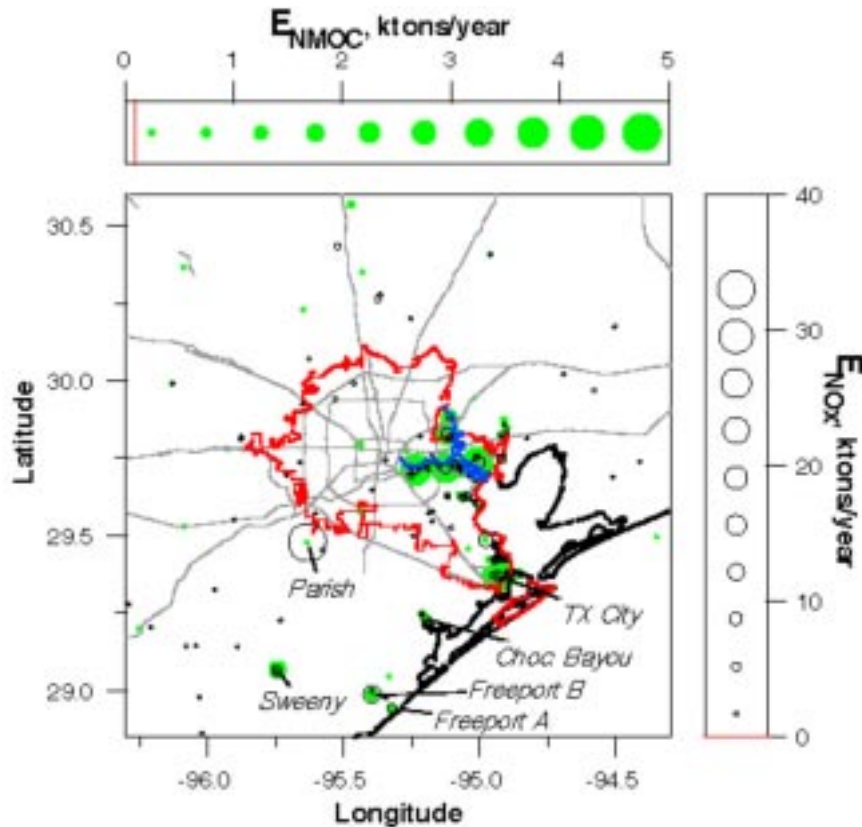


**Figure 3.** The greater Houston metropolitan area (red line). Locations of point emission sources are shown sized according to VOC emission source strengths (“ $E_{\text{VOC}}$ ”, filled green circles) and  $\text{NO}_x$  emission source strengths (“ $E_{\text{NO}_x}$ ”, open black circles) according to the legends provided.

### Initial VOC reactivity In the Houston area

Aircraft measurements on August 27 and 28 show that the primary OH reactivity in the coalesced petrochemical plume beginning north of Texas City and extending downwind over and past the Ship Channel was due to reaction with petrochemical emissions of reactive alkenes and their photoproducts  $\text{CH}_2\text{O}$  and  $\text{CH}_3\text{CHO}$ . Because of the limited number of VOC samples on any single flight, this conclusion is best illustrated using the full data set from all 14 Electra research flights in the Houston area (Figure 2). Derived total OH loss rates to measured VOC compounds from *in-situ* and canister measurements within the boundary layer during the 2000 Houston study are plotted (circles) as a function of sampling location in Figure 4. The symbols in this figure are sized by the magnitude of OH reactivity with measured VOCs and colored by the fractional contribution of alkenes to the total reactivity.

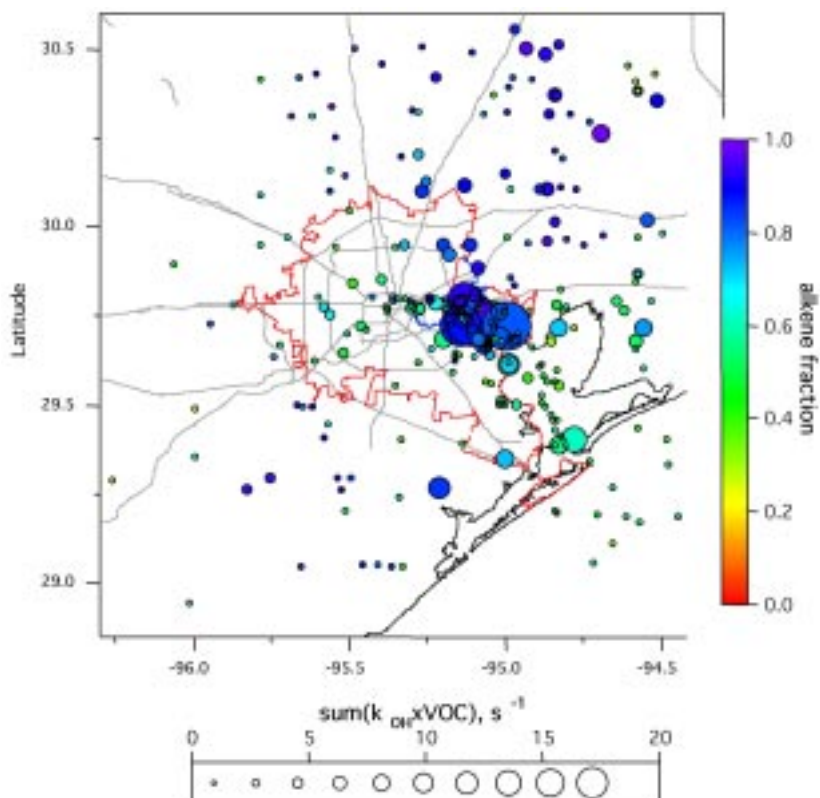


**Figure 4.** 200 x 200 km map of the study area showing locations of *in-situ* and whole-air canister hydrocarbon measurements (circles) taken below 1.5 km aircraft altitude, sized by  $\Sigma (k_{\text{OH}}[\text{VOC}])$  and colored by  $(\Sigma(k_{\text{OH}}[\text{alkene}]))/(\Sigma(k_{\text{OH}}[\text{VOC}])),$  the fractional contribution of alkenes to the total.

The data shown in Figure 4 demonstrate that OH reactivity from the measured VOC compounds was substantially enhanced above the petrochemical source regions relative to the urban area or the surrounding rural areas. Emissions plumes were encountered in different directions downwind depending on the prevailing wind direction on a particular

day; for example, in Figure 4 the Texas City plume enhancements can be found both east over Galveston Bay, or west and inland. Independent of wind direction, the maximum reactivity on every flight was clearly localized over the Ship Channel. The samples in the Sweeny, Freeport, and Chocolate Bayou plumes on August 27 and 28, discussed above, are included in Plate 6 but show relatively low reactivity compared to the Ship Channel region. Alkenes strongly dominated the total reactivity. Above the Ship Channel the contribution from alkenes was typically >80% (Figure 4). The contribution from elevated mixing ratios of propene and ethene dominated, with the two compounds constituting >70% of the measured total directly over the source areas. Generally, propene contributed a factor of approximately 2 more than did ethene, and all other alkenes contributed substantially less, to derived OH reactivity in the Ship Channel source region.

The remainder of alkene reactivity was primarily due to isoprene, likely from a combination of anthropogenic and biogenic sources, and 1,3-butadiene; however, on average these dienes contributed less than 10% of the Ship Channel total. Samples taken immediately downwind of the Texas City petrochemical complexes suggest proportionally greater contributions from the branched alkanes 2-methylpropane and 2-methylbutane, but these did not exceed 10% of the total calculated OH reactivity close to the source region. Given the varied nature of the petrochemical industrial facilities in the Houston area, other compounds were occasionally substantially enhanced, presumably when a VOC sample was taken very close to an individual source of that particular compound. With few exceptions, however, propene and ethene dominated the reactivity toward OH of the emissions mix from the petrochemical industry in this area.

In contrast to the Ship Channel area, measurements taken in the Houston urban core exhibited substantially lower OH reactivity, with values typically  $<2.0 \text{ s}^{-1}$  and similar to that of other major urban areas studied to date. While a major fraction of reactivity in the urban core is due to alkenes emitted from transportation sources, the resulting mixing ratios were sufficiently low that the total OH reactivity was small compared to air masses sampled directly over petrochemical source regions in the Ship Channel.

### **Ozone formation rate and yield**

Ozone production takes place rapidly in the coalesced plume downwind of the Ship Channel industrial facilities, consistent with the findings from the isolated petrochemical plumes discussed above. This is illustrated by a time series of ozone data taken along the E-W transect at  $30.1^\circ$  latitude within the boundary layer (Figure 5). Plume locations from sources in the Ship Channel (blue line, in inset map in Figure 6), the Houston urban area (red line), and the W.A. Parish power plant (black circle) are shown as heavy overlays along the flight track (dotted line). The upper time series in Figure 5 shows the directly emitted compounds  $\text{NO}_y$ ,  $\text{CO}_2$ , and  $\text{CO}$ ; these tracers and  $\text{SO}_2$  (not shown) were used to differentiate between the various plumes, whose edges are approximately defined by the vertical dashed lines. The lower time series shows the photoproducts ozone and  $\text{CH}_2\text{O}$  measured along this transect, which was flown approximately 43 km north, or 2.7

hours transport time, downwind of the Ship Channel and the I-10 corridor just north of downtown Houston.

Differences are apparent between the three plumes in the amount of ozone produced by this time downwind. Petrochemical plume mixing ratios of ozone approaching 140 ppbv were coincident with  $\text{CH}_2\text{O}$  of 14 ppbv, which were the highest values for either species encountered during this flight; much smaller enhancements are found in the urban and power plant plumes. Differences in  $\text{NO}_y$  mixing ratios between the three plumes were much less pronounced (Figure 5, top panel), suggesting that the rapidity of ozone formation was primarily due to the enhanced VOC reactivity characteristic of Houston-area petrochemical emissions. Rapid ozone production leading to the accumulation of very high, spatially localized surface ozone mixing ratios has been a unique feature of the Houston area; these findings point toward petrochemical industrial emissions as the primary cause of the observed high ozone events.

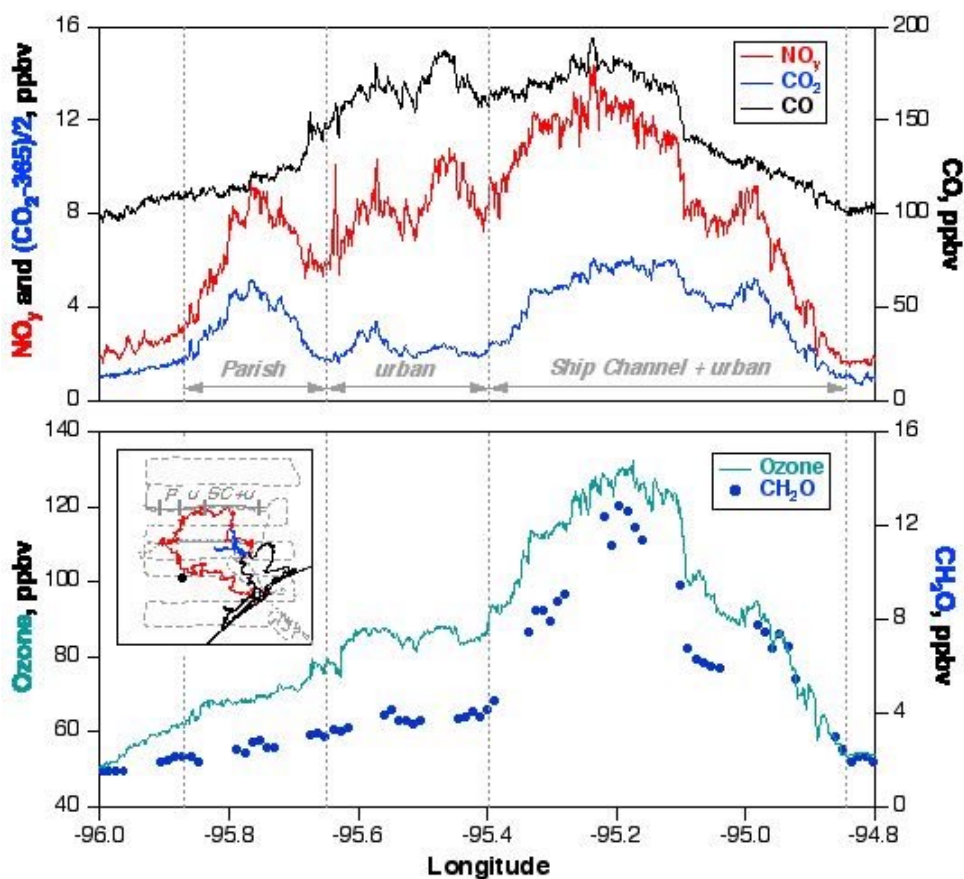


**Figure 5.** The inset map shows the E-W transect at  $30.1^\circ$  latitude on August 28, 2000 (solid gray line) along the aircraft flight track (dotted gray line). Locations of plumes from the W.A. Parish power plant “P”, the Houston urban core “u”, and the combined Ship Channel and urban plume “SC+u” along this transect are indicated by the vertical lines in the inset map and in the time series.

Ozone formation yield is inferred from data taken in the most fully oxidized transects downwind. The geographical extent of the photochemically processed Ship

Channel/Texas City plume on August 28 is defined by substantial enhancements in CO<sub>2</sub> and SO<sub>2</sub>, with relatively smaller enhancements in CO, observed on the northernmost transect downwind (Figure 6). At this transect, ~5.6 hours downwind of the Ship Channel, the coalesced petrochemical plume (NO<sub>x</sub>/NO<sub>y</sub>) ratio was  $0.19 \pm 0.02$ , indicating extensive photooxidation of primary NO emissions had occurred during transport. Coalesced petrochemical plume ozone data from this transect are plotted in Figure 6 versus measured (NO<sub>y</sub> - NO<sub>x</sub>). These data are highly correlated ( $r^2 = 0.978$ ) with a linear-least-squares fitted slope suggesting that, neglecting depositional loss of HNO<sub>3</sub> during transport, roughly 12 molecules of ozone had been generated per NO<sub>x</sub> molecule oxidized [Trainer *et al.*, 1993] at this distance downwind on August 28. For comparison, a slope of 11 is derived from ozone plotted vs. (NO<sub>y</sub> - NO<sub>x</sub>) using the August 27 flight data from the northernmost transect, showing consistency from day to day. These high apparent yields are consistent with the range of ozone yields derived using data from the isolated and resolved plumes from the petrochemical complexes at Sweeny, Freeport, and Chocolate Bayou, described above. Again, these derived yields are substantially larger than recent measurements suggest for both urban and power plant plumes, reflecting the extremely reactive mix of VOC and the elevated (VOC/NO<sub>x</sub>) ratios in plumes from petrochemical industrial complexes in the Houston area. Similarity in derived ozone yields between the two days, with no substantial emission upsets reported to TNRCC, indicates these values are representative for emissions during normal operation of the multiple Ship Channel and Texas City petrochemical complexes under the meteorological conditions of those two days.

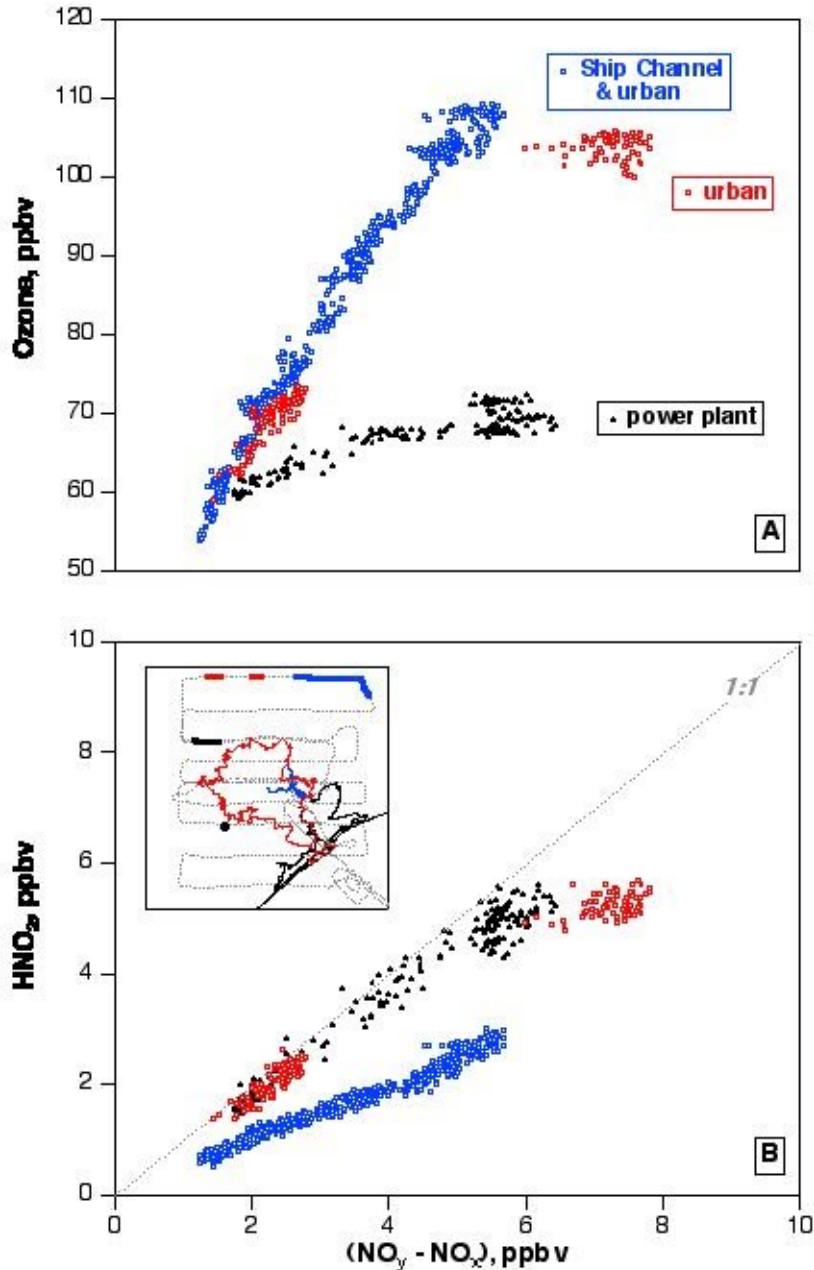


**Figure 6.** Transect data for the W.A. Parish (black,  $\text{NO}_x/\text{NO}_y = 0.24$ ), Houston urban (red,  $\text{NO}_x/\text{NO}_y = 0.19$ ), and Ship Channel/Texas City petrochemical plumes (blue,  $\text{NO}_x/\text{NO}_y = 0.19$ ) for the August 28th flight. Location of these plume transects are given by the colored overlays along the flight track shown in the inset map. Markedly different enhancements in ozone as a function of  $\text{NO}_x$  oxidized are apparent (A), consistent with initial VOC/ $\text{NO}_x$  ratios observed immediately downwind of the sources and with large differences in the fraction of  $\text{HNO}_3$  generated (B) at these distances downwind.

## Findings

The principal reactions leading to the rapid ozone formation characteristic of the Houston area are shown to involve oxidation of petrochemical emissions of propene and ethene. This is encouraging for successfully simulating Houston-area petrochemical plume ozone production in 3-D atmospheric models that rely on simplified, or lumped, VOC reaction schemes [Dodge, 2000]. The chemical solvers in most 3-D models treat oxidation of the light alkenes explicitly and should be entirely appropriate for modeling prompt ozone formation in the Houston area. The principal shortcoming in successful model simulations of prompt ozone formation appears to be the substantial underestimate of petrochemical alkene emissions in inventory tabulations. It will be difficult for chemically explicit 3-D models of appropriate spatial resolution to reproduce ozone observations in the Houston area until routine petrochemical VOC emissions rates are more realistically included in inventories.

Apparent ozone formation rates and yields derived on these two days for the isolated complexes and the coalesced Ship Channel plumes are qualitatively similar and are ascribed to similarly elevated (alkene/NO<sub>x</sub>) emissions ratios from the aggregated petrochemical facilities at each complex. These rates and yields are substantially higher than those derived on the same day under similar meteorological conditions for the Houston urban plume and that from the W.A. Parish power plant. Further, the urban and power plant yields are qualitatively similar to those reported for other urban areas and rural power plants. Finally, the hourly-, daily-, and annually-averaged emissions suggest that these observations are the result of typical operation of the power plants and petrochemical industrial facilities in the area. Such consistency suggests that the Texas 2000 mission data are representative of the normal effects of various anthropogenic emissions sources on tropospheric ozone in the Houston area. We emphasize that while derived values reported here are subject to substantial day-to-day variability according to meteorological conditions, the differences in ozone formation rates and yields between the three anthropogenic source types are expected to remain.

The chemistry required to capture the important features of prompt ozone production in Houston is thus dependent on a limited set of all possible VOCs known to be emitted from petrochemical sources [Derwent, 2000; Watson *et al.*, 2001]. These findings ultimately suggest that correctly estimating emissions of reactive light alkenes should be emphasized in constructing accurate VOC emissions inventories for Houston-area petrochemical industrial sources. Finally, these reactive light alkenes should represent the primary focus of current and future VOC emissions control measures designed to reduce tropospheric ozone formation from these individual facilities. Reduction in emissions of ethene and propene alone would account for over 75% of initial VOC reactivity and by inference the majority of the prompt ozone formed in the petrochemical plumes studied here. Reductions in emissions of alkanes, other alkenes, and aromatic compounds would be substantially less effective in mitigating rapid ozone formation in high yield downwind of these sources.

## Particle Production

The data collected on these same flights can be used to compare and contrast the formation and growth of fine particles downwind of the different source regions in the Houston area. The relative contribution of each of the major sources of particle volume in the Houston area is difficult to determine from observed concentrations alone because of the different horizontal dimensions of the plumes. To account for varying plume dimension, we have integrated the observed enhancement above background in particle volume across the width of the plume. This integration relies upon subjective interpretation of the eastern and western boundaries of each plume, determined largely from the  $\text{SO}_2$ ,  $\text{NO}_y$ , and  $\text{O}_3$  mixing ratios. For the total of 8 transects north of the Houston city limits on 27 and 28 August and (Figure 7), and the integrated particle volume in the ship channel plume exceeded that from the plume of the Parish power plant by a factor of  $4.0 \pm 1.5$ , with no systematic variation with downstream distance. Assuming that the pollution plume is vertically well mixed, and using an approximate PBL height (1.4 km

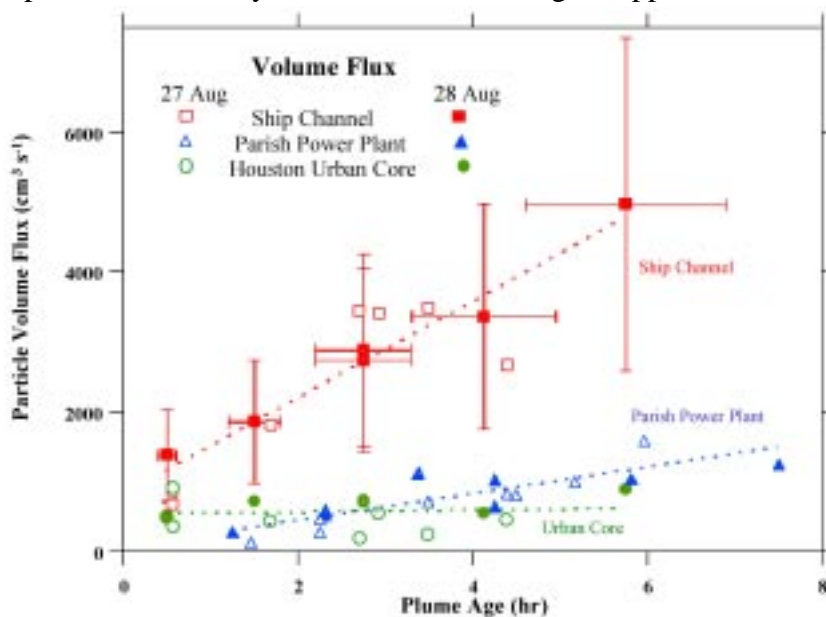


**Figure 7.** Particle volume downwind of major source types in the Houston area.

on 28 August), determined during aircraft soundings at the termini of some of the transects, particle mass fluxes have been estimated.

Integrated particle enhancement within the Houston urban plume between the Parish and ship channel plumes are extremely difficult to estimate because 1) there is only a small enhancement in particle volume above concentrations measured west of the Parish plume and east of the ship channel plume, and 2) the Parish and ship channel plumes extend into the urban plume on either side. By assuming that the region of minimum particle volume between the two industrial plumes represents relatively unadulterated urban air and then estimating a width for the urban plume based on CO concentrations, we can make a crude estimate of the particle enhancement due to the urban core of Houston. The

estimated contribution from the urban core is <10% of that from the combined Parish and ship channel sources at distances >40 km from the downtown area.

There are three major findings to this work: 1) The urban core of Houston is a relatively minor source of particle number and volume (mass) concentrations compared with the large industrial sources located along the ship channel and with the Parish coal-fired power plant just southwest of the city; and 2) substantial increases in particle volume concentration with increasing plume age, indicating condensation of gas-phase compounds, have been found only in plumes with detectable enhancements in SO<sub>2</sub>; 3) particle growth in the plume of the Parish power plant is generally consistent with the condensation of the oxidation products of SO<sub>2</sub> alone when the plume does not pass over substantial sources of VOCs, while particle growth within the VOC-rich ship channel plume exceeds that expected from solely from SO<sub>2</sub> oxidation.

## Task D-1: Improvement of Inventories

### (Alkene/NO<sub>x</sub>) emission ratios

Ratios of co-emitted species from a single large source are, to first order, independent of dilution over time during transport downwind and, when chemical transformation and deposition are negligible, are given by the slope of a linear fit to measured data. Ratios measured downwind in plumes will differ from the emissions ratio if chemical reaction or physical removal rates differ for the two species in question. We use plume transect data to estimate the emissions ratios of (ethene/NO<sub>x</sub>) and (propene/NO<sub>x</sub>) for the Sweeny, Freeport, and Chocolate Bayou facilities, account for differential chemical loss with respect to OH, and compare to emissions ratios calculated from the 2000 TNRCC point source database (PSDB) inventory. We note that some differences exist between the 1999 inventory used by Wert et al. [2002], and the 2000 inventory used in the present work, which has only recently become available, for the Texas 2000 study period. These inventory tabulations are not static over time, reflecting changes in operating conditions, plant activity, and addition of new facilities or shutting down older units. Changes from the 1999 to the 2000 inventory are also due to a substantially smaller fraction of VOC emissions reported as “unspecified” in 2000. The PSDB inventory is the basis for the predictive and regulatory modeling by TNRCC and EPA.

(Ethene/NO<sub>x</sub>) ratios measured in transects within 5 km of the Freeport and Chocolate Bayou facilities were not significantly affected by differential chemical or physical removal; the inferred emissions ratios are therefore judged to be accurate to within the combined measurement uncertainties of  $\pm 17\%$ . The closest Sweeny plume transects took place ca. 22 km or 1.4 hr downwind; given the larger OH reaction rate for propene relative to NO<sub>x</sub> the resulting estimated (propene/NO<sub>x</sub>) emission ratio is subject to the largest uncertainty. We judge the estimated (propene/NO<sub>x</sub>) emissions ratio for Sweeny is only accurate to within a factor of two. These estimated emissions data are presented in Table 1 along with the ratios calculated from annual emissions rates listed in the 2000 PSDB inventory. The data in Table 1 show that substantial discrepancies, many times larger than the measurement uncertainty, exist between the measurement-inferred emission ratios and those calculated from the 2000 inventory values. Small differences in the inventory (alkene/NO<sub>x</sub>) ratios between Table 1 in this report and those in Table 4 of Wert et al. [2002] are due to the different inventory reporting years.

**Table 1.** Tabulated NO<sub>x</sub> and alkene emission rates and ratios, and measurement-inferred emission ratios, for selected petrochemical complexes and an electric utility power plant.

Complex	E <sub>NO<sub>x</sub></sub> <sup>1</sup>	E <sub>ethene</sub> <sup>1</sup>	tabulated ethene/NO <sub>x</sub>	measured ethene/NO <sub>x</sub>	E <sub>propene</sub> <sup>1</sup>	tabulated propene/NO <sub>x</sub>	measured propene/NO <sub>x</sub>
Sweeny	12.6	0.6	0.05	3.6	0.4	0.03	2.0
Freeport	34.8	1.8	0.05	1.5	0.4	0.01	0.5
Chocolate Bayou	7.2	0.6	0.08	2.0	0.7	0.10	4.0
W.A. Parish	66.5	-	-	-	-	-	-

<sup>1</sup>Sum of annually-averaged emissions (kmoles/hr) listed in the 2000 TNRCC PSDB for the boxes in Figure 3.

Such large discrepancies could arise from inaccuracy either in the tabulated inventory values of NO<sub>x</sub>, of alkenes, or of both, for the petrochemical complexes in question. The discrepancy could also arise if the actual NO<sub>x</sub> emissions were extremely low, or the alkene emissions extremely high, from all three facilities simultaneously during both the August 27 and 28 plume studies compared to the annual averages. In the following section we show that the NO<sub>x</sub> emissions were relatively constant over time and are reasonably well estimated in the inventory.

*NO<sub>x</sub> emissions were constant over time.* The NO<sub>x</sub> emissions information is derived from continuous emission monitoring systems (CEMS) data for many of the largest NO<sub>x</sub> sources at each complex; these data are believed to be accurate to better than ±30% on average [Placet *et al.*, 2000; Ryerson *et al.*, 1998]. Petrochemical facilities are typically operated continuously, so that variation in their NO<sub>x</sub> output over time can be minimal (C. Wyman, personal communication, 2001). As an example, total hourly-averaged NO<sub>x</sub> emissions rates reported by the largest of the four facilities in the Chocolate Bayou area differed by less than 5% for the August 27 and 28 plume study periods reported here. Further, very little variation is apparent over the eleven days of hourly-averaged emission rates for NO<sub>x</sub> (264 consecutive hours, average±sigma=(7.9±0.2), max=8.5, min=7.5, with units of 10<sup>23</sup> molec/s) reported by this facility (August 22-September 1, 2000, including the plume study periods). The 2000 PSDB annually-averaged NO<sub>x</sub> emission rate is further consistent within 15% with that derived from the hourly averages from this facility. In addition, the available daily-averaged NO<sub>x</sub> emissions data from the second-largest facility show variations of less than 10% (eleven consecutive days, average±sigma=(2.7±0.2), max=3.0, min=2.5, with units of 10<sup>23</sup> molec/s). Annual averages suggest these two facilities account for 91% of the total NO<sub>x</sub> emissions from the Chocolate Bayou source region. Similar arguments can be constructed for the facilities in the Sweeny and Freeport source regions (Figure 3). These findings suggest that for the August 27 and 28 plume studies the emissions rates derived from hourly-, daily-, and annually-averaged NO<sub>x</sub> inventories are comparable, and that NO<sub>x</sub> emissions from the three isolated petrochemical source regions were quite constant and representative of normal operating conditions of these complexes.

*NO<sub>x</sub> emissions are well represented by the available inventories.* The overall accuracy of the NO<sub>x</sub> emissions rates for these three complexes is evaluated by comparing to emissions rates inferred from plume mass flux of NO<sub>y</sub>, calculated from near-field aircraft transect data [Brock *et al.*, 2002; Ryerson *et al.*, 1998; Ryerson *et al.*, 2001; Trainer *et al.*, 1995; White *et al.*, 1976], to the available inventory values. Mass flux estimates from aircraft data taken in well-resolved plumes are subject to several sources of uncertainty, including depositional losses, venting to the free troposphere, incomplete mixing within the boundary layer, and variability in wind speeds. These uncertainties and their evaluation are discussed extensively in Ryerson *et al.* [1998]. Examination of the multiple plume transect data on these two days suggests that the NO<sub>y</sub> mass flux was relatively well conserved over time. Plume NO<sub>y</sub>/SO<sub>2</sub> ratios remained constant, within  $\pm 30\%$ , between successive transects on these two days (e.g., see Figure 8 in Brock *et al.* [2002] for the analysis of the W.A. Parish plume), suggesting minimal differential loss of NO<sub>y</sub> relative to SO<sub>2</sub> and/or CO<sub>2</sub>. Further, the total estimated mass of NO<sub>y</sub> in each petrochemical plume remained constant within  $\pm 30\%$  over time downwind of each complex, in turn suggesting that depositional loss of HNO<sub>3</sub> was relatively small compared to the total NO<sub>y</sub> on the timescales considered here. Thus, NO<sub>y</sub> appears to have been approximately conserved during the course of these plume studies. Given additional uncertainties in wind speed histories and boundary layer heights, for the isolated petrochemical plumes studied here, we conservatively estimate the uncertainty in derived NO<sub>y</sub> mass flux to be a factor of two. Comparison of the aircraft-derived NO<sub>y</sub> flux estimates to the annually-averaged NO<sub>x</sub> inventory emissions values shows agreement within  $\pm 50\%$ , well within the uncertainty in deriving mass fluxes for these isolated facilities for these two days. This level of agreement rules out the inventory NO<sub>x</sub> values as the primary source of inventory-measurement (alkene/NO<sub>x</sub>) ratio discrepancies of factors of 20 to nearly 70, mentioned above. These discrepancies are roughly a factor of 2 smaller than those noted in Wert *et al.* [2002] using the 1999 PSDB inventory; while the total VOC emissions numbers remained approximately constant, more complete speciation in the 2000 inventory accounted for much of the change.

*Alkene emissions are consistently underestimated.* Inventory values of alkene emissions are therefore implicated as the primary cause of the large discrepancies in (alkene/NO<sub>x</sub>) emissions ratios. Hourly and daily ethene, propene, and butadiene emissions data from facilities in, e.g., the Chocolate Bayou source region suggest that total emissions of these alkenes showed minimal variability, within  $\pm 20\%$  of the average value over the August 22-September 1 time period, encompassing the two plume study days. Similarities observed between plumes sampled on August 27 and 28, further consistent with the larger Electra data set from the month-long Texas 2000 project, suggest that the instantaneous VOC emissions were representative of normal operations on both days and generally consistent with the annual average. No substantial upsets, or non-routine emission events, were recorded for these facilities for the plume intercepts studied here. We conclude that consistently large discrepancies between measurement-derived and tabulated (alkene/NO<sub>x</sub>) ratios are due to consistently and substantially underestimated VOC emissions from the petrochemical facilities [Wert *et al.*, 2002].

### Sensitivity of model estimates to emission inputs

The analysis of canister and *in-situ* samples collected in the Houston area using the NCAR Electra aircraft clearly demonstrate that low molecular weight olefins are the major contributor to VOC reactivity (Figure 4). Therefore, the discrepancies in light olefin emissions documented above would be expected to have a dramatic effect on model estimates of ozone and other photochemical products in the Houston area. A number of model comparisons were performed to evaluate the sensitivity of model estimates to the choice of VOC emission inputs.

*Plume model estimates* - The first sensitivity study was performed using a simple reactive plume model. This model includes a full description of the inorganic and photochemical processes and uses explicit chemistry for ethylene and propylene. Plume dilution is matched to aircraft measurements of plume dimensions. This model was used to analyze several plumes from petrochemical facilities for August 27 and 28, 2000 when the Electra sampled these plumes under stable flow conditions with the plumes superimposed on clean background air from the Gulf of Mexico (Figure 8).

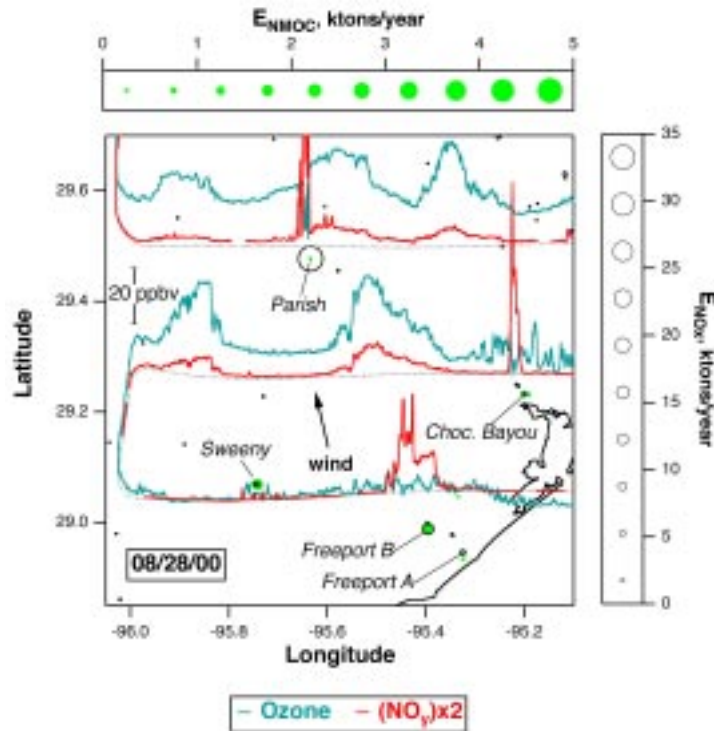


**Figure 8.** Electra flight track on August 28, 2000 with O<sub>3</sub> and NO<sub>y</sub> traces and sources included. The plumes from the Freeport and Sweeny facilities are evident in the pollutant traces. The wind was from the SSE.

The plumes from these facilities were modeled using emissions taken from the TCEQ inventory and using observationally derived emissions. A comparison of the emission values derived by these two methods is provided in Table 2, [Wert et al, 2002].

**Table 2.** TCEQ inventory and measurement-derived estimates of NO<sub>x</sub> and VOC emissions for the Freeport and Sweeny facilities on August 28, 2000.

Petrochemical Facility	Measurements (kmol/hr)			Inventory (kmol/hr)		
	NO <sub>x</sub>	Ethylene	Propylene	NO <sub>x</sub>	Ethylene	Propylene
Freeport B	30	45	15	31	0.9	0.3
Sweeny	15	54	30	14	0.5	0.3

The measured and reported emission factors for NO<sub>x</sub> compare very well while the discrepancies in the VOC estimates are evident. When the observationally derived NO<sub>x</sub> and VOC emission values are employed the reactive plume model reproduces the ozone and formaldehyde profiles remarkably well (Figure 9). However, when the model is initialized with NO<sub>x</sub> and VOC emissions taken from the TCEQ inventory the performance is significantly degraded. Using the inventory values, less than 10% of the measured formaldehyde, and 40% of the measured ozone enhancement over background levels were simulated (Figure 9).

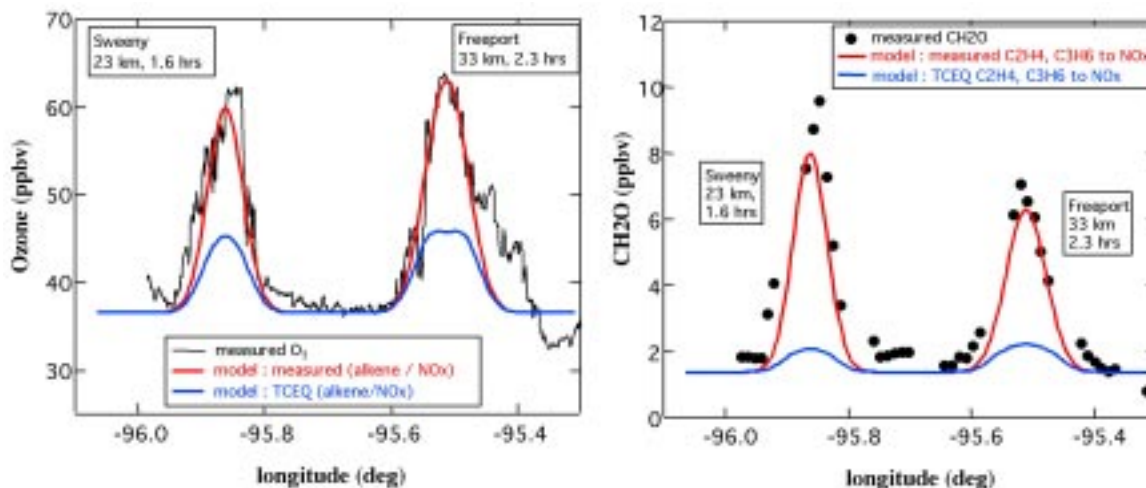


**Figure 9.** Comparison of ozone (left) and formaldehyde (right) estimates using a plume model initialized with precursor emissions from the TCEQ inventory (blue) and estimated from measurements on the NCAR Electra. Data are from August 28.

*Photochemical grid model estimates* - When emissions ratios of ethylene and propylene to NO<sub>x</sub> derived from the aircraft observations are compared to EPA or TCEQ emissions inventories for the Sweeny, Freeport, Chocolate Bayou and Texas City petrochemical complexes, the inventories are low by factors of 30 to 80 for both species. The errors in the emissions inventories for the ship channel region east and southeast of Houston are not as easy to estimate due to the large number and dense distribution of individual ethylene and propylene petrochemical sources that are not always co-located with NO<sub>x</sub>

sources. Yet the aircraft observations suggest the ship channel region is the largest source of ethylene and propylene (Figure 5) in the broader Houston-Galveston area. A method was therefore developed to modify the emissions of propylene and ethylene from petrochemical sources within the emissions inventories, based on the emissions errors observed at the 4 isolated facilities. Source attribution from the EPA NET-96 point source inventory was used to aggregate NMHC emissions at each facility in one of 3 classes: propylene production, ethylene production, and a general “fugitive emissions” source that includes 15 of the main NMHC source categories at each site (i.e. flares, storage and transfer, wastewater treatment, and catalytic cracking). Linear fits of the emission of either propylene or ethylene determined from the measurements were applied to total NMHC emissions from the 3 emission aggregate types at the 4 facilities. The following table shows the results of the linear fits. Each entry is a multiplication factor that must be applied to the total NMHC emissions for each aggregate source type (left column) to obtain the observed emissions of either  $C_2H_4$  or  $C_3H_6$ .

**Table 3.** Multiplication factors used to adjust inventory-based emissions to make them consistent with observations.

	$C_2H_4$	$C_3H_6$
Fugitive emissions	1.7	0
$C_3H_6$ production	0	52
$C_2H_4$ production	22	15

The results of this table are then applied to the emissions inventories for the greater Houston-Galveston region to modify ethylene and propylene emissions for all other petrochemical sites.

The NOAA/FSL air quality forecast model (MM5-CHEM) [Grell et al., 2000] is used to assess the impact of the modified emissions inventory on ozone, and ozone precursors. Several key photochemical relationships (i.e.  $O_3$  versus  $NO_y$  minus  $NO_x$ , and formaldehyde versus  $NO_y$  minus  $NO_x$ ) are found to match observations significantly better over the ship channel region when the modified emissions inventory is applied to the photochemical model. The impact the modified emissions inventory has on predicted  $O_3$  for August 30, 2000 is shown in Figure 10. The maximum of 165 ppbv in the modified emissions case is much more consistent with the 180 ppbv observed by the NCAR-Electra aircraft observed near the same region on this day.

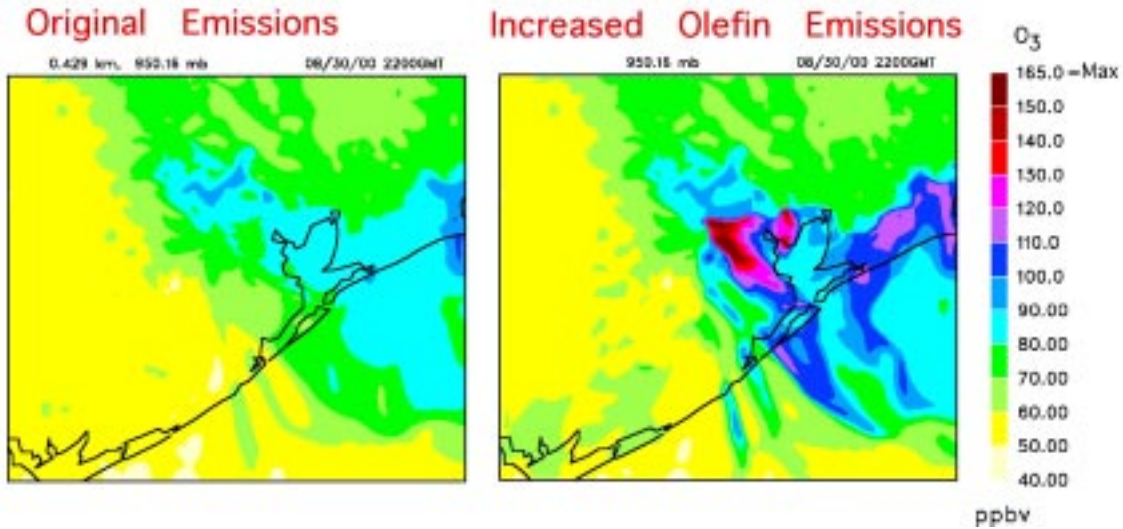


**Figure 10.** Ozone estimates for the Houston area for August 30, 2000 using the MM5-CHEM model initialized with precursor emissions taken from the Net-99 inventory (left) and with emissions adjusted using factors from Table 2 (right).

### Finding

The photochemical model simulations are very sensitive to the choice of VOC emission rates used for the petrochemical facilities in the Houston area. The simulations conducted using observationally based emissions, which are significantly enhanced over those found in the traditional inventories, produced significantly better agreement with measurements made on the NCAR Electra and those from the surface regulatory network.

---

## References

- Brock, C.A., M. Trainer, T.B. Ryerson, J.A. Neuman, D.D. Parrish, J.S. Holloway, D.K.J. Nicks, G.J. Frost, G. Hübler, and F.C. Fehsenfeld, Particle growth in urban and industrial plumes in Texas, *Journal of Geophysical Research (in press)*, 2002.
- Derwent, R.G., Ozone formation downwind of an industrial source of hydrocarbons under European conditions, *Atmospheric Environment*, *34*, 3689-3700, 2000.
- Dodge, M.C., Chemical oxidant mechanisms for air quality modeling: critical review, *Atmospheric Environment*, *34*, 2103-2130, 2000.
- EPA, National Air Quality and Emissions Trends Report, 1999, United States Environmental Protection Agency, Research Triangle Park, 2001.
- Grell, G.A.; Emeis, S.; Stockwell, W.R.; Schoenemeyer, T.; Forkel, R.; Michalakes, J.; Knoche, R.; Seidl, W. Application of a Multiscale, Coupled MM5/Chemistry Model to the Complex Terrain of the VOTALP Valley Campaign; *Atmos. Environ.*, *34*, 1435-1453, 2000.
- Kleinman, L.I., P.H. Daum, D.G. Imre, Y.-N. Lee, L.J. Nunnermacker, S.R. Springston, J. Weinstein-Lloyd, and J. Rudolph, Ozone production rate and hydrocarbon reactivity in 5 urban areas: a cause of high ozone concentration in Houston, *Geophysical Research Letters*, *29*, 10.1029/2001GL014569, 2002.
- Liu, S.C., M. Trainer, F.C. Fehsenfeld, D.D. Parrish, E.J. Williams, D.W. Fahey, G. Hübler, and P.C. Murphy, Ozone production in the rural troposphere and the implications for regional and global ozone distributions, *Journal of Geophysical Research*, *92*, 4191-4207, 1987.
- Neuman, J.A., L.G. Huey, R.W. Dissly, F.C. Fehsenfeld, F. Flocke, J.C. Holocek, J.S. Holloway, G. Hübler, R.O. Jakoubek, D.K.J. Nicks, D.D. Parrish, T.B. Ryerson, D.T. Sueper, and A.J. Weinheimer, Fast-response airborne in situ measurements of HNO<sub>3</sub> during the Texas 2000 Air Quality Study, *Journal of Geophysical Research (in press)*, 2002.
- Placet, M., C.O. Mann, R.O. Gilbert, and M.J. Niefer, Emissions of ozone precursors from stationary sources: a critical review, *Atmospheric Environment*, *34*, 2183-2204, 2000.
- Ryerson, T.B., M. Trainer, J.S. Holloway, D.D. Parrish, L.G. Huey, D.T. Sueper, G.J. Frost, S.G. Donnelly, S. Schaufli, E.L. Atlas, W.C. Kuster, P.D. Goldan, G. Hübler, J.M. Meagher, and F.C. Fehsenfeld, Observations of ozone formation in power plant plumes and implications for ozone control strategies, *Science*, *292*, 719-723, 2001.

Ryerson, T.B., M.P. Buhr, G. Frost, P.D. Goldan, J.S. Holloway, G. Hübler, B.T. Jobson, W.C. Kuster, S.A. McKeen, D.D. Parrish, J.M. Roberts, D.T. Sueper, M. Trainer, J. Williams, and F.C. Fehsenfeld, Emissions lifetimes and ozone formation in power plant plumes, *Journal of Geophysical Research*, *103*, 22,569-22,583, 1998.

Sillman, S., Ozone production efficiency and loss of NO<sub>x</sub> in power plant plumes: Photochemical model and interpretation of measurements in Tennessee, *Journal of Geophysical Research*, *105*, 9189-9202, 2000.

Trainer, M., B.A. Ridley, M.P. Buhr, G. Kok, J. Walega, G. Hübler, D.D. Parrish, and F.C. Fehsenfeld, Regional ozone and urban plumes in the southeastern United States: Birmingham, a case study, *Journal of Geophysical Research*, *100*, 18,823-18,834, 1995.

Trainer, M., D.D. Parrish, M.P. Buhr, R.B. Norton, F.C. Fehsenfeld, K.G. Anlauf, J.W. Bottenheim, Y.Z. Tang, H.A. Weibe, J.M. Roberts, R.L. Tanner, L. Newman, V.C. Bowersox, J.F. Meagher, K.J. Olszyna, M.O. Rodgers, T. Wang, H. Berresheim, K.L. Demerjian, and U.K. Roychowdhury, Correlation of ozone with NO<sub>y</sub> in photochemically aged air, *Journal of Geophysical Research*, *98*, 2917-2925, 1993.

Trainer, M., E.-Y. Hsie, S.A. McKeen, R. Tallamraju, D.D. Parrish, F.C. Fehsenfeld, and S.C. Liu, Impact of natural hydrocarbons on hydroxyl and peroxy radicals at a remote site, *Journal of Geophysical Research*, *92*, 11,879-11,894, 1987a.

Trainer, M., E.J. Williams, D.D. Parrish, M.P. Buhr, E.J. Allwine, H.H. Westberg, F.C. Fehsenfeld, and S.C. Liu, Models and observations of the impact of natural hydrocarbons on rural ozone, *Nature*, *329*, 705-707, 1987b.

Watson, J.G., J.C. Chow, and E.M. Fujita, Review of volatile organic compound source apportionment by chemical mass balance, *Atmospheric Environment*, *35*, 1567-1584, 2001.

Wert, B.P., M. Trainer, A. Fried, T.B. Ryerson, B. Henry, W. Potter, S.G. Donnelly, S. Schauffler, E.L. Atlas, D.K.J. Nicks, P.D. Goldan, W.C. Kuster, D.D. Parrish, J.S. Holloway, J.A. Neuman, W.M. Angevine, J. Stutz, A. Hansel, A. Wisthaler, C. Weidinmyer, G.J. Frost, G. Hübler, D.T. Sueper, and F.C. Fehsenfeld, Signatures of alkene oxidation in airborne formaldehyde measurements during TexAQS 2000, *Journal of Geophysical Research (submitted)*, 2002.

White, W.H., J.A. Anderson, D.L. Blumenthal, R.B. Husar, N.V. Gillani, J.D. Husar, and W.E.J. Wilson, Formation and transport of secondary air pollutants: ozone and aerosols in the St. Louis urban plume, *Science*, *194*, 187-189, 1976.

# Appendix

The data analyses described in the following manuscripts were supported in part with funds provided by the Texas Commission on Environmental Quality.

1. **Signatures of Terminal Alkene Oxidation in Airborne Formaldehyde Measurements During TexAQS 2000**, by B. P. Wert, M. Trainer, A. Fried, T. B. Ryerson, B. Henry, W. Potter, W.M. Angevine, E. Atlas, S.G. Donnelly, F.C. Fehsenfeld, G.J. Frost, P.D. Goldan, A. Hansel, J.S. Holloway, G. Hubler, W.C. Kuster, D.K. Nicks Jr., J.A. Neuman, D.D. Parrish, S.Schauffle, J. Stutz, D.T. Sueper, C. Wiedinmyer, and A. Wisthaler
2. **Particle growth in urban and industrial plumes in Texas**, by Charles A. Brock, Michael Trainer, Thomas B. Ryerson, J. Andrew Neuman, David D. Parrish, John S. Holloway, Paul Goldan, William Kuster, Gregory Frost, Gerhard Hübler, Christine Wiedinmyer, and Fred C. Fehsenfeld J. Charles Wilson, J. Michael Reeves, Bernard G. Lafleur, and Henrike Hilbert
3. **Effect of petrochemical industrial emissions of reactive alkenes and NO<sub>x</sub> on tropospheric ozone formation in Houston, TX**, by T.B. Ryerson, M. Trainer, W.M. Angevine, C.A. Brock, R.W. Dissly, F.C. Fehsenfeld, G.J. Frost, P.D. Goldan, J.S. Holloway, G. Hübler, R.O. Jakoubek, W.C. Kuster, J.A. Neuman, D.K. Nicks Jr., D.D. Parrish, J.M. Roberts, and D.T. Sueper



**Signatures of Terminal Alkene Oxidation in Airborne  
Formaldehyde Measurements During TexAQS 2000,**

by

B. P. Wert, M. Trainer, A. Fried, T. B. Ryerson, B. Henry, W. Potter, W.M. Angevine, E.  
Atlas, S.G. Donnelly, F.C. Fehsenfeld, G.J. Frost, P.D. Goldan, A. Hansel, J.S.  
Holloway, G. Hubler, W.C. Kuster, D.K. Nicks Jr., J.A. Neuman, D.D. Parrish,  
S.Schauffle, J . Stutz, D.T. Sueper, C. Wiedinmyer, and A. Wisthaler



## Signatures of Terminal Alkene Oxidation in Airborne Formaldehyde Measurements During TexAQS 2000

B. P. Wert<sup>1,2</sup>, M. Trainer<sup>3</sup>, A. Fried<sup>1</sup>, T. B. Ryerson<sup>3</sup>, B. Henry<sup>1</sup>, W. Potter<sup>1,4</sup>, W.M. Angevine<sup>3,5</sup>, E. Atlas<sup>1</sup>, S.G. Donnelly<sup>1</sup>, F.C. Fehsenfeld<sup>3</sup>, G.J. Frost<sup>3,5</sup>, P.D. Goldan<sup>3</sup>, A. Hansel<sup>6</sup>, J.S. Holloway<sup>3,5</sup>, G. Hubler<sup>3,5</sup>, W.C. Kuster<sup>3</sup>, D.K. Nicks Jr.<sup>3,5</sup>, J.A. Neuman<sup>3,5</sup>, D.D. Parrish<sup>3</sup>, S.Schauffler<sup>1</sup>, J. Stutz<sup>7</sup>, D.T. Sueper<sup>3</sup>, C. Wiedinmyer<sup>1</sup>, and A. Wisthaler<sup>6</sup>

<sup>1</sup> The National Center for Atmospheric Research, Atmospheric Chemistry Division, P.O. Box 3000, Boulder, Colorado, 80307, USA.

<sup>2</sup> also with University of Colorado, Department of Chemistry and Biochemistry, Boulder, Colorado 80309, USA.

<sup>3</sup> National Oceanic and Atmospheric Administration, Aeronomy Laboratory, Boulder, CO, USA.

<sup>4</sup> also with University of Tulsa, Department of Chemistry and Biochemistry, Tulsa, Oklahoma, 74104, USA.

<sup>5</sup> also with University of Colorado, Cooperative Institute for Research in Environmental Sciences, Boulder, CO 80309, USA.

<sup>6</sup> University of Innsbruck, Institute for Ionphysics, Innsbruck, Austria.

<sup>7</sup> University of California Los Angeles, Department of Atmospheric Sciences, Los Angeles, CA, 90095, USA.

Rev. 9/12/2002; for resubmission to JGR.

**Abstract.** Airborne formaldehyde (CH<sub>2</sub>O) measurements were made by tunable diode laser absorption spectroscopy (TDLAS) at high time resolution (1 and 10 s) and precision ( $\pm 400$  and  $\pm 120$  pptv ( $2\sigma$ ), respectively) during the Texas Air Quality Study (TexAQS) 2000. Measurement accuracy was corroborated by in-flight calibrations and zeros, and by overflight comparison with a ground-based DOAS system. Throughout the campaign, the highest levels of CH<sub>2</sub>O precursors and VOC reactivity were measured in petrochemical plumes. Correspondingly, CH<sub>2</sub>O and ozone production were greatly enhanced in petrochemical plumes, compared with plumes dominated by power plant and

mobile source emissions. The photochemistry of several isolated petrochemical facility plumes was accurately modeled using three non-methane hydrocarbons (NMHCs): ethene, propene (both anthropogenic), and isoprene (biogenic), and was in accord with standard OH-initiated chemistry. Measurement-inferred facility emissions of ethene and propene were far larger than reported by inventories. Substantial direct CH<sub>2</sub>O emissions were not detected from petrochemical facilities. The rapid production of CH<sub>2</sub>O and ozone observed in a highly polluted plume (30+ ppbv CH<sub>2</sub>O, 200+ ppbv ozone) originating over Houston was well replicated by a model employing only two NMHCs, ethene and propene.

## **I. Introduction.**

Gas phase formaldehyde (CH<sub>2</sub>O) is a ubiquitous component of the troposphere, and is typically the most abundant carbonyl compound found in the boundary layer atmosphere. CH<sub>2</sub>O is largely produced in situ, as an intermediate in the oxidation of a large array of volatile organic compounds (VOCs). However, only a small number of VOCs are both abundant and efficient CH<sub>2</sub>O producers. In the polluted boundary layer the terminal alkenes are generally the most important CH<sub>2</sub>O precursors, particularly isoprene (C<sub>5</sub>H<sub>8</sub>), ethene (C<sub>2</sub>H<sub>4</sub>), and propene (C<sub>3</sub>H<sub>6</sub>) [Dodge, 1990; Lee, Y.-N. et al., 1998; Goldan et al., 2000]. In many cases, the important CH<sub>2</sub>O precursors also contribute substantially to total hydrocarbon hydroxyl radical (OH) reactivity ( $\Sigma [k_x \text{OH} * [\text{VOC}_x]]$ ), and thereby total VOC reactivity. Here  $k_x$  is the bimolecular rate constant for reaction of OH with each VOC. Due to the heterogeneous spatial distribution of CH<sub>2</sub>O precursors, and the relatively short lifetime of CH<sub>2</sub>O (2 - 4 hours in the sunlit

troposphere), continental boundary layer CH<sub>2</sub>O concentrations span nearly two orders of magnitude [Grosjean, 1991; Fried *et al.*, 1997; Lee, Y.-N. *et al.*, 1998], providing a sensitive indicator of recent VOC oxidation.

CH<sub>2</sub>O is also emitted directly into the atmosphere by incomplete fossil fuel combustion [Sigsby *et al.*, 1987; Altshuller *et al.*, 1993; Anderson *et al.*, 1996], biomass burning [Lee, M. *et al.*, 1998; Yokelson *et al.*, 1999], industrial processes, and vegetative emissions [Carlier *et al.*, 1996]. However, primary CH<sub>2</sub>O emissions are typically small relative to photochemical production. Using ambient measurements, Li *et al.* [1994] have estimated that the amount of CH<sub>2</sub>O directly emitted from eastern North America is 16 times less than that produced by the oxidation of emitted anthropogenic and biogenic VOCs.

Since VOC oxidation also drives tropospheric ozone production in the polluted boundary layer [Haagen-Smit, 1952; Chameides *et al.*, 1992; Sillman, 1999], CH<sub>2</sub>O measurements are useful to deconvolving sources of ozone pollution, an issue central to urban and regional air quality. For instance, CH<sub>2</sub>O measurements made during the 1995 Southern Oxidant Study (SOS 95), based in Nashville, Tennessee, were used to corroborate the contribution of biogenic isoprene to regional ozone production [Lee, Y.-N. *et al.*, 1998]; and satellite measurements of CH<sub>2</sub>O have been used to evaluate biogenic isoprene emissions over North America [Chance *et al.*, 2000; Palmer *et al.*, 2001]. To similar ends, the present study utilizes high time resolution airborne CH<sub>2</sub>O measurements collected during the Texas Air Quality Study (TexAQS) 2000 to examine the role of various hydrocarbons in the photochemistry of the Houston, Texas area.

During the 1990's ozone levels in exceedance of National Ambient Air Quality Standards (NAAQS) were regularly reported for the greater Houston, Texas metropolitan area. On average, only Los Angeles reported more intense episodes of ozone pollution during this period [Lin *et al.*, 2001]. Over 4 million people live in the greater Houston metropolitan area [U.S. Census, 2000], resulting in large mobile source emissions of VOCs and NO<sub>x</sub> [TNRCC, 1996]. One of the largest electric utility power plants in the nation, the W.A. Parish facility, is located just outside of Houston [Nicks *et al.*, 2002] (see Figure 1). In addition, a large fraction of the United States' olefin production capacity is found in the Houston-Galveston-Brazoria area, with an especially high density located along the Ship Channel inside Houston city limits (see Figure 1). Biogenic emissions are also a source of VOCs in and around Houston, although detailed vegetation surveys [Wiedinmyer *et al.*, 2001] indicate that these emissions should be substantially less than in areas such as Tennessee [Geron *et al.*, 1994; Goldan *et al.*, 2000].

The TexAQS 2000 mission was conducted to elucidate the role of such emissions, along with meteorology, in Houston's intense photochemical pollution [Kleinman *et al.*, 2002]. The study was conducted from mid-August to mid-September 2000, and involved the combined efforts of the Texas Natural Resource Conservation Commission (TNRCC), the National Oceanic and Atmospheric Administration (NOAA), the National Center for Atmospheric Research (NCAR), Brookhaven National Laboratories (BNL), the University of Texas, Baylor University, and many other laboratories and universities. Multiple well-instrumented aircraft and ground sites were employed.

The present study addresses four primary questions utilizing airborne CH<sub>2</sub>O observations collected during TexAQS 2000: 1) What were the major sources of CH<sub>2</sub>O

(and CH<sub>2</sub>O precursors) in the Houston atmosphere? 2) Can the fast CH<sub>2</sub>O measurements reported here be used to accurately extrapolate intermittent, lower resolution CH<sub>2</sub>O precursor measurements made on the same aircraft? 3) To what extent did the important CH<sub>2</sub>O precursors contribute to rapid ozone production in the Houston area? and 4) Were emission inventories accurate with respect to the important CH<sub>2</sub>O precursors?

### **III. Experimental.**

#### **III.1 Airborne Sampling.**

The measurements considered here were made from the NCAR L-188C Electra aircraft. CH<sub>2</sub>O measurements were made by the NCAR tunable diode laser absorption spectrometer (TDLAS). Supporting measurements included 1 Hz ozone, CO [*Holloway et al.*, 2000], CO<sub>2</sub>, NO, NO<sub>2</sub>, NO<sub>y</sub> [*Ryerson et al.*, 2000], HNO<sub>3</sub> [*Huey et al.*, 1998; *Neuman et al.*, 2002], SO<sub>2</sub>, size-resolved aerosol number [*Brock et al.*, 2000], and spectrally-resolved actinic flux. Peroxyacyl nitrate compounds were measured once every 3.5 min by gas-chromatography (GC) [*Flocke et al.*, 2002]. Acetaldehyde was measured by proton transfer mass spectrometry (PTRMS) [*Lindinger et al.*, 1998]. Thirty-nine whole-air canister samples, typically integrated over 8 s, were acquired on each flight at the discretion of the flight scientist; subsequent GC analysis provided an extensive suite of speciated VOCs (see Table 1) [*Schauffler et al.*, 1999]. In situ GC samples were acquired once every 15 minutes, measuring a different subset of VOCs, including a limited suite of oxygenates [*Goldan et al.*, 2000].

Flights surveyed the greater Houston metropolitan area on eight different days. Two days each were dedicated to exploring the Dallas-Ft. Worth area, and power plant

plumes throughout eastern Texas. Flight tracks usually involved multiple crosswind intercepts of one or several plumes at a number of distances downwind, in order to characterize the temporal evolution of the plume chemistry. The bulk of sampled plumes were either of mobile source (urban), petrochemical facility, or power plant origin, with many plumes representing some combination of these emission types. In order to capture mid-day photochemistry and the daily ozone maximum, flights typically took off between 1000 and 1100 CST, and lasted for about 6 hours.

### **III.2. TDLAS System.**

The TDLAS and its forerunner systems have been described [Fried et al., 1998, 2002; Wert et al., 2002a], thus only a short summary is included here. Gas-phase CH<sub>2</sub>O was measured by probing the 2831.6417 cm<sup>-1</sup> ro-vibrational line with a tunable diode laser coupled to a 100 m pathlength astigmatic Herriott absorption cell. Extensive field and laboratory analysis has shown that the TDLAS inlet and Herriott cell produce only minimal sampling artifacts under the conditions encountered during TexAQS [Wert et al., 2002b]. Frequent instrument zeros were acquired, and flowing gas phase standards were generated via a permeation oven, the accuracy of which has been determined to be ± 6% [Gilpin et al., 1997; Fried et al., 1998 & 2002]. During the first portion of the TexAQS intensive, ambient CH<sub>2</sub>O measurements were made at 10 s resolution. Data integration was reduced to 1 s beginning on the September 1<sup>st</sup> flight, and this resolution was maintained for the remainder of the mission. Estimated TDLAS precision during the TexAQS mission was 120 parts-per-trillion-by-volume (pptv) for 10 s measurements, and 400 pptv for 1 s measurements (reported at the 2σ level) [Wert et al., 2002a]. Ambient

measurements covered roughly 50% of the total flight time, excluding takeoff and landing.

Extensive tests have found that only methanol ( $\text{CH}_3\text{OH}$ ) interferes with this technique. Laboratory studies using the same TDLAS arrangement as in TexAQS have shown the methanol interference to be +3.8% at equal methanol and  $\text{CH}_2\text{O}$  concentrations [Fried *et al.*, 2002; Wert *et al.*, 2002a], consistent with independent measurements made at Rice University [Richter, 2001]. Thus ambient methanol levels of 10 parts-per-billion-by-volume (ppbv) would cause the TDLAS  $\text{CH}_2\text{O}$  measurement to be too high by 380 pptv. TDLAS  $\text{CH}_2\text{O}$  data were corrected using an algorithm derived from 144 coincident measurements of methanol (in situ GC) and  $\text{CH}_2\text{O}$  made on the Electra. Given the 1 to 3 ppbv  $\text{CH}_2\text{O}$  boundary layer background in the Houston area, and the emphasis of the present study on plume chemistry, the methanol bias and associated correction were largely negligible for the data of interest (< 10%). All analyses in this paper utilize methanol corrected data.

Further evidence for the accuracy of the TDLAS  $\text{CH}_2\text{O}$  measurement was provided by comparison with UCLA's ground-based Differential Optical Absorption Spectrometer (DOAS) [Stutz and Platt, 1997; Harder *et al.*, 1997] during TexAQS; these two systems were also successfully compared throughout the SOS 99 campaign [Wert *et al.*, 2002a]. During TexAQS the Electra aircraft conducted overflights of the La Porte airport, the site of extensive chemical instrumentation including the UCLA DOAS. TDLAS data was averaged for a 5 to 10 s period of closest approach in all but one case, corresponding to a path comparable in length (0.5 to 1 km) and height (40 to 60 m flight altitude) to that of the DOAS (1.9 km pathlength, 2 to 50 m height above ground).

Ground based O<sub>3</sub> and CO measurement variability was acceptably small during the DOAS integration periods (20 min to 1 hr). Bivariate regression of the TDLAS and DOAS CH<sub>2</sub>O data produced the relationship:  $(\text{TDLAS CH}_2\text{O}) = 0.95 * (\text{DOAS CH}_2\text{O}) - 0.70$  ppbv ( $n = 6$ ,  $\chi^2 = 5.5$ ), with slope and intercept uncertainties of 0.15 and 0.65, respectively (see Fig. 2). CH<sub>2</sub>O measurements made by three separate DOAS paths at La Porte (0.75, 1.9, and 5.5 km pathlengths) agreed well during all overflight periods but one, indicating good mixing. The overflight associated with conditions of poor mixing was that which yielded the high concentration point. Removal of this point produces a slope of 1.23 ( $\pm 0.29$ ). These results suggest that systematic measurement errors associated with the two different techniques are small ( $< \approx 10\%$ ).

### **III.3. Photochemical Model.**

The photochemical model used in the current study is similar to earlier plume simulations by, for example, *Hov and Isaksen* [1981] and *Sillman* [2000], where the plume of a power plant was followed in an idealized Lagrangian fashion and the vertical and horizontal spreading were explicitly described. In the present model the vertical dispersion of the plume was controlled by the growth of the Planetary Boundary Layer (PBL), and diffusive vertical transport was calculated as described in *Trainer et al.* [1991]. The maximum height of the PBL was scaled to approximate observed conditions. Horizontal spreading of the plume was described by a diffusion coefficient chosen to approximate the observed growth in plume width as a function of distance. The advective wind was a free parameter that controlled the peak concentration in the plume, and was chosen according to measurements aboard the aircraft, or radar profile measurements made from the ground. Horizontal grid resolution was fixed at 500 m and

the plume was emitted into a 100 m x 500 m x 500 m grid cell. Plume spreading and photochemistry were concurrently calculated within this grid framework. The chemistry was based on *Trainer et al.* [1987, 1991] where the reaction rates and products were updated according to JPL97 [*DeMore et al.*, 1997] and *Atkinson* [1997]. Photolysis rates were calculated by the TUV radiative transfer model of *Madronich* [1987] and validated by comparison with actinic flux measurements made on the Electra. The TUV model is based upon the discrete ordinates model modified to solve the radiative transfer equation in pseudo-spherical coordinates [*Dahlbeck and Stamnes*, 1991].

#### **IV. Results.**

##### **IV.1 TexAQS CH<sub>2</sub>O Distributions.**

As depicted in Figure 3, the vertical distribution of CH<sub>2</sub>O measured during TexAQS shows a rapid decay above the boundary layer (0.5 to 2.5 km [*Christoph Senff*, private communication]), indicative of surface CH<sub>2</sub>O precursor sources and the short lifetime of CH<sub>2</sub>O under summer conditions. The regional distribution of CH<sub>2</sub>O maximums observed below 1000 m flight altitude is shown in Figure 1, at a grid cell resolution of 0.2° latitude by 0.2° longitude (22 by 19 km respectively). Of primary interest to the present study are the high CH<sub>2</sub>O levels found in the greater Houston metropolitan area on many days. These large mixing ratios of between 10 and 32 ppbv were observed in plumes substantially smaller in spatial extent than the Houston metropolitan area. In contrast to Houston, Dallas-Ft. Worth had CH<sub>2</sub>O levels that were much lower (2 to 6 ppbv) and more spatially uniform. Measurements of the Dallas-Ft. Worth plume are compared with those from Houston, as the populations of the cities are

similar (Dallas-Ft. Worth: Dallas and Tarrant counties, 3.6 million people; Houston: Harris, Fort Bend, Brazoria, and Galveston counties, 4.2 million people) [U.S. Census, 2000]. The only power plant plumes with CH<sub>2</sub>O levels significantly above background were those from the Welsh and Monticello plants (up to 17 ppbv CH<sub>2</sub>O over a very limited area), which encountered strong biogenic isoprene emissions (see Figure 1).

#### **IV.2 Houston Area CH<sub>2</sub>O Precursor Distributions.**

To provide an assessment of the relative CH<sub>2</sub>O production expected from measured VOCs, the present analysis calculates the “CH<sub>2</sub>O production potential” of individual VOC samples [Lee, Y.-N. *et al.*, 1998]. For a given VOC mixture, the CH<sub>2</sub>O production potential is here expressed as  $\Sigma (k_x \text{OH} * [\text{VOC}_x] * (\gamma \text{CH}_2\text{O}_{(\text{VOC}_x)}))$ . Note that in this analysis the CH<sub>2</sub>O yield term ( $\gamma \text{CH}_2\text{O}$ ) reflects only the first generation products of OH-initiated VOC oxidation; production from moderately lived intermediates such as acetaldehyde (CH<sub>3</sub>CHO) is not considered. Molar CH<sub>2</sub>O yields used for the most abundant reactive CH<sub>2</sub>O precursors were: ethene (1.6) [Niki *et al.*, 1981], propene (1.0) [Niki *et al.*, 1978], and isoprene (0.6) [Carter and Atkinson, 1996]. For the alkanes yields of 0.1 to 0.3 were typically used (exceptions include methane (1) and isobutane (0.8)); the yields of alkynes and most aromatics were set to zero [Lee, Y.-N. *et al.*, 1998]. OH reaction rate constants were taken from Atkinson [1990; 1997] and DeMore *et al.* [1997].

CH<sub>2</sub>O production potentials were calculated for 390 VOC samples collected in canisters aboard the Electra at flight altitudes less than 1000 m during TexAQS, producing the Houston-Galveston area distribution depicted in Figure 4. A distinct maximum in CH<sub>2</sub>O production potential is clearly evident in the vicinity of the Houston Ship Channel. Of the VOC samples taken in this area, six yielded production potentials

between 13 and 63  $\text{s}^{-1}$ . Only two other samples acquired during TexAQS had  $\text{CH}_2\text{O}$  production potentials greater than 10  $\text{s}^{-1}$ . One of these samples was taken in a plume downwind of Texas City, an area of concentrated petrochemical industry south of Houston (see Figure 1). The other was measured in a plume intercepted over eastern Texas, from a petrochemical facility that reported the largest ethene emissions in Texas (Eastman Chemical) [TNRCC, 1999]. On average, the terminal alkenes, largely ethene and propene, composed 95% of total  $\text{CH}_2\text{O}$  production potential and 91% of total hydrocarbon OH reactivity in these eight highly polluted samples. Additional sources of substantial  $\text{CH}_2\text{O}$  production potential were the Sweeny, Freeport, and Chocolate Bayou petrochemical facilities south of Houston (2 to 9  $\text{s}^{-1}$ ); these three facilities will be collectively referred to as the “isolated petrochemical facilities.” The forested region northeast of Houston also featured somewhat elevated  $\text{CH}_2\text{O}$  production potentials (1 to 3  $\text{s}^{-1}$ ) due largely to isoprene. In all such cases, the bulk of the  $\text{CH}_2\text{O}$  precursors must have been emitted within about an hour prior to sampling, given the rapid mid-day summertime photochemistry.

The industrial origin of the eight highest  $\text{CH}_2\text{O}$  production potential samples ( $> 10 \text{ s}^{-1}$ ) was confirmed by ethene/ethyne and propene/ethyne ratios [Ryerson *et al.*, 2002]. Strong industrial signatures (ethene/ethyne  $\geq 3$  and/or propene/ethyne  $\geq 1$ ) were identified in 98 canister samples acquired over the greater Houston metropolitan area. These samples had a median ethene/ethyne ratio of 4.9, propene/ethyne ratio of 1.6,  $\text{CH}_2\text{O}$  production potential of 2.9  $\text{s}^{-1}$ , and OH hydrocarbon reactivity of 3.1  $\text{s}^{-1}$ . The  $\text{CH}_2\text{O}$  production potential of these 98 samples was due largely to the terminal alkenes (78%), with ethene contributing 30%, propene 22%, and isoprene 14% (1-butene,

isobutene, 1,3 butadiene, 3-methyl-1-butene, and 1-pentene also contributed to a lesser degree). Terminal alkenes were also responsible for a majority (71%) of the total OH hydrocarbon reactivity of these samples.

Seven VOC samples, acquired on five different days between 1130 and 1600 CST were selected as representative of Houston mobile source emissions based upon chemical ratios (ethene/ethyne < 1.7 and propene/ethyne < 0.5), CO mixing ratios (> 150 ppbv), CO<sub>2</sub> mixing ratios (< 375 ppmv), location over the Houston urban core, and wind direction. Median CH<sub>2</sub>O production potential (0.6 s<sup>-1</sup>) and OH hydrocarbon reactivity (0.7 s<sup>-1</sup>) for these samples were substantially lower than seen in the industrially influenced samples. All nine canister samples acquired over the Dallas-Ft. Worth metropolitan area yielded similar signatures, consistent with the lower, more spatially uniform CH<sub>2</sub>O levels measured throughout the Dallas-Ft. Worth plume (see Figure 1). These observations suggest that the CH<sub>2</sub>O species should represent an excellent proxy for the important reactive VOCs in the Houston atmosphere, the utility of which is explored in the remainder of this paper.

#### **IV.3 Houston Area Plumes.**

Measurements of CH<sub>2</sub>O in the Houston area are now examined for consistency with the precursor distributions discussed above. Complicating this however, lifetimes of ethene (3 to 8 hrs) and propene (1 to 2.5 hrs) are short (lifetime ranges calculated for OH =  $1 \times 10^7$  molec cm<sup>-3</sup>, O<sub>3</sub> = 120 ppbv, and OH =  $4.5 \times 10^6$  molec cm<sup>-3</sup>, O<sub>3</sub> = 60 ppbv, respectively) [Atkinson, 1997]. Therefore, regressions of CH<sub>2</sub>O versus CH<sub>2</sub>O production potentials did not yield strong correlations; this lack of correlation was accentuated by variable meteorology and limited VOC measurements.

Instead, levels of CH<sub>2</sub>O in Houston area plumes are compared for transects of roughly equivalent photochemical age. Plume sources were determined using tracers including SO<sub>2</sub>, CO, and CO<sub>2</sub> [Ryerson *et al.*, 2002; Brock *et al.*, 2002]. Based on these tracers, distinct power plant (W.A. Parish), mobile source (Houston urban), and petrochemical (Ship Channel) dominated plumes were identified in the August 28<sup>th</sup> 30.1° latitude east/west flight transect appearing in Figures 5 and 6. These plumes had passed over the core of the Houston metropolitan area 2.5 to 3 hrs (40 km) previously. Peak NO<sub>y</sub> levels in each of the three plumes were roughly comparable (9 to 14 ppbv), and consistent NO<sub>x</sub>/NO<sub>y</sub> ratios (0.21 to 0.27) indicated that the three plumes were well processed and of similar photochemical age. As shown in Figure 6, levels of CH<sub>2</sub>O in the petrochemically dominated plume were much higher (up to 13 ppbv) than those of the mobile source (up to 4.5 ppbv) and power plant plumes (up to 3 ppbv).

Within individual plumes transects, tight positive correlations were found between CH<sub>2</sub>O and directly emitted species (CO, CO<sub>2</sub> and NO<sub>y</sub>), as well as secondary photoproducts (ozone, HNO<sub>3</sub>, and acetaldehyde), as listed in Table 2 for two petrochemically dominated plumes. Figure 7 depicts such relationships graphically, showing CH<sub>2</sub>O and coincidentally measured NO<sub>y</sub> and ozone from a Ship Channel dominated plume transect. Associated correlation coefficient ( $r^2$ ) values were greater than 0.95 for the 20-km-wide plume cross section, indicating that the relationship of CH<sub>2</sub>O, NO<sub>y</sub>, and ozone was very uniform throughout the plume (see Table 2). Note that these good correlations are largely the result of mixing/dilution, as will be discussed below.

When comparing plumes of different sources, large differences were observed in such  $\text{CH}_2\text{O}$ /"tracer" relationships. This is clearly evident in the survey of petrochemical, mobile source (urban), and power plant plumes presented in Table 3.  $\text{CH}_2\text{O}/\text{NO}_y$  slopes for petrochemical plumes, including the Ship Channel plume (see Fig. 7b), were between 0.8 and 3.1. In contrast,  $\text{CH}_2\text{O}/\text{NO}_y$  slopes ranged from 0.2 to 0.4 for the Houston and Dallas-Ft. Worth plumes (mobile source dominated), and the W. A. Parish plume (power plant). Reported  $\text{CH}_2\text{O}$ /tracer slopes were determined from individual plume transects where  $\text{NO}_x/\text{NO}_y$  ratios were generally between 0.2 and 0.3. Some uncertainty in this comparison arises due to  $\text{HNO}_3$  loss [Trainer *et al.*, 2000], and the relatively short lifetime of  $\text{CH}_2\text{O}$  that will cause such ratios to change significantly with the photochemical age of the airmass (see Table 2). Nonetheless, the striking and consistent  $\text{CH}_2\text{O}/\text{NO}_y$  slope differences found between plumes of different source types on multiple days provides further evidence that petrochemical emissions are indeed the dominant source of extreme  $\text{CH}_2\text{O}$  concentrations in Houston.

The tightly positively correlated  $\text{CH}_2\text{O}/\text{O}_3$  slopes repeatedly measured in mobile source, power plant, and petrochemical plumes (see Tables 2 & 3 and Fig. 7c), suggest that oxidation of  $\text{CH}_2\text{O}$  precursors (including photolysis of  $\text{CH}_2\text{O}$  itself) played a major role in ozone production. This is consistent with the observation that  $\text{CH}_2\text{O}$  precursors were responsible for a substantial fraction of total OH hydrocarbon reactivity, especially in the most polluted VOC samples. As depicted in Figure 6,  $\text{CH}_2\text{O}$  and ozone levels observed the same basic trends in the August 28<sup>th</sup> Houston plumes. Measurements from September 1<sup>st</sup>, a highly polluted day (see Figs. 7a & c, 8a & b), also show  $\text{CH}_2\text{O}$  and ozone tracking one another. It should be noted that a spatial (temporal) offset was

observed between the CH<sub>2</sub>O and ozone gradients, as expected, due to the longer lifetime and slower relative net production rate of ozone. Throughout the TexAQS campaign, high CH<sub>2</sub>O levels, often 10 - 20+ ppbv above background, were always found coincident with exceedance levels of ozone (> 120 ppbv).

#### **IV.4 Isolated Petrochemical Facility Plumes.**

Using the model discussed above, we now analyze several petrochemical plumes to determine if measured ethene and propene emissions can account for the majority of observed CH<sub>2</sub>O and ozone, and if measurements are consistent with NO<sub>x</sub> and VOC inventories. For this exercise, plume measurements from the isolated petrochemical facilities, Freeport, Sweeny, and Chocolate Bayou are used [Ryerson, *et al.*, 2002; Brock *et al.*, 2002]. These facilities primarily conducted olefin-producing processes, and are analogous to many of the larger petrochemical facilities located along the Houston Ship Channel [C. Wiedinmyer and G. Frost, personal communication]. On the 27<sup>th</sup> and 28<sup>th</sup> of August, plumes from these facilities were superimposed on clean background air, the result of prevailing winds from the Gulf of Mexico (see Fig. 5). This kept the plumes largely unperturbed by other emission sources for several hours. Plume model results presented here are for the 28<sup>th</sup>, as intermittent CH<sub>2</sub>O instrument problems were encountered on the 27<sup>th</sup>. Sufficient CH<sub>2</sub>O data were collected on the 27<sup>th</sup> to demonstrate that the Freeport and Sweeny plumes exhibited consistent behavior on both days. Emission estimates inferred from aircraft observations are reported for Freeport and Sweeny, but not Chocolate Bayou, as VOC data were collected only on the very edge of the Chocolate Bayou plume. Measurements of acetaldehyde and CH<sub>2</sub>O were used to apportion emissions of ethene and propene, since propene oxidation produces

acetaldehyde while ethene oxidation does not [Niki *et al.*, 1978 & 1981; Grosjean *et al.*, 1996a & b; Calvert *et al.*, 2000; Bacher *et al.*, 2001].

Model NO<sub>x</sub> and VOC inputs were derived from observations made 1 to 2 hours downwind of the petrochemical complexes on both August 27<sup>th</sup> and 28<sup>th</sup>, between about 12:00 and 13:00 CST. It was assumed that by this time the boundary layer was well mixed vertically and the measurements at the flight altitude of 500 to 600 m were representative of the whole boundary layer (species ratios were constant). Uncertainty in estimated NO<sub>x</sub> emission rates for the isolated petrochemical facilities was largely due to model parameters such as wind speed ( $\pm 1 \text{ m s}^{-1}$ ), and boundary layer heights. Considering these uncertainties, the adopted and reported NO<sub>x</sub> emission rates for the isolated petrochemical complexes compared favorably (see Table 4). Previous plume studies provide precedent for this good agreement [Ryerson *et al.*, 1998].

Estimates of VOC emissions were derived using measured plume VOC/NO<sub>x</sub> ratios, with corrections applied for VOC and NO<sub>x</sub> losses occurring between the point of emission and measurement. For the Freeport plume, six separate VOC measurements were made at a variety of downwind distances. One VOC sample apiece was collected from the Sweeny and Chocolate Bayou plumes. Due to the dominance of ethene and propene in these samples, the model assumed that VOC emissions for each facility were composed exclusively of these two terminal alkenes. Isoprene was also measured in all plumes, the majority of which was attributed to biogenic emissions from the discontinuous forests of the region, based upon VOC samples taken outside of the plumes and biogenic inventories [Wiedinmyer *et al.*, 2001]. A background isoprene flux

common to all of the plumes was therefore included in the model ( $5.2 \times 10^{15}$  molec  $\text{m}^{-2} \text{s}^{-1}$ ).

Using these observationally derived  $\text{NO}_x$  and VOC emission values, the model accurately replicated measured ethene, propene,  $\text{CH}_2\text{O}$ , acetaldehyde,  $(\text{NO}_y - \text{NO}_x)$ ,  $(\text{NO}_y - (\text{NO}_x + \text{HNO}_3))$ , and ozone concentrations. As noted above, observationally derived  $\text{NO}_x$  values were effectively equivalent to inventory values. Figure 9 provides an overview of results for the  $29.3^\circ$  latitude intercept of the Sweeny and Freeport plumes. Not only did the model successfully simulate the rapid  $\text{CH}_2\text{O}$  enhancement in the plume, it also accurately captured the  $\text{CH}_2\text{O}$  background due to the area-wide isoprene emissions (see Fig. 9b). Ethene and propene emission apportionment was corroborated by agreement with both  $\text{CH}_2\text{O}$  and acetaldehyde (Fig. 9b & c). It is important to note that in all cases the model needed only standard OH-initiated VOC oxidation to achieve good agreement with observations. The observed “shoulder” feature seen on the east side of the Freeport plume, particularly apparent in the ozone measurement (Fig. 9d), was due to incursion of the Freeport A complex plume into the Freeport B complex plume. The model only attempted to replicate the larger Freeport B plume (see Fig. 5).

The Freeport and Sweeny plumes were also modeled using  $\text{NO}_x$  and VOC emissions taken directly from TNRCC inventories, along with the measurement-inferred biogenic isoprene background. Note that the only real difference between this and the previously discussed model case was the magnitude of the industrial VOC inputs (see Table 4). When using such inputs, less than 10% of the measured  $\text{CH}_2\text{O}$ , and 40% of the measured ozone enhancement over background levels were predicted (see Figs. 9b and 9d, dotted grey lines). In this case, modeled  $\text{CH}_2\text{O}$  and ozone production was largely due

to the presence of the isoprene background, with TNRCC inventory VOCs contributing minimally. On a related note, inclusion of a large measured isobutane emission to the Chocolate Bayou model case (not depicted) produced very little additional CH<sub>2</sub>O and ozone, due to the much lower reactivity of alkanes.

One potential weakness of the above analysis was its reliance on just a handful of canister measurements to characterize the VOC emissions of the isolated petrochemical facilities. However, since CH<sub>2</sub>O is efficiently produced by the dominant reactive VOCs in these plumes, it represents a good surrogate for plume VOCs. The very robust positive CH<sub>2</sub>O/tracer correlations measured in the plumes (see Tables 2 & 3) show that facility emissions were sufficiently collocated, and atmospheric mixing adequately strong, as to rapidly (0.5 - 1 hr) produce plumes of constant species ratios, despite the fact that the facilities were not perfect point sources. The strong boundary layer mixing necessary to create this measured horizontal uniformity would also be expected to produce vertically homogeneous species ratios as well. Therefore, plume VOC/NO<sub>x</sub> ratios measured at flight altitudes of 500 to 600 m by the Electra should be representative of the entire boundary layer vertical profile, except for very fresh plumes (< 0.5 hr under moderate winds) and perhaps for plumes affected by special meteorological conditions such as coastal effects. Support for this conclusion is provided by airborne LIDAR ozone measurements made during TexAQS that showed strong vertical mixing [Senff, private communication], as well as limited in situ measurement profiles made by the Electra.

Measurement derived VOC emissions for the Freeport and Sweeny plumes used in this model exercise were estimated to be accurate within at least a factor of two. This was based upon the high degree of agreement achieved between predicted and measured

secondary photoproducts, particularly CH<sub>2</sub>O and acetaldehyde, and the plume uniformity demonstrated by CH<sub>2</sub>O/tracer relationships. Also accounted for were the uncertainties associated with NO<sub>x</sub> emissions, wind speeds (plume ages), and boundary layer heights. Consistent CH<sub>2</sub>O/tracer slopes were found on each day the Freeport (3 days) and Sweeny plumes (2 days) were intercepted, as listed in Table 2 for intercepts of comparable photochemical ages (NO<sub>x</sub>/NO<sub>y</sub> ratios), suggesting that the VOC emissions deduced here were the consequences of standard operations rather than unreported unusual emission events (“upsets”). As seen in Table 4, derived ethene and propene emissions for the Freeport and Sweeny facilities are 50 - 100 times larger than reported (1999 TNRCC VOC inventory), and in sum about 20 times larger than total reported VOC emissions. Analysis of the Chocolate Bayou plume produced similar disparities.

#### **IV.5 Primary CH<sub>2</sub>O Emissions.**

The isolated petrochemical facility plumes were also used to assess the importance of primary petrochemical CH<sub>2</sub>O emissions. If primary emissions were large, they would need to be considered in assessments of emissions and photochemistry made using CH<sub>2</sub>O data. Only small enhancements of CH<sub>2</sub>O were found in close proximity intercepts of the isolated petrochemical facility plumes however, providing an upper limit on direct emissions. In the Freeport plume, CH<sub>2</sub>O levels were 1 - 2 ppbv above background about 20 min downwind (8 km), on both the 27<sup>th</sup> and 28<sup>th</sup> of August (see the 29.1° lat pass in Fig. 5). A similar enhancement was also measured 30 min (7 km) downwind of the Chocolate Bayou facility on the 27<sup>th</sup>. In all cases, plume CH<sub>2</sub>O levels dramatically increased downwind of these initial intercepts despite dilution, consistent with rapid photochemical production of CH<sub>2</sub>O from emitted VOCs, rather than primary

emission. In addition, the model achieved good agreement with observations invoking only photochemistry. The dominance of in situ CH<sub>2</sub>O production was also supported by extensive, continuous PTRMS measurements of propene, acetaldehyde, and CH<sub>2</sub>O made at the La Porte ground site near the Ship Channel [Karl *et al.*, 2002]. Direct CH<sub>2</sub>O emissions from mobile sources are not expected to contribute importantly to peak daytime Houston CH<sub>2</sub>O abundances either, based upon work by Zweidinger *et al.* [1988], Altshuller [1993], and others, and the much lower measured CH<sub>2</sub>O levels in the Houston and Dallas-Ft. Worth mobile source plumes.

#### **IV.6 Photochemistry of a Highly Polluted Plume.**

Ozone exceedance events measured over Houston by the Electra typically involved ozone enhancements of 60 – 150+ ppbv above background. In comparison, ozone enhancements associated with the isolated petrochemical facility plumes did not exceed 30 ppbv above background. Therefore to test the premise that petrochemical ethene and propene emissions are central to Houston's most extreme ozone pollution, the September 1<sup>st</sup> Houston plume (see Figures 7, 8; Table 2) was modeled using an approach similar to that employed with the isolated petrochemical plumes. This plume was dominated by Ship Channel emissions and had maximum observed ozone levels of 245 ppbv, and CH<sub>2</sub>O levels of 32 ppbv.

Emission estimates for the September 1<sup>st</sup> plume were complicated by the diversity and size of the petrochemical source area, and the mobile source emission background, which although of secondary importance was still substantial. Based on a survey of VOC/NO<sub>x</sub> measurements made in the plume, corrected for differential losses, an equal molar emission rate for NO<sub>x</sub>, ethene, and propene (252 kmol hr<sup>-1</sup> each) was estimated.

NMHCs other than ethene and propene contributed only weakly to total hydrocarbon OH reactivity measured in the plume and were left out. The point of this modeling exercise was to assess whether the oxidation of observed ethene and propene could alone account for the general rate and magnitude of extreme CH<sub>2</sub>O and ozone production, rather than to provide a detailed check of emission inventories. Use of these simplified inputs yielded good measurement-model agreement. Figure 10 depicts results for the 94.6° longitude, 4 hr (50 km) downwind intercept (see Table 2), featuring CH<sub>2</sub>O concentrations of 3 to 27 ppbv, and ozone of 50 to 200 ppbv; NO<sub>y</sub> partitioning (not shown) was also accurately replicated.

## **V. Summary and Conclusions.**

TDLAS CH<sub>2</sub>O measurements made during TexAQS 2000 yielded several important insights concerning terminal alkene emissions and photochemistry in Houston. These insights were amplified by the high resolution (1 and 10 s) of the measurements, the first time such resolution has been achieved in the field for CH<sub>2</sub>O.

Results reported here indicate that measured petrochemical ethene and propene levels were alone sufficient to explain the highest CH<sub>2</sub>O and ozone levels measured in several Houston area plumes, including levels over 30 and 200 ppbv, respectively. No evidence was found for strong direct emissions of CH<sub>2</sub>O. While enhanced concentrations of VOCs other than ethene and propene were measured in Houston, their lower reactivities rendered them far less important to rapid ozone formation. In addition, the successful modeling indicates that OH-initiated terminal alkene oxidation is the dominant source of ozone in Houston, and that other oxidants such as Cl radicals (and thereby alkanes) play a comparatively modest role, consistent with studies by *Tanaka* [2002].

Modeling of the isolated petrochemical facilities using measurement derived VOC emissions confirms that ethene and propene emissions are far larger than inventories indicate. Given that these facilities are expected to be representative of the Houston petrochemical industry, and that similar disparities exist between inventory and measured VOC/NO<sub>x</sub> ratios for the Ship Channel, it is highly likely that VOC emission inventory deficits are widespread in Houston. Accurate emission inventories will be critical to the success of three-dimensional modeling efforts and the development of efficient ozone control strategies for Houston.

**Acknowledgements.** The TexAQS 2000 mission would not have been possible without the able and diligent efforts of the Southern Oxidants Study (SOS) and Texas National Resource Conservation Commission (TNRCC). We are also very grateful to the National Center for Atmospheric Research (NCAR) Research Aviation Facility (RAF) for providing the Electra aircraft on short notice. NCAR is sponsored by the University Corporation for Atmospheric Research (UCAR). In addition to the National Science Foundation (NSF) Global Troposphere Chemistry Program (GTCP) funds that have supported the long-term development of the NCAR TDLAS system, the work described here was funded in part by grants from the National Oceanic and Atmospheric Administration (NOAA) Climate and Global Change Program, and from the SOS program of the US Environmental Protection Agency (EPA). Coauthors Armin Hansel and Armin Wisthaler were supported by NOAA grant NA06GP0483.

**References.**

- Anderson, L.G., J.A. Lanning, R. Barrell, J. Miyagishima, R.H. Jones, and P. Wolfe, Sources and sinks of formaldehyde and acetaldehyde: an analysis of Denver's ambient concentration data, *Atmos. Env.*, 30, 2113-2123, 1996.
- Altshuller, A.P., Production of aldehydes as primary emissions and from secondary atmospheric reactions of alkenes and alkanes during the night and early morning hours, *Atmos. Envir.*, 27A, 21-32, 1993.
- Atkinson, R., Gas-phase tropospheric chemistry of organic compounds: a review, *Atmos. Env.*, 24A, 1-41, 1990.
- Atkinson, R., Gas-phase tropospheric chemistry of volatile organic compounds: 1. Alkanes and alkenes, *J. Phys. Ref. Chem. Ref. Data*, 26, 215-290, 1997.
- Bacher, C., G. S. Tyndall, and J.J. Orlando, The atmospheric chemistry of glycolaldehyde, *J. Atmos. Chem.*, 39, 171-189, 2001.
- Brock, C.A., F. Schroder, B. Karcher, A. Petzold, R. Busen, M. Fiebig, Ultrafine particle size distributions measured in aircraft exhaust plumes, *J. Geophys. Res.*, 105, 26555-26568, 2000.

Brock, C.A., M. Trainer, T.B. Ryerson, A.J. Neuman, D.D. Parrish, J.S. Holloway, D.K.J. Nicks, G.J. Frost, G. Hübler, and F.C. Fehsenfeld, Particle growth in urban and industrial plumes in Texas, *J. Geophys. Res.* (submitted), 2002.

Calvert, J. G., R. Atkinson, J.A. Kerr, S. Madronich, G.K. Moortgat, T.J. Wallington, and G. Yarwood, *The Mechanisms of Atmospheric Oxidation of the Alkenes*, Oxford University Press, New York, 2000.

Carter, W.P.L. and R. Atkinson, Development and evaluation of a detailed mechanism for the atmospheric reactions of isoprene and NO<sub>x</sub>, *Int. J. Chem. Kinet.*, 28, 497-530, 1996.

Chameides, W.L., F. Fehsenfeld, M.O. Rodgers, C. Cardelino, J. Martinez, D. Parrish, W. Lonneman, D.R. Lawson, R.A. Rasmussen, P. Zimmerman, J. Greenberg, P. Middleton, and T. Wang, Ozone precursor relationships in the ambient atmosphere, *J. Geophys. Res.*, 97, 6037-6055, 1992.

Chance, K. P. I. Palmer, R.J.D. Spurr, R.V. Martin, T.P. Kurosu, and D.J. Jacob, Satellite observations of formaldehyde over North America from GOME, *Geophys. Res. Lett.*, 27, 3461-3464, 2000.

Dahlback, A., and K. Stamnes, A new spherical model for computing the radiation field available for photolysis and heating at twilight, *Planet. Space Sci.*, 39, 671-683, 1991.

DeMore, W.B., S.P. Sander, D.M. Golden, R.F. Hampson, M.J. Kurylo, C.J. Howard, A.R. Ravishankara, C.E. Kolb, and M.J. Molina, Chemical kinetics and photochemical data for use in stratospheric modeling, JPL Publ.;97-4, 1997.

Dodge, M., Formaldehyde production in photochemical smog as predicted by three state-of-the-science chemical oxidant mechanisms. *J. Geophys. Res.*, 95, 3635- 3648, 1990.

Flocke, F. et al., The behavior of PANs and the budget of total reactive nitrogen (NO<sub>y</sub>) during the TOPSE campaign, in preparation, 2002.

Fried, A., S. McKeen, S. Sewell, J. Harder, B. Henry, P. Goldan, B. Kuster, E. Williams, K. Baumann, R. Shetter, and C. Cantrell, Photochemistry of formaldehyde during the 1993 Tropospheric OH Photochemistry Experiment, *J. Geophys. Res.*, 102, 6283 - 6296, 1997.

Fried, A., B. Henry, B. Wert, S. Sewell, and J.R. Drummond, Laboratory, ground-based, and airborne tunable diode laser systems: performance characteristics and applications in atmospheric studies, *Appl. Phys. B.*, 67, 317 – 330, 1998.

Fried, A., Y.-N. Lee, G. Frost, B. Wert, B. Henry, G. Hübler, and T. Jobson, Airborne CH<sub>2</sub>O measurements over the North Atlantic during the 1997 NARE campaign:

instrument comparisons and distributions, *J. Geophys. Res.*, *107*, 10.1029/2000JD000260, 2002a.

Geron, C.D., A.B. Guenther, and T.E. Pierce, An improved model for estimating emissions of volatile organic compounds from forests in the eastern United States, *J. Geophys. Res.*, *99*, 12773-12791, 1994.

Gilpin, T., E. Apel, A. Fried, B. Wert, J. Calvert, Z. Genfa, P. Dasgupta, J.W. Harder, B. Heikes, B. Hopkins, H. Westberg, T. Kleindienst, Y.-N. Lee, X. Zhou, W. Lonneman, and S. Sewell, Intercomparison of six ambient [CH<sub>2</sub>O] measurement techniques, *J. Geophys. Res.*, *102*, 21161-21188, 1997.

Goldan, P.D., D.D. Parrish, W.C. Kuster, M. Trainer, S.A. McKeen, J. Holloway, B.T. Jobson, D.T. Sueper, and F.C. Fehsenfeld, Airborne measurements of isoprene, CO, and anthropogenic hydrocarbons and their implications, *J. Geophys. Res.*, *105*, 9091-9105, 2000.

Grosjean, D., Ambient levels of formaldehyde, acetaldehyde, and formic acid in southern California: results of a one-year base-line study, *Environ. Sci. Technol.*, *4*, 710-715, 1991.

Grosjean, E., J. B. De Andarde, and D. Grosjean. Carbonyl products of the gas-phase reaction of ozone with simple alkenes, *Environ. Sci. Technol.*, *30*, 975-983, 1996a.

Grosjean, E., and D. Grosjean. Carbonyl products of the gas-phase reaction of ozone with symmetrical alkenes, *Environ. Sci. Technol.*, *30*, 2036-2044, 1996b.

Haagen-Smit, A.J., Chemistry and physiology of Los Angeles smog, *Ind. Eng. Chem.*, *44*, 1342-1346, 1952.

Harder, J.W., A. Fried, S. Sewell, and B. Henry, Comparison of tunable diode laser and long-path ultraviolet/visible spectroscopic measurements of ambient formaldehyde concentrations during the 1993 OH Photochemistry Experiment, *J. Geophys. Res.*, *102*, 6267-6282, 1997.

Holloway, J.S., R. O. Jakoubek, D.D. Parrish, C. Gerbig, A. Volz-Thomas; S. Schmitgen, A. Fried, B. Wert, B. Henry and J.R. Drummond, Airborne intercomparison of vacuum ultraviolet fluorescence and tunable diode laser absorption measurements of tropospheric carbon monoxide, *J. Geophys. Res.*, *105*, 24251-24262, 2000.

Hov, O. And I.S.A. Isaksen, Generation of secondary pollutants in a power plant plume: A model study, *Atmos. Environ.*, *15*, 2367-2376, 1981.

Huey, G.L., E.J. Dunlea, E.R. Lovejoy, D.R. Hanson, R.B. Norton, F.C. Fehsenfeld, and C.J. Howard, Fast time response measurements of HNO<sub>3</sub> in air with a chemical ionization mass spectrometer, *J. Geophys. Res.*, *103*, 3355-3360, 1998.

Karl, T., et al., The use of Proton-Transfer Mass Spectrometry to characterize VOC sources at the La Porte super site during the Texas Air Quality Study 2000, (in preparation), 2002.

Kleinman, L.I., P.H. Daum, D. Imre, Y.-N. Lee, L.J. Nunnemacker, S.R. Springston, J. Weinstein-Lloyd, and J. Rudolph, Ozone production rate and hydrocarbon reactivity in 5 urban areas: a cause of high ozone concentration in Houston, *Geophys. Res. Lett.*, 29, 10.1029/2002GL014569, 2002.

Lee, M., B.G. Heikes, D.J. Jacob, G. Sachse, and B. Anderson, Hydrogen peroxide, organic hydroperoxide, and formaldehyde as primary pollutants from biomass burning, *J. Geophys. Res.*, 102, 1301-1309, 1998.

Lee, Y.-N., X. Zhou, L.I. Kleinman, L.J. Nunnemacker, S.R. Springston, P.H. Daum, L. Newman, W.G. Keigley, M.W. Holdren, C.W. Spicer, V. Young, B. Fu, D.D. Parrish, J. Holloway, J. Williams, J.M. Roberts, T.B. Ryerson, and F.C. Fehsenfeld, Atmospheric chemistry and distribution of formaldehyde and several multioxygenated carbonyl compounds during the 1995 Nashville/Middle Tennessee Ozone Study, *J. Geophys. Res.*, 103, 22449-22462, 1998.

Li, S.-M., K.G. Anlauf, H. A. Wiebe, and J.W. Bottenheim, Estimating primary and secondary production of HCHO in eastern North America based on gas phase

measurements and principal component analysis, *J. Geophys. Res.*, *21*, 669-672, 1994.

Lin, C.-Y.C., D.J. Jacob, and A.M. Fiore, Trends in exceedances of the ozone air quality standard in the continental United States, 1980-1998, *Atmos. Env.*, *35*, 3217-3228, 2001.

Lindinger, W., A. Hansel, and A. Jordan, Proton-transfer-reaction mass spectrometry (PTR-MS): on-line monitoring of volatile organic compounds at pptv levels, *Chemical Society Reviews*, *27*, 347-354, 1998.

Madronich, S., Photodissociation in the atmosphere, 1, Actinic flux and the effects of ground reflections and clouds, *J. Geophys. Res.*, *92*, 9740-9752, 1987.

Neuman, A.J., L.G. Huey, R.W. Dissly, F.C. Fehsenfeld, F. Flocke, J.C. Holocek, J.S. Holloway, G. Hübler, R.O. Jakoubek, D.K.J. Nicks, D.D. Parrish, T.B. Ryerson, D.T. Sueper, and A.J. Weinheimer, Fast-response airborne in situ measurements of HNO<sub>3</sub> during the Texas 2000 Air Quality Study, *J. Geophys. Res.* (in press), 2002.

Nicks, D.K., J.S. Holloway, T.B. Ryerson, R.W. Dissly, D.D. Parrish, G.J. Frost, M. Trainer, S.G. Donnelly, S.Schauffler, E.L. Atlas, G. Hubler, D.T. Sueper, and F.C. Fehsenfeld, Fossil-fueled power plants as a source of atmospheric carbon monoxide, *Atmos. Env.* (submitted), 2002.

Niki, H., P.D. Maker, C.M. Savage, and L.P. Breitenbach, Mechanism for hydroxyl radical initiated oxidation of olefin-nitric oxide mixtures in parts per million concentrations, *J. Phys. Chem.*, *82*, 135-137, 1978.

Niki, H., P.D. Maker, C.M. Savage, and L.P. Breitenbach, An FTIR study of mechanisms for the HO radical initiated oxidation of C<sub>2</sub>H<sub>4</sub> in the presence of NO: detection of glycolaldehyde, *Chem. Phys. Lett.*, *80*, 499-503, 1981.

Palmer, P.I., D.J. Jacob, K. Chance, R.V. Martin, R.J.D. Spurr, T.P. Kurosu, I. Bey, R. Yantosca, A. Fiore, and Q. Lin, Air mass factor formulation for spectroscopic measurements from satellites: application to formaldehyde retrievals from the Global Ozone Monitoring Experiment, *J. Geophys. Res.*, *106*, 14539-14550, 2001.

Richter, D., Portable mid-infrared gas sensors: development and applications, Ph.D. Thesis, Rice University, 2001.

Ryerson, T.B., M.P. Buhr, G.J. Frost, P.D. Goldan, J.S. Holloway, G. Hubler, B.T. Jobson, W.C. Kuster, S.A. McKeen, D.D. W. A. Parish, J.M. Roberts, D.T. Sueper, M. Trainer, J. Williams, and F.C. Fehsenfeld, Emission lifetimes and ozone formation in power plant plumes, *J. Geophys. Res.*, *103*, 22555-22568, 1998.

Ryerson, T.B., E.J. Williams, and F.C. Fehsenfeld, An efficient photolysis system for fast-response NO<sub>2</sub> measurements, *J. Geophys. Res.*, *105*, 26447-26461, 2000.

Ryerson, T.B., M. Trainer, J.S. Holloway, D.D. Parrish, L.G. Huey, D.T. Sueper, G.J. Frost, S.G. Donnelly, S. Schauffler, E. Atlas, W.C. Kuster, P.D. Goldan, G. Hübler, J.F. Meagher, F.C. Fehsenfeld, Observations of ozone formation in power plant plumes and implications for ozone control strategies, *Science*, 292, 719-723, 2001.

Ryerson, T.B., M. Trainer, D.K. Nicks Jr., A.J. Neuman, R.W. Dissly, J.S. Holloway, D.D. Parrish, D.T. Sueper, W.C. Kuster, P.D. Goldan, G. Hübler, W.M. Angevine, F.C. Fehsenfeld, S.G. Donnelly, S. Schauffler, E. Atlas, A.J. Weinheimer, F. Flocke, B.P. Wert, A. Fried, C.J. Senff, Effect of co-located petrochemical industrial emissions of reactive alkenes and NO<sub>x</sub> on tropospheric ozone formation, *J. Geophys. Res.* (to be submitted), 2002.

Schauffler, S. M., E.L. Atlas, and W. Travnicek, Distributions of brominated organic compounds in the troposphere and lower stratosphere, *J. Geophys. Res.*, 104, 21513-21535, 1999.

Seinfeld, J.H., Urban air pollution: state of science, *Science*, 243, 745-752, 1989.

Sigsby, J.E., S. Tejada, W. Ray, J.M. Lang, and J.W. Duncan, Volatile organic compound emissions from 46 in-use passenger cars, *Environ. Sci. Technol.*, 21, 466-475, 1987.

Sillman, S., The relation between ozone, NO<sub>x</sub> and hydrocarbons in urban and polluted rural environments, *Atmos. Env.*, *33*, 1821-1845, 1999.

Sillman, S., Ozone production potential and loss of NO<sub>x</sub> in power plant plumes: Photochemical model and interpretation of measurements in Tennessee, *J. Geophys. Res.*, *105*, 9189-9202, 2000.

Stutz, J. and U. Platt, Improving long-path differential optical absorption spectroscopy with a quartz-fiber mode mixer, *Applied Optics*, *36*, 1105-15, 1997.

Tanaka, P.L., et al., Direct evidence for chlorine-enhanced urban ozone formation in Houston, TX, *Env. Sci. Technol.* (submitted), 2002.

TNRCC, Sources of Air Pollution, <http://www.tnrcc.state.tx.us/air/aqp/pollsource.html>, 1996.

TNRCC, Point Source Database, 1999.

Trainer, M., E.Y. Hsie, S.A. McKeen, R. Tallamraju, D.D. Parrish, F.C. Fehsenfeld, and S.C. Liu, Impact of natural hydrocarbons on hydroxyl and peroxy radicals at a remote site, *J. Geophys. Res.*, *92*, 11879-11894, 1987.

Trainer, M., M.P. Buhr, C.M. Curran, F.C. Fehsenfeld, E.Y. Hsie, S.C. Liu, R.B. Norton, D.D. Parrish, E.J. Williams, B.W. Gandrud, B.A. Ridley, J.D. Shetter, E.J. Allwine, and H.H. Westberg, Observations and modeling of the reactive nitrogen photochemistry at a rural site, *J. Geophys. Res.*, *96*, 3045-3063, 1991.

Trainer, M., D.D. Parrish, P.D. Goldan, J. Roberts, and F.C. Fehsenfeld, Review of observation-based analysis of the regional factors influencing ozone concentrations, *Atmos. Env.*, *34*, 2045-2061, 2000.

U.S. Census Bureau, United States Census 2000, [www.census.gov](http://www.census.gov), 2000.

Wiedinmyer, C., A. Guenther, M. Estes, I.W. Strange, G. Yarwood, and D.T. Allen, A land use database and examples of biogenic isoprene emission estimates for the state of Texas, USA, *Atmos. Env.*, *35*, 6465-6477, 2001.

Wert, B.P., A. Fried, S. Rauenbuehler, and J. Walega, Design and performance of a tunable diode laser absorption spectrometer for airborne formaldehyde measurements, *J. Geophys. Res.* (submitted), 2002a.

Wert, B.P., A. Fried, B. Henry, and S. Cartier, Evaluation of inlets used for the airborne measurement of formaldehyde, *J. Geophys. Res.*, *107*, 10.1029/2001JD001072, 2002b.

Yokelson, R.J., J.G. Goode, and W.M. Hao, Emissions of formaldehyde, acetic acid, methanol, and other trace gases from biomass fires in North Carolina measured by airborne Fourier transform infrared spectroscopy, *J. Geophys. Res.*, *104*, 30109-30125, 1999.

Zweidinger, R.B., J.E. Sigsby, S.B. Tejada, F.D. Stump, D.L. Dropkin, W.D. Ray, and J.W. Duncan, Detailed hydrocarbon and aldehyde mobile source emissions from roadway studies, *Environ. Sci. Technol.*, *22*, 956-962, 1988.

Figure Captions:

Fig. 1: Regional distribution of CH<sub>2</sub>O maximums measured below 1000 m flight altitude, for 0.2° latitude by 0.2° longitude grid cells. The solid circles show the location of NO<sub>x</sub> emitters and are sized according to reported NO<sub>x</sub> emissions. Labels are provided for cities (Houston and Dallas-Ft. Worth), utility power plants (W.A. Parish, Monticello, and Welsh), isolated petrochemical facilities (Sweeny, Freeport, and Chocolate Bayou), and areas of concentrated petrochemical production (Ship Channel and Texas City) discussed in the text.

Fig. 2: Bivariate regression of CH<sub>2</sub>O measurements made by the NCAR TDLAS on the Electra aircraft and the UCLA DOAS at the La Porte site during close overflights.

Fig. 3: The vertical distribution of CH<sub>2</sub>O measurements made during TexAQS 2000. Median CH<sub>2</sub>O values for 1000 m flight altitude bins are denoted by the solid circle symbols.

Fig. 4: Measured Houston-Galveston VOC distribution, coded by size for CH<sub>2</sub>O production potential, and by color for the percentage of terminal alkene contribution to total OH hydrocarbon reactivity.

Fig. 5: Measurements of CH<sub>2</sub>O in the Houston area on August 28<sup>th</sup> below 1000 m flight altitude. The solid circles show the location of NO<sub>x</sub> emitters, and are sized according to

reported  $\text{NO}_x$  emissions. General wind direction is shown by the arrow in the bottom left corner.

Fig. 6: Mixing ratios of  $\text{CH}_2\text{O}$  and other species in a cross section of the Houston plume acquired at  $30.1^\circ$  latitude on August 28th, showing distinct power plant (W. A. Parish), mobile source (Houston urban) and petrochemical (Ship Channel) dominated plumes.

Fig. 7: Measurements of  $\text{CH}_2\text{O}$ ,  $\text{NO}_y$ , and ozone in a cross section of the September 1<sup>st</sup> Ship Channel dominated plume, 2 hours downwind of the Ship Channel [a]. Regressions of  $\text{CH}_2\text{O}$  vs.  $\text{NO}_y$  [b] and ozone [c] (see Table 2 for slopes and correlation coefficients).

Fig. 8a & b. Measured  $\text{CH}_2\text{O}$  [a] and ozone [b] mixing ratios in the Houston-Galveston area on Sept 1<sup>st</sup> at flight altitudes less than 1000 m. General wind direction is shown by the arrow in the upper left corner of [a].

Fig. 9: Measurements and corresponding model results for the  $29.3^\circ$  latitude intercept of the Sweeny and Freeport plumes (2.3 hrs downwind of Freeport). Shown are ethene and propene [a],  $\text{CH}_2\text{O}$  [b], acetaldehyde [c], and ozone [d] mixing ratios.

Fig. 10: Measured and modeled  $\text{CH}_2\text{O}$  versus ozone, for the September 1st intercept of the Ship Channel dominated plume at  $-94.6$  longitude (4 hrs downwind of the Ship Channel).

Table 1: VOCs measured by the NCAR Whole Air Sampler (WAS).

<b>Alkanes</b>		<b>Alkenes</b>	<b>Aromatics</b>
methane	n-octane	ethene	benzene
ethane	n-nonane	propene	toluene
propane	n-decane	1-butene	ethyl benzene
isobutene	cyclopentane	isobutene	m & p-xylene
n-butane	cyclohexane	t-2-butene	o-xylene
isopentane	dimethyl cyclopentane	c-2-butene	styrene
n-pentane	dimethyl cyclohexane	1,3-butadiene	isopropyl benzene
n-hexane		3-methyl-1-butene	n-propyl benzene
2,2-dimethyl butane		1-pentene	1,2,3-trimethyl benzene
2,3-dimethyl butane		isoprene	1,2,4-trimethyl benzene
3-methyl pentane		t-2-pentene	1,3,5-trimethyl benzene
2-methyl hexane		c-2-pentene	
3-methyl hexane		2-methyl-2-butene	<b>Alkynes</b>
2,2,4-trimethyl pentane		cyclopentene	ethyne
n-heptane		$\alpha$ -pinene	

Table 2: Slopes of CH<sub>2</sub>O versus several other species measured in the September 1<sup>st</sup> Ship Channel dominated plume, and the August 28<sup>th</sup> Freeport plume.

Dist (km)	Age (hrs)	NO <sub>x</sub> /NO <sub>y</sub>	CH <sub>2</sub> O/NO <sub>y</sub>	r <sup>2</sup>	CH <sub>2</sub> O/CO	r <sup>2</sup>	CH <sub>2</sub> O/O <sub>3</sub>	r <sup>2</sup>	CH <sub>2</sub> O/HNO <sub>3</sub>	r <sup>2</sup>
<b>Sept 1<sup>st</sup> Ship Channel Dominated Plume</b>										
10	0.8	0.69	0.47	0.73	0.21	0.89	0.68	0.87	7.7	0.87
25	2	0.49	0.79	0.99	0.18	0.95	0.41	0.96	5.0	0.94
50	4	0.29	0.73	0.84	0.13	0.92	0.16	0.86	2.5	0.80
75	6	0.24	0.87	0.98	0.09	0.97	0.15	0.98	2.8	0.96
100	8	0.22	0.74	0.89	0.05	0.91	0.12	0.86	1.9	0.77
<b>Aug 28<sup>th</sup> Freeport Plume</b>										
8	0.6	0.77	0.14	0.90	0.07	0.50	na	na	na	na
33	2.3	0.36	1.35	0.95	0.31	0.94	0.25	0.99	3.7	0.92
60	4.2	0.29	0.87	0.93	0.10	0.84	0.15	0.95	2.2	0.85

Table 3: Slopes of CH<sub>2</sub>O versus NO<sub>y</sub> and ozone measured in plumes of petrochemical, mobile source (urban), and power plant origin.

Plume Source	Date	NO <sub>x</sub> /NO <sub>y</sub>	CH <sub>2</sub> O/NO <sub>y</sub>	r <sup>2</sup>	CH <sub>2</sub> O/O <sub>3</sub>	r <sup>2</sup>
<b>Petrochemical</b>						
Freeport	27-Aug	0.37	0.85	0.93	0.19	0.97
Freeport	28-Aug	0.36	1.35	0.95	0.25	0.99
Freeport	6-Sep	0.31	1.30	0.78	0.18	0.84
Sweeny	27-Aug	0.27	1.85	0.92	0.11	0.85
Sweeny	28-Aug	0.32	1.66	0.99	0.12	0.97
Choc. Bayou	28-Aug	0.29	3.13	0.98	0.33	0.99
Ship Channel	27-Aug	0.24	1.28	0.96	0.15	0.91
Ship Channel	28-Aug	0.29	0.92	0.82	0.13	0.88
Ship Channel	1-Sep	0.24	0.87	0.98	0.15	0.98
<b>Mobile Source (urban)</b>						
Houston	28-Aug	0.21	0.36	0.81	0.11	0.53
Dallas-Ft. Worth	7-Sep	0.28	0.25	0.86	0.095	0.80
<b>Power Plant</b>						
W.A.Parish	28-Aug	0.21	0.24	0.83	0.08	0.94

Table 4: Measurement derived inputs used for modeling the Freeport and Sweeny plumes (August 28<sup>th</sup>), along with corresponding inventory values. Note: Inventory numbers from the 1999 and 2000 TNRCC Point Source Database; Freeport B = 6 sources;  $28.94^{\circ} \leq \text{lat} \leq 29.02$ ,  $-95.44^{\circ} \leq \text{lon} \leq -95.36^{\circ}$ ; Sweeny = 5 sources;  $29.04^{\circ} \leq \text{lat} \leq 29.10^{\circ}$ ,  $-95.80^{\circ} \leq \text{lon} \leq -95.7^{\circ}$

Petrochemical Facility	Measurement Derived (kmol/hr)			Inventory (kmol/hr)			
	NO <sub>x</sub>	Ethene	Propene	NO <sub>x</sub>	Ethene	Propene	Total VOCs
	Freeport B	30	45	15	31	0.9	0.3
Sweeny	15	54	30	14	0.5	0.3	3.7

Fig. 1:

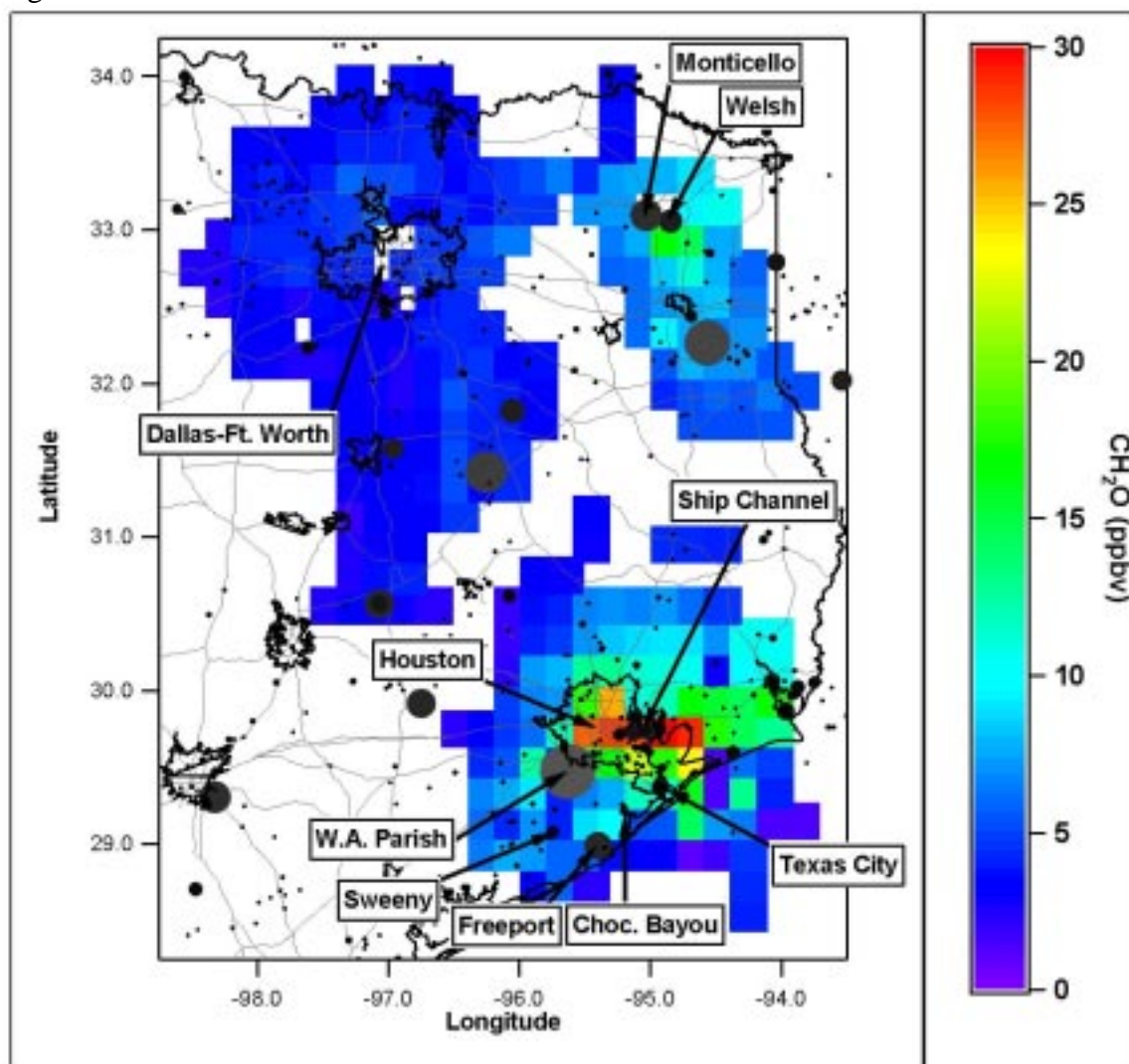


Fig. 2:

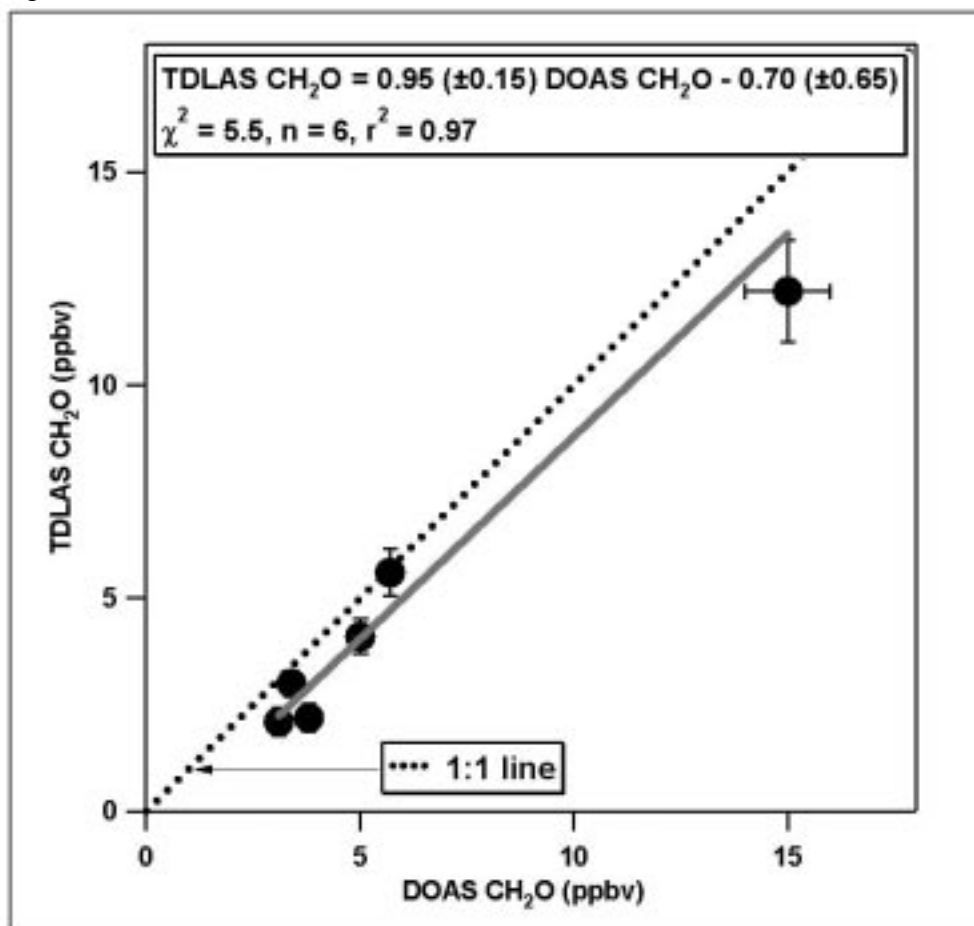


Fig. 3:

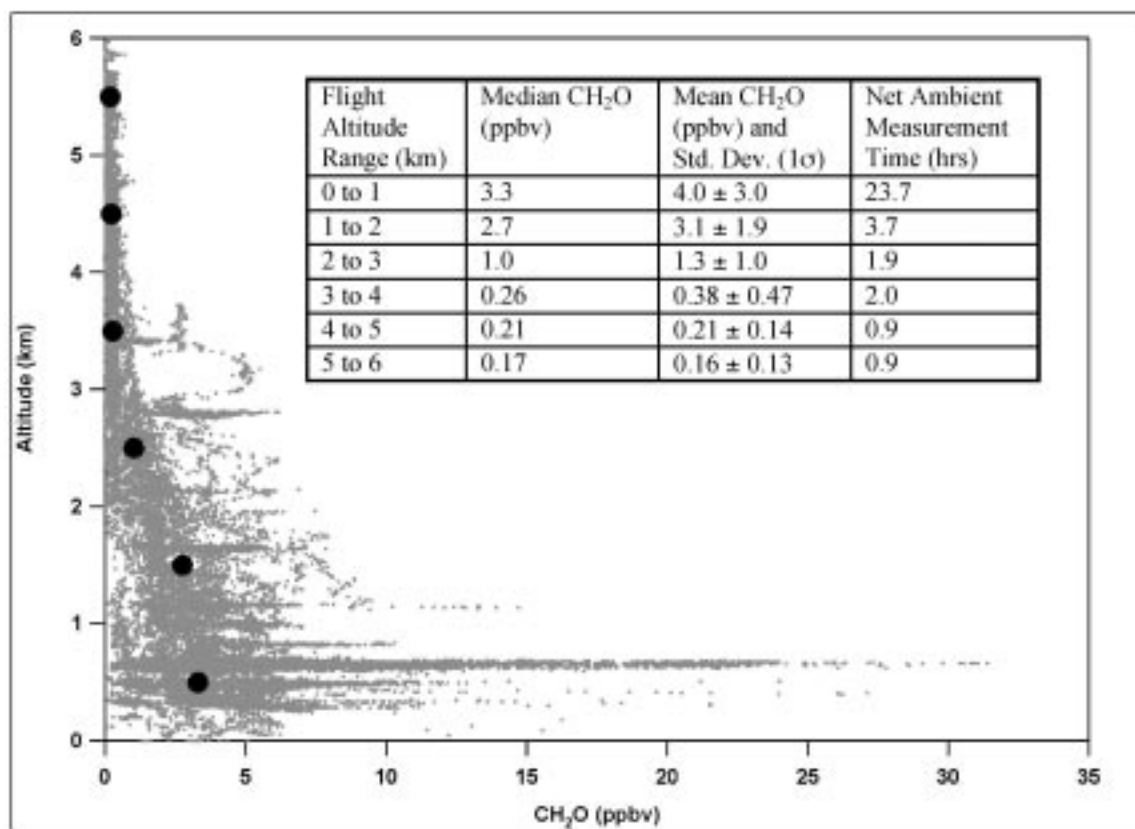


Fig. 4:

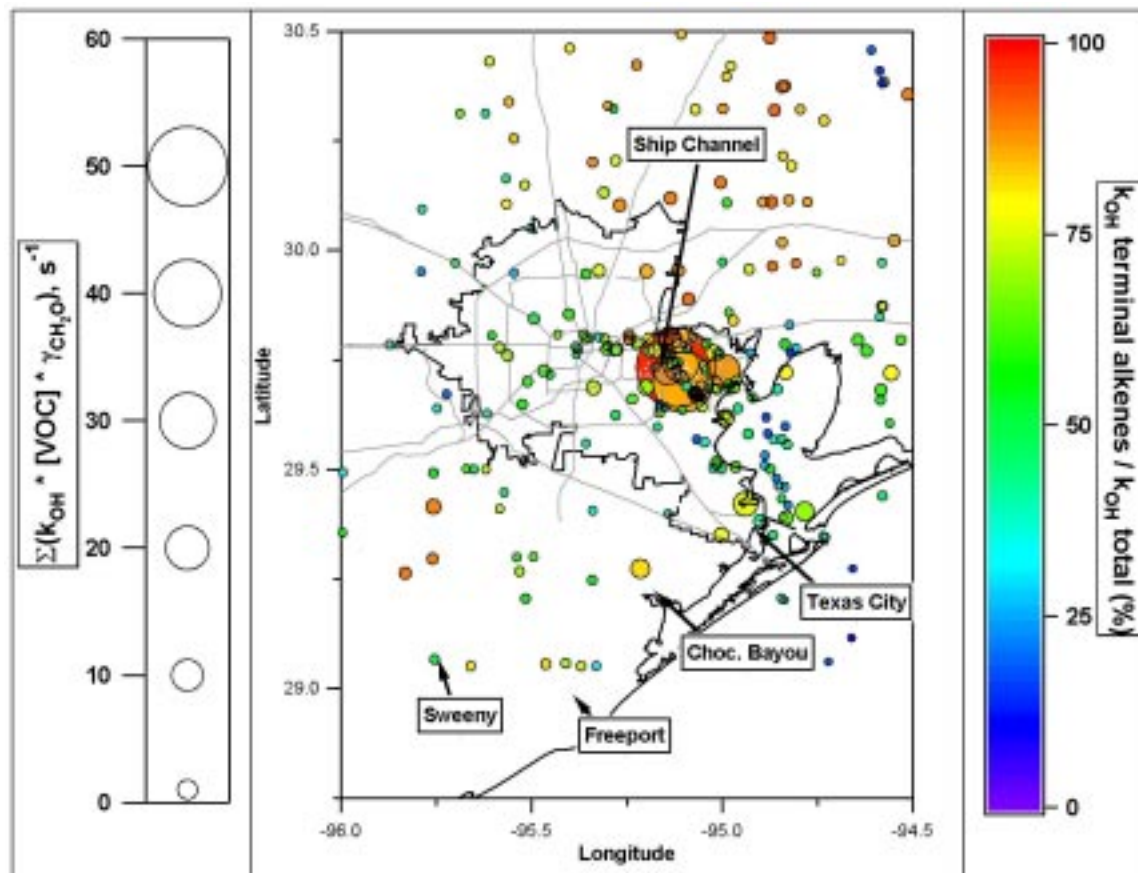


Fig. 5:

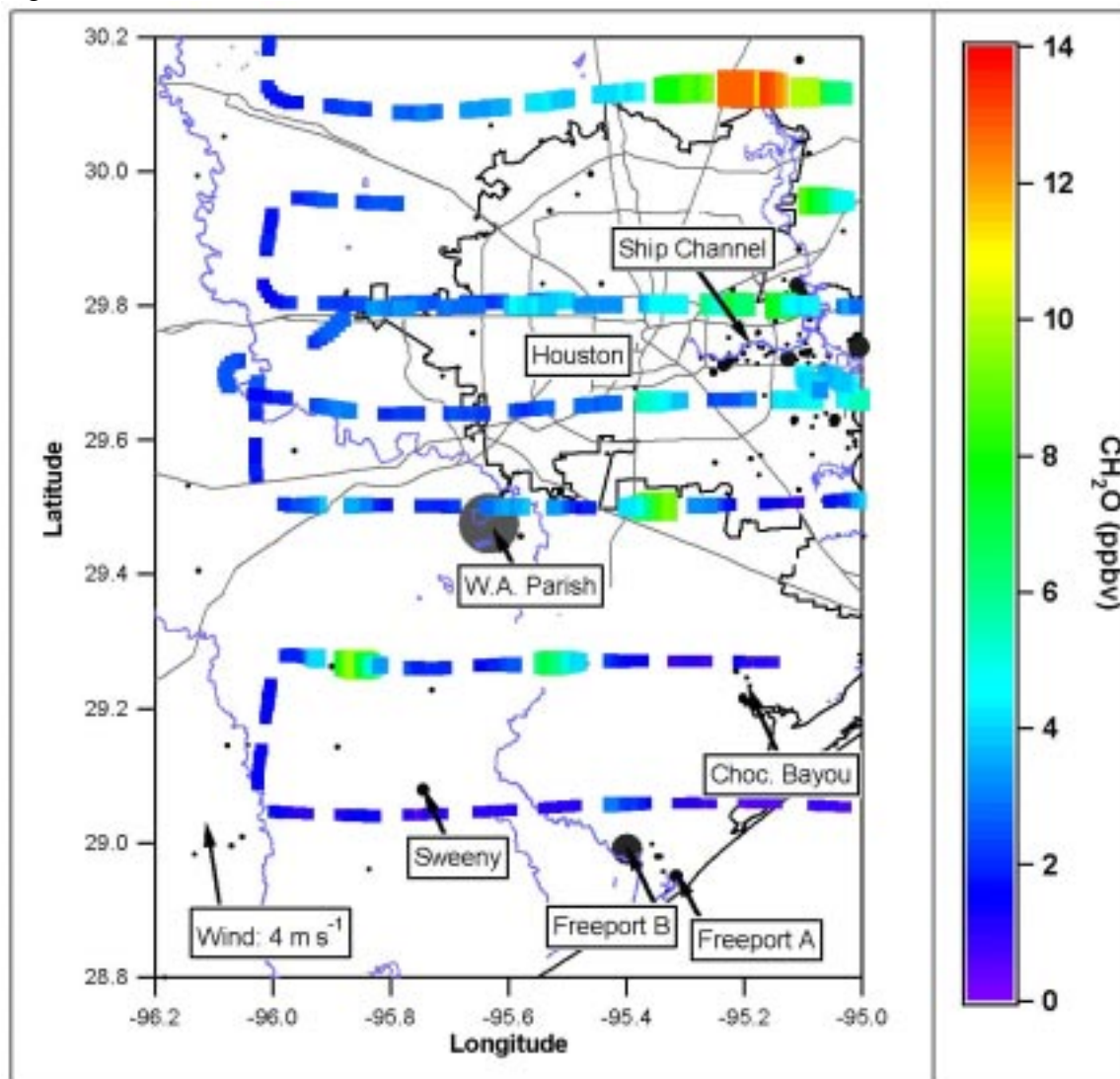


Fig. 6:

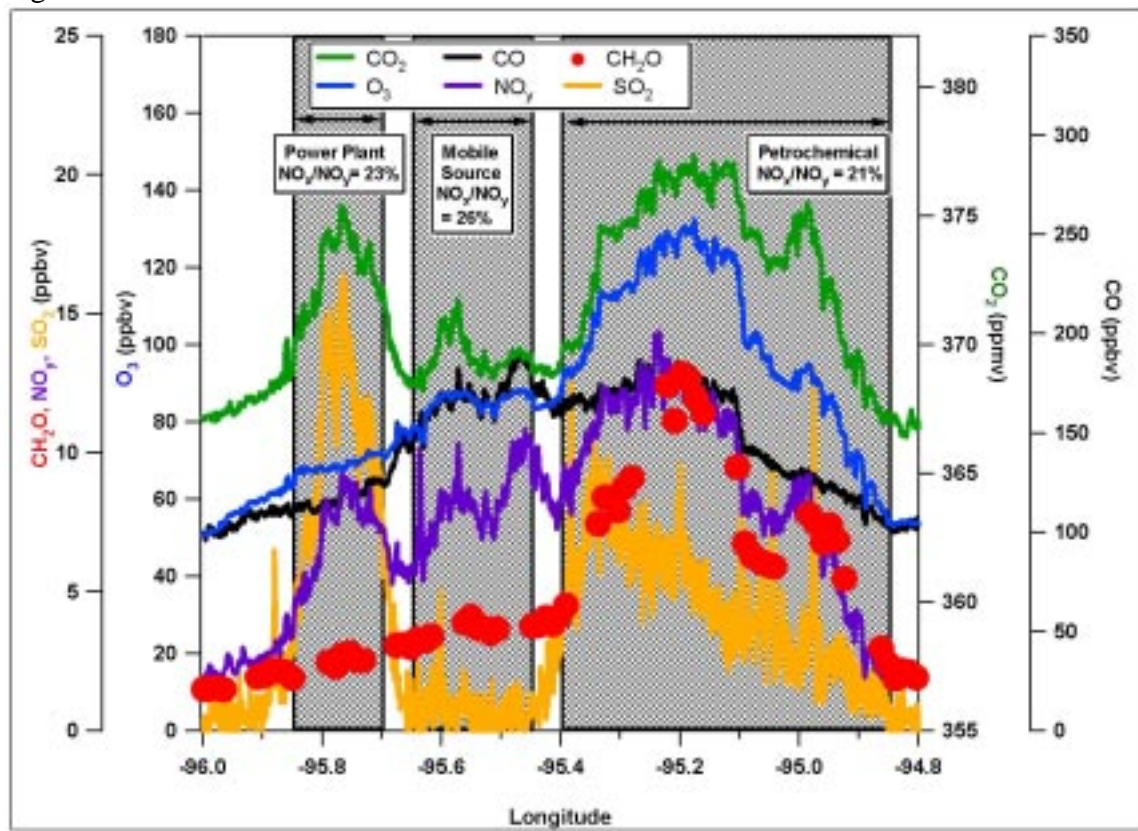


Fig. 7.

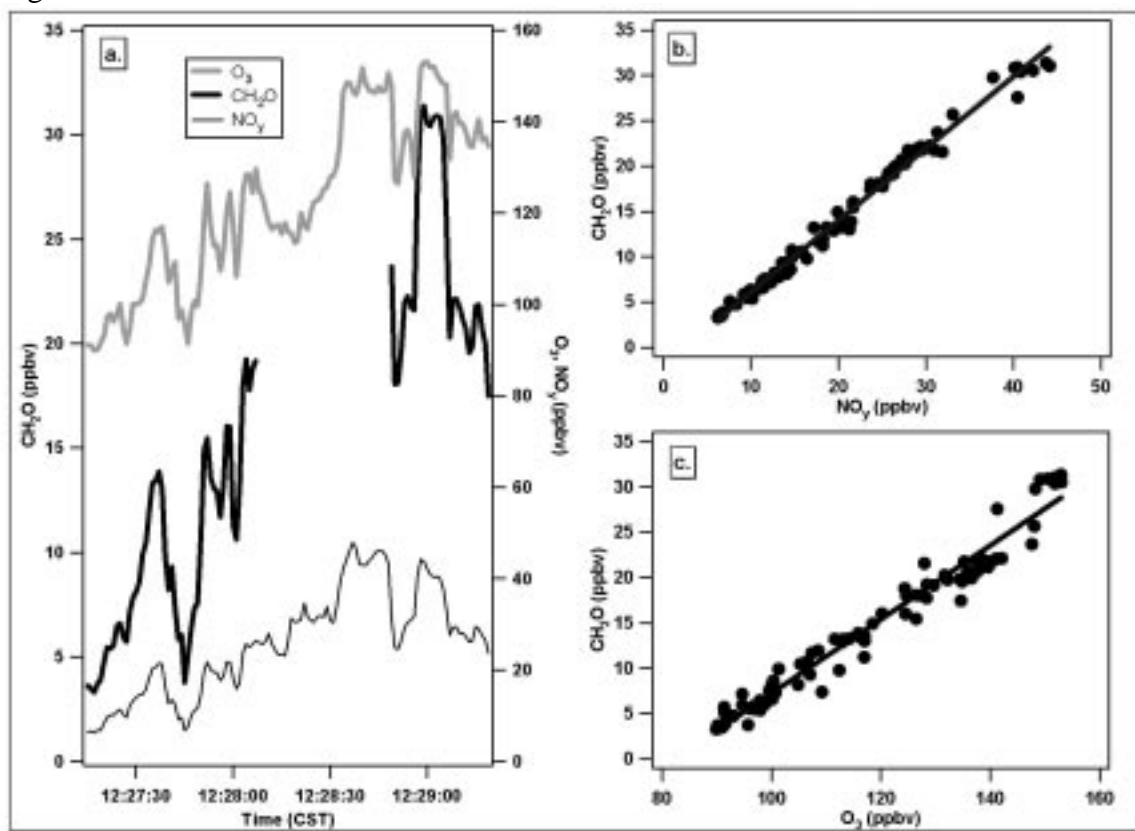


Fig. 8a &amp; b.

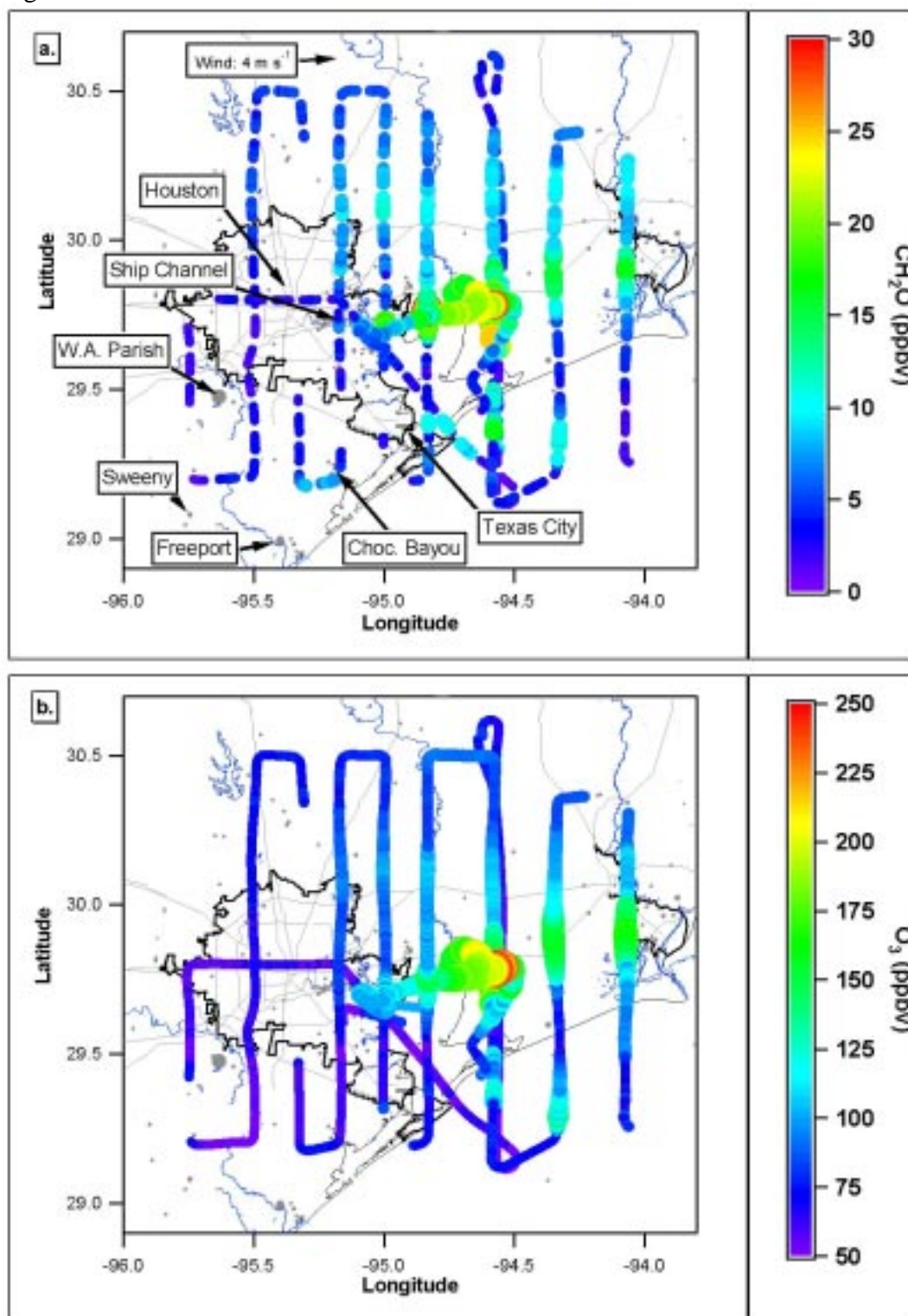


Fig 9.

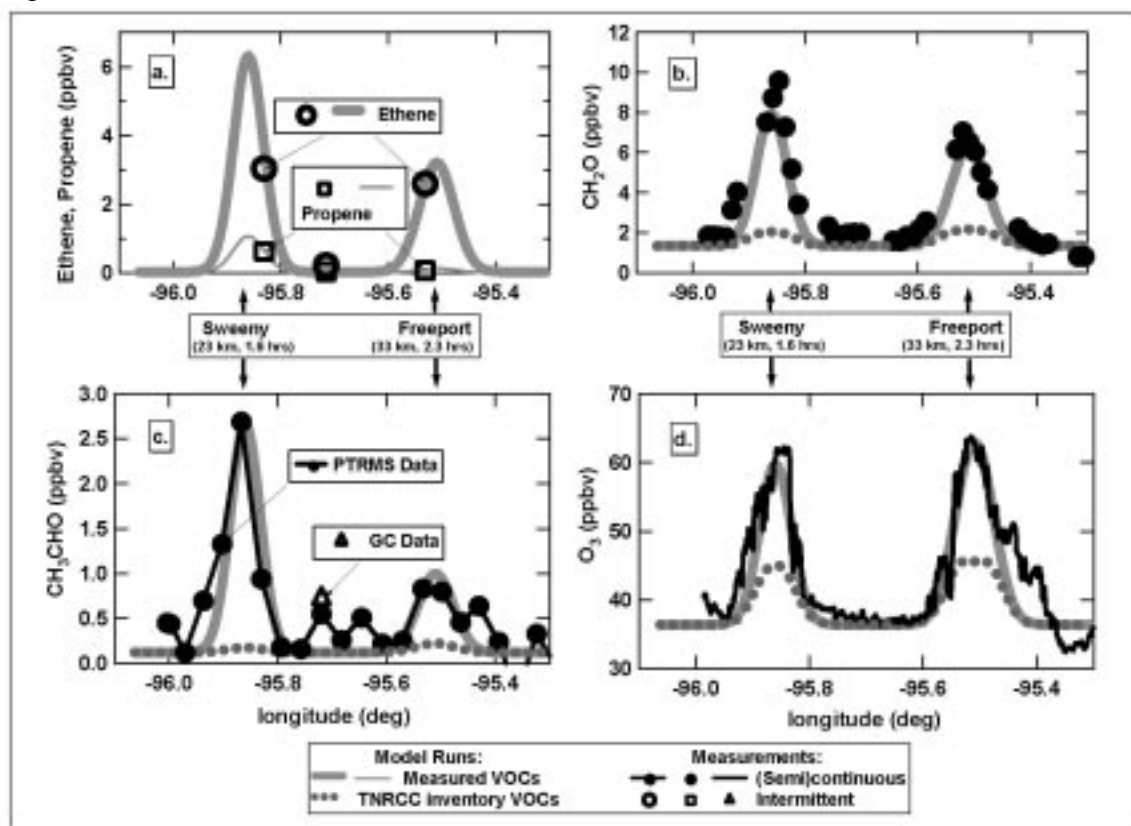
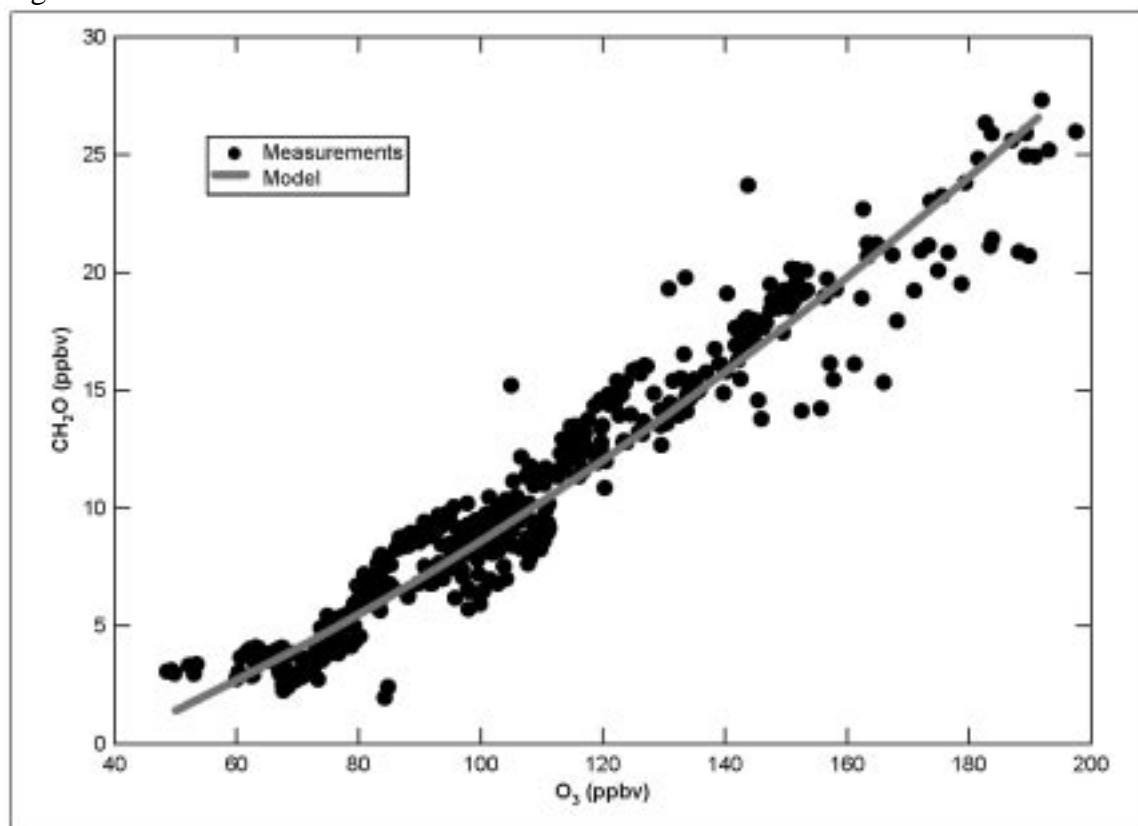


Fig. 10.





# **Particle growth in urban and industrial plumes in Texas**

**by**

Charles A. Brock, Michael Trainer, Thomas B. Ryerson, J. Andrew Neuman, David D. Parrish, John S. Holloway, Paul Goldan, William Kuster, Gregory Frost, Gerhard Hübler, Christine Wiedinmyer, and Fred C. Fehsenfeld J. Charles Wilson, J. Michael Reeves, Bernard G. Lafleur, and Henrike Hilbert



## Particle growth in urban and industrial plumes in Texas

Charles A. Brock,<sup>1</sup> Michael Trainer, Thomas B. Ryerson, J. Andrew Neuman,<sup>1</sup> David D. Parrish, John S. Holloway,<sup>1</sup> Dennis K. Nicks Jr.,<sup>1</sup> Gregory J. Frost,<sup>1</sup> Gerhard Hübler,<sup>1</sup> and Fred C. Fehsenfeld<sup>1</sup>

Aeronomy Laboratory, National Oceanic and Atmospheric Administration, Boulder, Colorado, USA

J. Charles Wilson, J. Michael Reeves, Bernard G. Lafleur, and Henrike Hilbert

Department of Engineering, University of Denver, Denver, Colorado, USA

Elliot L. Atlas, Stephen G. Donnelly, Sue M. Schauffler, Verity R. Stroud, and Christine Wiedinmyer

Atmospheric Chemistry Division, National Center for Atmospheric Research, Boulder, Colorado, USA

Received 11 July 2002; revised 17 September 2002; accepted 30 September 2002; published 7 February 2003.

[1] Particle size distributions and gas-phase particle precursors and tracer species were measured aboard an aircraft in the plumes downwind from industrial and urban sources in the vicinity of Houston, TX during the daytime in late August and early September 2000. Plumes originating from the Parish gas-fired and coal-fired power plant, petrochemical industries along the Houston ship channel, the petrochemical facilities near the Gulf coast, and the urban center of Houston were studied. Most of the particle mass flux advected downwind of Houston came from the industries and electrical utilities at the periphery of the city rather than from sources in the urban core. In SO<sub>2</sub>-rich plumes that did not contain elevated concentrations of volatile organic compounds (VOCs), particle volume increased with increasing plume oxidation (age) at a rate consistent with condensation and neutralization of the gas-phase oxidation products of SO<sub>2</sub>. In plumes that were rich in both SO<sub>2</sub> and VOCs, observed particle growth greatly exceeded that expected from SO<sub>2</sub> oxidation, indicating the formation of organic particulate mass. In plumes that were enhanced in VOCs but not in SO<sub>2</sub>, and in the plume of the Houston urban center, no particle volume growth with increasing plume oxidation was detected. Since substantial particle volume growth was associated only with SO<sub>2</sub>-rich plumes, these results suggest that photochemical oxidation of SO<sub>2</sub> is the key process regulating particle mass growth in all the studied plumes in this region. However, uptake of organic matter probably contributes substantially to particle mass in petrochemical plumes rich in both SO<sub>2</sub> and VOCs. Quantitative studies of particle formation and growth in photochemical systems containing nitrogen oxides (NO<sub>x</sub> = NO + NO<sub>2</sub>), VOCs, and SO<sub>2</sub> are recommended to extend those previously made in NO<sub>x</sub>-VOC systems. *INDEX TERMS*: 0305 Atmospheric Composition and Structure: Aerosols and particles (0345, 4801); 0322 Atmospheric Composition and Structure: Constituent sources and sinks; 0345 Atmospheric Composition and Structure: Pollution—urban and regional (0305); 0365 Atmospheric Composition and Structure: Troposphere—composition and chemistry; *KEYWORDS*: aerosols, particles, plumes, oxidation, urban, industrial

**Citation:** Brock, C. A., et al., Particle growth in urban and industrial plumes in Texas, *J. Geophys. Res.*, 108(D3), 4111, doi:10.1029/2002JD002746, 2003.

### 1. Introduction

[2] The metropolitan area of Houston, TX is home to more than four million people and the largest grouping of petrochemical industrial plants in the United States. During the

summer, emissions of NO<sub>x</sub> and volatile organic compounds (VOCs) in combination with intense solar radiation and appropriate meteorological conditions lead to ozone concentrations that frequently exceed United States regulatory standards, sometimes by more than a factor of 2. The Houston metropolitan area may also be at risk of exceeding the proposed standards for the concentration of dry mass of aerosol particles with diameters <2.5 μm (PM<sub>2.5</sub>). The sources of PM<sub>2.5</sub> in the Houston area are believed to include the gas-phase photooxidation of SO<sub>2</sub> and reactive organic

<sup>1</sup>Also at Cooperative Institute for Research in Environmental Sciences, University of Colorado, Boulder, Colorado, USA.

compounds, followed by condensation of the lower vapor pressure oxidation products. Other sources of  $PM_{2.5}$  in the Houston area include dispersed, fixed urban sources such as light industry, cooking, and combustion, mobile sources such as diesel soot emissions and roadway-generated particles, and sea spray and windblown dust. A quantitative understanding of the relationship between emissions of primary particles and precursor gases and downwind aerosol properties is needed to develop effective mitigation strategies.

[3] The primary goal of the Texas Air Quality Study (TexAQS) 2000 was to improve understanding of the chemical and meteorological causes of ozone exceedance episodes in the Houston–Galveston and Dallas metropolitan areas [Kleinman *et al.*, 2002; Wert *et al.*, 2003; T. B. Ryerson *et al.*, Effect of co-located petrochemical industrial emissions of reactive alkenes and  $NO_x$  on tropospheric ozone formation, submitted to *Journal of Geophysical Research*, 2002, hereinafter referred to as Ryerson *et al.*, submitted manuscript, 2002]. A further goal of the study was to investigate the sources and characteristics of aerosol particles in the study region. Airborne and surface observations, as well as modeling and forecasting tools, were used to achieve these program goals.

[4] From 16 August to 13 September 2000 measurements of particulate and gas-phase pollutants and tracer species were made on the Lockheed Electra aircraft, leased by the National Oceanic and Atmospheric Administration (NOAA) from the National Center for Atmospheric Research (NCAR), in a variety of power plant, petrochemical, and urban plumes in eastern Texas and Oklahoma. These flights, and those of other research aircraft, were supported by a network of Houston-area ground-based sites measuring photochemically active compounds, tracer species, photochemical oxidation products, and radiative and meteorological variables. Meteorological parameters were measured from a network of microwave wind profilers, and two additional sites were extensively instrumented with a variety of instruments for measuring gas-phase concentrations and the microphysical, optical, and chemical properties of aerosol particles. Meteorological and chemical modeling and efforts to refine emissions inventories were also integral components of the TexAQS 2000 program. This work will focus on reporting and interpreting particle size distribution measurements obtained aboard the Electra in plumes from specific sources in the Houston metropolitan area under meteorological conditions typified by relatively steady, moderate wind speeds. The major sources of enhanced particle volume and number are determined, their relative magnitudes are quantified, and the processes leading to particle production in this region in summertime are discussed.

## 2. Instruments and Methods

### 2.1. Particle Instruments

[5] Data collected aboard the Electra aircraft from a five-channel condensation particle counter (CPC) [Brock *et al.*, 2000], a laser optical particle counter (OPC) [Jonsson *et al.*, 1995], and a white-light OPC were combined to determine dry particle size distributions from 0.004 to 8  $\mu\text{m}$  diameter with 1-s time resolution. Performance and calibration of the CPC and laser OPC, which together measure particle size distributions from 0.004 to 1.0  $\mu\text{m}$ , are described by Brock *et*

*al.* [2002]. The size distribution of particles with diameters from 0.4 to 8  $\mu\text{m}$  was measured with a modified Climec 208A white-light OPC (Climec Instruments, Redlands, CA).

[6] Before, during, and after the TexAQS 2000 field project, the three particle instruments were calibrated with nearly monodisperse  $(\text{NH}_4)_2\text{SO}_4$  particles with diameters from 0.05 to 1.6  $\mu\text{m}$ . These particles were generated from an aqueous solution using an atomizer. The aerosol flow was dried and introduced into a cylindrical differential mobility analyzer (DMA) designed and built at the NOAA Aeronomy Laboratory. The particles were exposed to a 20 mCi bipolar ion source and classified within the DMA by electrical mobility. The nearly monodisperse particle stream was then introduced into the sampling plumbing at the location where the inlet sample line entered the aircraft fuselage. The concentration of calibration particles introduced at the inlet was determined with a separate CPC (Model 3760, TSI Inc., St. Paul, MN). Additionally, the size response of the Climec OPC, but not its counting efficiency, was determined for particles with diameters from 1.6 to 8  $\mu\text{m}$  using polystyrene spheres and glass beads. Further calibrations of the five-channel CPC were also performed as described by Brock *et al.* [2000] prior to TexAQS 2000 using particles with diameters from 0.004 to 0.8  $\mu\text{m}$  in diameter.

### 2.2. Low-Turbulence Inlet (LTI)

[7] The aerosol instruments sampled ambient air through a new inlet that uses active boundary layer suction to virtually eliminate turbulence while decelerating the 100  $\text{m s}^{-1}$  airflow to  $\sim 6 \text{ m s}^{-1}$  (Figure 1). This LTI was developed at the University of Denver. The LTI was mounted on the forwardmost window just aft of the cockpit and forward of upwash flow around the wing root area. The enhanced efficiencies with which particles of different sizes are transmitted through the LTI has been estimated by numerical simulation of particle trajectories within the external flow approaching the inlet tip, as well as within the decelerating and diverging internal flow within the inlet. Calculated enhancements in the sample airstream relative to the ambient air were negligible for particles with aerodynamic diameters  $< 1 \mu\text{m}$ , and factors of approximately 1.1, 1.3, and 1.7 for particles with aerodynamic diameters of 3, 5, and 8  $\mu\text{m}$ , respectively. The data were corrected for these effects. After exiting the LTI, the sample airstreams were extracted from the center of the LTI flow and transported in stainless steel tubing distances  $< 3 \text{ m}$  to each of the instruments. The aerosol sample streams to the two OPCs were dried to  $< 20\%$  relative humidity with Nafion diffusion dryers.

### 2.3. Uncertainty Analysis

[8] A Monte Carlo simulation was used to propagate the random uncertainties due to calibration of particle size and concentration, and to in-flight measurement of flow rate, temperature, and pressure, through the numerical data processing algorithms, assuming typical background conditions measured during TexAQS 2000. The resulting estimated measurement precision for particle number is  $\pm 15\%$  for 1-s data, while that for particle volume is  $\pm 34\%$  with a sensitivity of  $0.4 \mu\text{m}^3 \text{ cm}^{-3}$  for 1-s data. These precisions vary somewhat depending on the measured size distribution due to the differing accuracies of the three particle sizing instruments. Possible biases, due mainly to

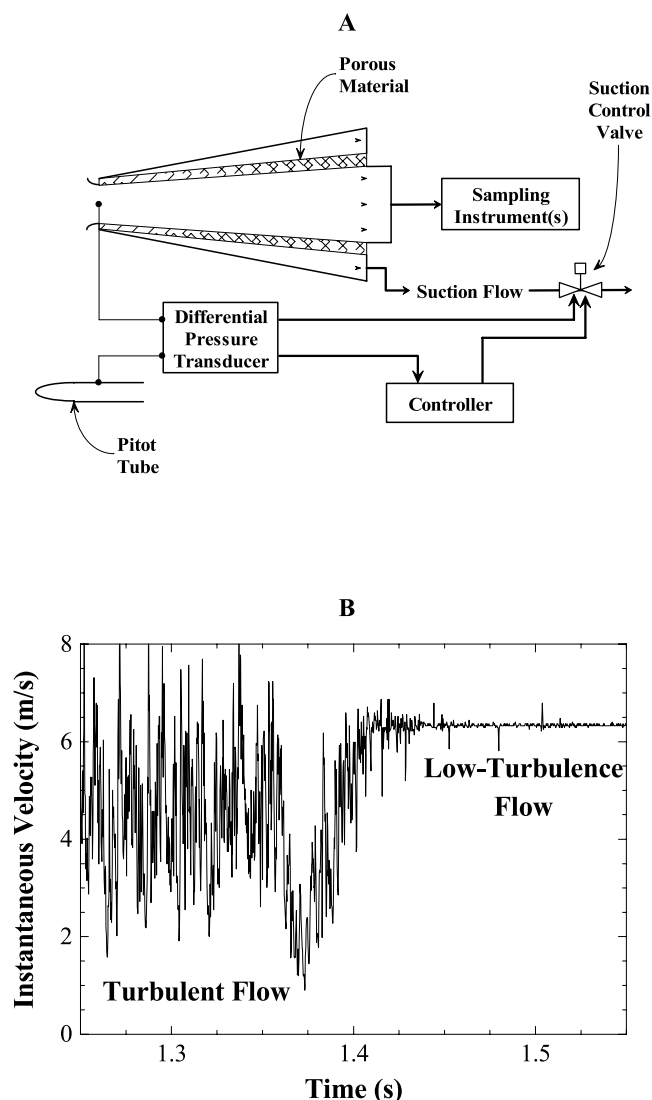


**Figure 1.** (a) Schematic diagram of the LTI used on the Electra aircraft during TexAQS 2000. Turbulent air is removed by suction through a porous material as it develops near the inlet wall, leaving a laminar core of air for the sampling instruments. Size-dependent particle enhancements occur where the sample flow decelerates and diverges. (b) Turbulence levels in the core sample flow at the diffuser exit as the suction flow is turned on.

uncertainties in particle refractive index and to uncharacterized sampling losses, are estimated to be <10% and <35% for particle number and volume concentrations, respectively. All particle parameters are reported in quantity per cubic centimeter of air at standard temperature and pressure (1013 hPa and 273.2 K).

#### 2.4. Additional Measurements

[9] The analysis presented here makes use of measurements of photochemically reactive gases and tracer compounds to identify plumes, estimate dilution, and evaluate the mass budget of condensable compounds. These gas-phase measurements include NO, NO<sub>2</sub>, NO<sub>y</sub>, O<sub>3</sub>, SO<sub>2</sub>, CO, CO<sub>2</sub>, and HNO<sub>3</sub> [Ryerson *et al.*, 1998; Neuman *et al.*, 2002]. All of these compounds were measured continuously

with demonstrated instrumental response times of 1 s or faster (except for SO<sub>2</sub>, with a response time of ~3 s) and accuracy and precision quantified by in-flight calibration and zeroing. Generally, the uncertainty of the SO<sub>2</sub> measurement was within ±10% for SO<sub>2</sub> levels well above the detection limit of approximately 0.5 ppbv. However, for the data on the two flights presented here this accuracy was sporadically degraded by short-term transients of up to several ppbv due to operational difficulties with the in-flight calibration system. These difficulties are considered in assigning the confidence limits to the results of the following analyses. Uncertainties for NO<sub>y</sub> and HNO<sub>3</sub>, which are used quantitatively in this analysis, are ±(100 pptv + 10%) and ±(130 pptv + 10%), respectively. Individual whole-air canister samples were collected periodically over ~8-s intervals and were subsequently analyzed by chromatographic techniques [Heidt *et al.*, 1989; Schauffler *et al.*, 1999]. Analyzed species included alkyl nitrate compounds, alkanes, alkenes, alkynes, and several aromatic compounds with known secondary organic aerosol yields. Meteorological and navigational parameters reported by the Research Aviation Facility of NCAR (<http://raf.atd.ucar.edu/Bulletins/bulletin9.html>) were also used in the analysis.

### 3. Observations

[10] In this report, particle formation and growth in plumes observed on 27 and 28 August 2000 downwind of four clearly identifiable sources will be discussed. These sources are (Figure 2): (1) the Houston ship channel/west Galveston Bay area, containing multiple large petrochemical complexes and shipping and rail hubs within a low-density urban setting; (2) the Parish power plant, a coal-fired and natural gas-fired electric generation facility with no SO<sub>2</sub> gas scrubbers and located in open farmland southwest of Houston; (3) the Houston urban core, dominated by mobile tailpipe and dispersed local emissions; and (4) isolated large petrochemical complexes south of Houston.

[11] On both 27 and 28 August 2000, continuous southerly winds ranging from 3 to 6 m s<sup>-1</sup> were reported within the planetary boundary layer (PBL) throughout the Houston study area. The mid-PBL wind velocities on these days will be approximated as 4.5 ± 1 m s<sup>-1</sup>. The relative constancy, direction and speed of the wind make it possible to readily identify the sources of many plumes, to track their locations >60 km downwind, and to accurately determine, from downwind distance, the time since the measured plume parcel was emitted, or plume age. The NO<sub>x</sub>-O<sub>3</sub>-VOC photochemistry within plumes from different sources on these days is discussed in detail by Ryerson *et al.* (submitted manuscript, 2002). Because of the continuous advection and dilution, the mixing ratios of O<sub>3</sub> at ground-based monitoring sites in the Houston metropolitan area did not exceed regulatory criteria on either 27 or 28 August nor were such mixing ratios observed onboard the Electra. There were no substantial unusual emissions, or upsets, of gas-phase or particulate pollutants from industries in the area on either day according to emissions data reported to and provided by the Texas Natural Resource Conservation Commission (TNRCC). Thus, these days appear to be typical of moderately polluted, well-ventilated, summertime conditions in the Houston metropolitan area. While these conditions do not

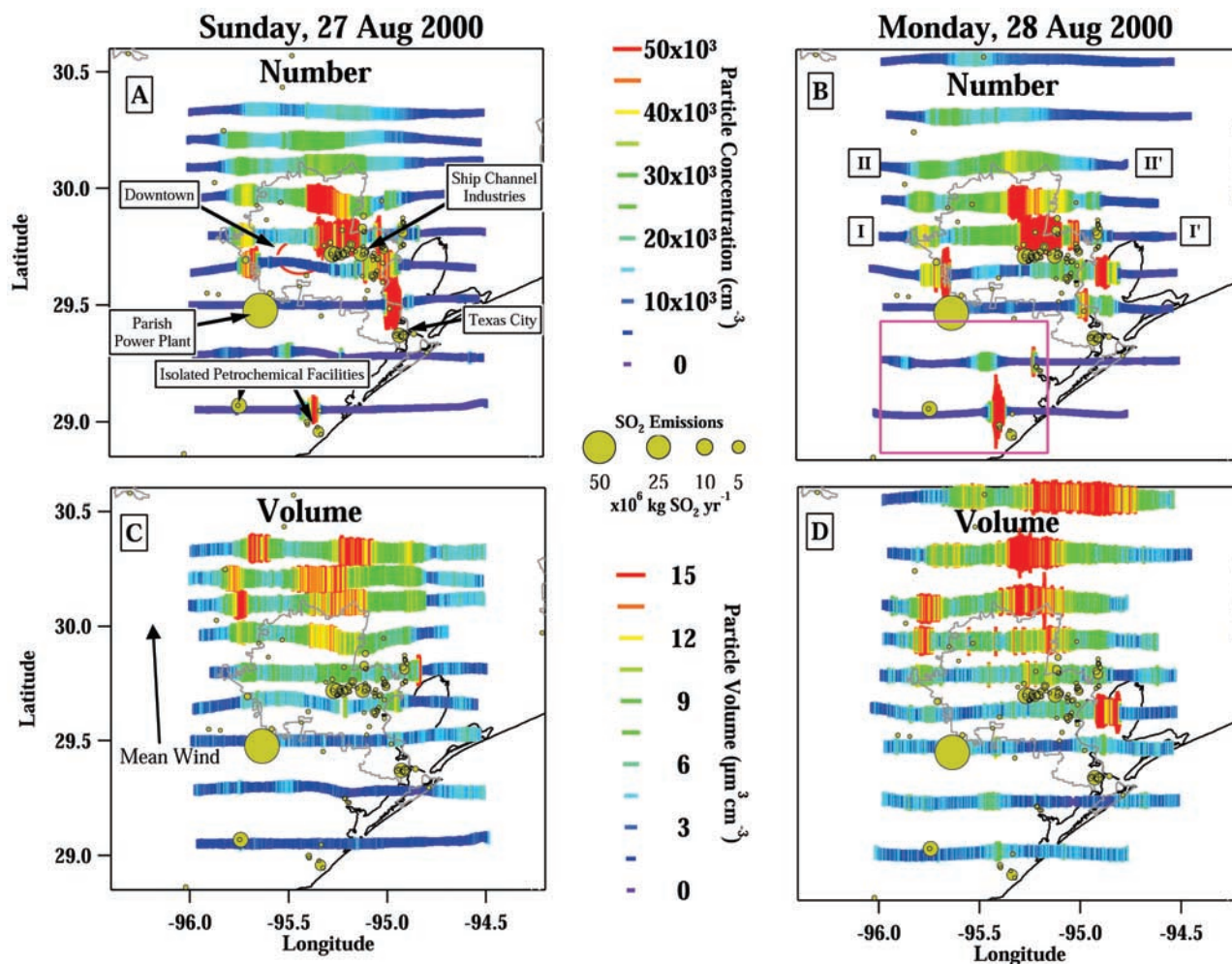


**Figure 2.** Map of the Houston area with flight track of the NCAR Electra aircraft during constant-latitude transects (approximately perpendicular to the prevailing southerly wind) within the PBL. The transects are color and size coded by particle number (a and b) and volume (c and d) concentration enhancements above background. (a) and (c) For 27 August 2000 and (b) and (d) for 28 August. Point sources of  $\text{SO}_2$  are indicated by the circles, sized by annual emissions according to the 1999 TNRCC inventory. The Houston metropolitan area is outlined in gray, while the Texas coastline is in black. Time series data from the transects indicated by I-I' and II-II' in (b) are shown in Figure 3. Area indicated by the magenta box in (b) is shown in Figure 4.

result in concentrations of pollutants in excess of regulatory standards, they provide a relatively simple meteorological scenario in which to contrast the effects of different types of emissions on particle formation and growth. On 27 August, a Sunday, particle emissions from urban diesel vehicle traffic were probably significantly lower than on 28 August [e.g., Dreher and Harley, 1998; Marr et al., 2002]. In contrast, inventoried emissions from stationary industrial sources were not substantially different on the two days.

[12] The Electra flew E-W transects approximately perpendicular to the southerly wind within the PBL at a typical height of 0.6–0.7 km above the surface on both days (Figure 2). The transects began well upwind of the Houston metropolitan area, proceeded over and downwind of Houston, and concluded >60 km downwind of the urban core. At the eastern or western termini of some of the transects, the aircraft climbed to determine the height of the PBL. Assuming approximately constant wind speed, as observed aboard

the Electra over the course of the ~6-hour flights and from surface profiler sites, the furthest transect downwind of the Houston urban core and ship channel area corresponded to a plume age of >4 hours on each day. Because of the wind direction, identifiable plumes from the Parish coal-fired and gas-fired power plant, the downtown urban core of Houston, and the petrochemical industries located along the Gulf coast and the Houston ship channel were advected side-by-side to the north (Figure 2), with some merging of the plumes with increasing downwind distance.

### 3.1. Houston Ship Channel Industrial Complex

[13] The Houston ship channel is a narrow waterway extending eastward from downtown Houston to Galveston Bay (Figure 2). Extensive petrochemical complexes and shipping and rail hubs line both sides of the waterway. Colocated with the industries are fossil fuel-fired electrical generation and process heat facilities, some of which emit

**Table 1.** Plume Distances, Approximate Ages, and Mean and Maximum Number and Volume Concentrations Measured Downwind of the Parish Power Plant, the Houston Urban Core, and the Houston Ship Channel and in Background Air Southwest of Houston<sup>a</sup>

Source	Date	Distance (km)	Plume Age (hours)	$N_{\text{mean}}$ ( $\times 10^4 \text{ cm}^{-3}$ )	$N_{\text{max}}$ ( $\times 10^4 \text{ cm}^{-3}$ )	$V_{\text{mean}}$ ( $\mu\text{m}^3 \text{ cm}^{-3}$ )	$V_{\text{max}}$ ( $\mu\text{m}^3 \text{ cm}^{-3}$ )		
Background	27 August	NA <sup>b</sup>	NA	~0.3	NA	~7	NA		
	28 August	NA	NA	~0.3	NA	~9	NA		
Ship Channel	27 August	8	0.5	3.5	8.0	10.7	16.3		
		27	1.7	2.0	4.5	11.0	18.1		
		44(a)	2.7	2.1	3.6	14.3	22.4		
		44(b)	2.7	1.3	2.5	10.2	14.5		
		56	3.5	1.2	2.1	12.3	17.7		
		69	4.3	1.4	2.1	14.9	23.7		
	28 August	8	0.5	4.1	12	14.3	21.0		
		8	0.5	3.6	8.3	12.5	28.6		
		24	1.5	3.2	6.8	16.0	23.4		
		44 (a)	2.7	2.2	4.1	17.9	43.4		
		44 (b)	2.7	2.3	4.8	16.6	31.4		
		66	4.1	1.1	2.0	19.2	38.1		
		92	5.7	0.5	0.8	17.3	26.6		
		Parish	27 August	23	1.4	3.4	6.3	9.0	12.2
				36	2.2	3.0	4.5	10.0	14.5
56	3.5			2.0	3.6	12.1	18.7		
71(a)	4.4			1.4	2.3	12.9	22.9		
71(b)	4.4			1.5	2.2	10.5	13.9		
83	5.1			1.1	2.1	11.2	18.8		
28 August	96	5.9	1.1	1.8	13.2	22.1			
	18	1.1	4.2	12	11.8	14.3			
	38(a)	2.3	2.4	4.2	13.4	19.1			
	38(b)	2.3	2.0	3.3	13.4	17.5			
	54	3.3	2.7	3.6	17.0	23.7			
	69(a)	4.3	1.9	2.9	16.9	24.6			
	69(b)	4.3	1.8	2.7	16.6	26.5			
	93	5.7	2.1	2.6	15.8	20.3			
	120	7.4	1.6	2.0	15.8	21.5			
	Urban Core	27 August	~8	~0.5	1.6	2.7	9.8	12.1	
27			1.7	2.1	2.7	10.0	12.4		
44 (a)			2.7	1.8	2.2	9.8	15.1		
44 (b)			2.7	1.8	2.4	11.5	16.9		
56			3.5	1.7	2.0	10.0	13.1		
69			4.3	1.4	2.2	10.2	12.9		
28 August		~8	~0.5	2.6	3.7	12.1	20.4		
		~8	~0.5	1.9	3.5	11.6	18.0		
		24	1.5	2.9	22	13.4	22.9		
		44 (a)	2.7	2.3	2.9	13.6	16.8		
		44 (b)	2.7	2.2	3.8	13.8	19.2		
		66	4.1	2.0	2.6	15.6	20.7		
		92	5.7	1.3	2.0	14.8	22.2		

<sup>a</sup>See text for uncertainties.<sup>b</sup>NA: Not applicable.

substantial amounts of SO<sub>2</sub> and NO<sub>x</sub>. The collocation of NO<sub>x</sub> and VOC emissions, combined with intense insolation and light winds, can result in extremely high photochemical reactivity and rapid and efficient ozone formation [Ryerson *et al.*, 2001; Neuman *et al.*, 2002; Kleinman *et al.*, 2002].

[14] On both 27 and 28 August, the individual and merged plumes from industries in the ship channel region were crossed at five different downwind distances (Table 1 and Figure 2). The plumes were distinguished by differing concentrations and ratios of the tracer species NO<sub>y</sub>, CO<sub>2</sub>, CO, and SO<sub>2</sub>, the photochemical reaction product O<sub>3</sub>, and the number and volume concentrations of particles (Figure 3). As an example, in the transect made at 8 km downwind of the ship channel on 28 August, individual plumes from several separate sources within the ship channel could be discerned, as could the urban plume and that from the Parish power plant (Figure 3a). By 44 km downwind of the ship channel, boundary layer mixing had merged the multiple individual

plumes from the ship channel to form a single coalesced plume with more uniform characteristics (Figure 3b). Also on this day, the plume from the Texas City industrial complex southeast of Houston could initially be identified over Galveston Bay (Figures 2b and 2d), but by 8 km downwind of the ship channel it was not possible to use the tracer measurements to discern the Texas City plume from the merged plume from the various ship channel industries. Further downwind, the western edge of the ship channel plume gradually blended with that from the Houston urban core, which was identifiable by elevated mixing ratios of CO from mobile sources and a relative lack of SO<sub>2</sub> and CO<sub>2</sub> from industrial sources.

[15] Particle volume concentrations within the plume from the ship channel industries increased substantially with increasing downwind distance, despite the dilution of the plume by entrainment of air with lower particle loadings from the west and east (Table 1 and Figures 2 and 3). On 28

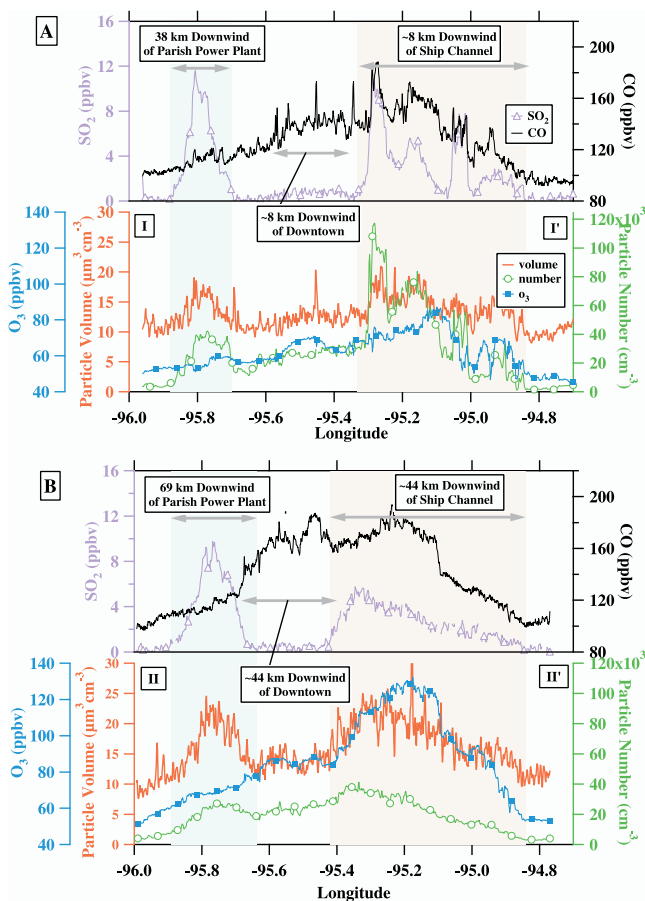


**Figure 3.** Measurements of  $\text{SO}_2$ ,  $\text{CO}$ ,  $\text{O}_3$ , and particle number and volume concentrations on 28 August 2000 downwind of the Parish power plant (shaded blue), the Houston urban core (unshaded), and the Houston ship channel industries (shaded peach). (a) Transect I-I' on Figure 2, just downwind of the urban center and ship channel. (b) Transect II-II' on Figure 2, further downwind at the northern edge of the Houston metropolitan area. Substantial increases in particle volume above background are clearly associated with the power plant and industrial plumes, indicated by enhanced  $\text{SO}_2$  mixing ratios.

August, the peak enhancement above background in dry particle volume concentration was  $>17 \mu\text{m}^3 \text{cm}^{-3}$  near the center of the plume at a distance of 92 km downwind. Assuming a dry particle density of  $\sim 1.5 \text{ g cm}^{-3}$ , this corresponds to an enhancement above background in particle mass concentration of  $>25 \mu\text{g m}^{-3}$ . The value, measured under well-ventilated meteorological conditions, may be compared with the proposed annual and 24-hour  $\text{PM}_{2.5}$  national ambient air quality standards of 15 and  $65 \mu\text{g m}^{-3}$ , respectively. Particle volume enhancements exceeding  $12 \mu\text{m}^3 \text{cm}^{-3}$  above background were found for  $>45 \text{ km}$  along the flight path in this furthest transect  $>90 \text{ km}$  downwind of the ship channel (Figure 2d). This substantial horizontal dispersion of enhanced particle volume concentrations illustrates the potential influence of the Houston-area petrochemical industries on regional air quality.

[16] In contrast to particle volume concentrations, particle number concentration maximized close to the sources (Table 1 and Figures 2a and 2b). The aerosol in these

regions of high concentration was dominated by particles with diameters  $<0.05 \mu\text{m}$  which are unlikely to have been directly emitted but rather were formed from condensation from the gas phase [e.g., Brock et al., 2002]. The highest particle concentrations were found in  $\text{SO}_2$ -rich portions of the  $\sim 0.5$ -hour-old ship channel plume, indicating recent gas-to-particle formation from the oxidation products of  $\text{SO}_2$ . These observations are consistent with many earlier laboratory and field observations indicating that the oxidation products of  $\text{SO}_2$  are critically important in the formation of new particles in polluted air, even when VOC concentrations are quite high [e.g., Flagan et al., 1991; Hoppel et al., 2001]. The rapid decrease in particle number concentration in the ship channel plume with increasing plume age is qualitatively consistent with expected high rates of coagulation of these nucleation-mode particles with themselves and with larger particles, combined with dilution by air with relatively low particle concentrations.

### 3.2. Parish Power Plant

[17] The W.A. Parish power plant is a large coal-fired and natural gas-fired electrical generation facility located southwest of the Houston metropolitan area. The plant emits approximately  $5.7 \times 10^7 \text{ kg yr}^{-1}$  of  $\text{SO}_2$  and  $3.2 \times 10^7 \text{ kg yr}^{-1}$  of  $\text{NO}_x$  (as  $\text{NO}_2$ ). Compared with other Houston-area sources, it is not a large direct emitter of particulate matter or VOCs. On both 27 and 28 August 2000, the plume from the Parish power plant was advected northward over agricultural and suburban areas at the western edge of the Houston metropolitan area. On 27 August, transects were made perpendicular to the well-mixed plume at six downwind distances (Table 1 and Figures 2a and 2c) corresponding to approximate plume ages from 1.4 to 5.9 hours. On 28 August, transects across the well-mixed plume were also made at six distances, corresponding to approximate plume ages from 1.1 to 7.4 hours (Table 1 and Figures 2b and 2d).

[18] Although the photochemical evolution of the Parish plume was very similar on both 27 and 28 August, greater downwind coverage of the plumes by the aircraft makes the 28th better for in-depth study. By 38 km (2.3 hours) downwind distance (plume age) on 28 August, the eastward edge of the Parish plume had begun to blend with that from the Houston urban area (Figure 3a). By this time, peak enhancements above background in particle volume concentration of  $\sim 8 \mu\text{m}^3 \text{cm}^{-3}$  were observed within the Parish plume, while particle number concentrations reached  $\sim 4 \times 10^4 \text{ cm}^{-3}$  (Table 1). At 69 km (4.3 hours) distance from the power plant, the particle volume enhancement above background had reached its observed maximum of  $\sim 16 \mu\text{m}^3 \text{cm}^{-3}$ . As in the plume from the ship channel, particle number concentrations, dominated by particles with diameters  $<0.05 \mu\text{m}$  produced from gas-to-particle conversion, reached a maximum close to the source and decreased rapidly with increasing plume age.

### 3.3. Houston Urban Core

[19] On both 27 and 28 August, the plume from the urban core of Houston was advected downwind between the plumes of the Parish power plant to the west and the petrochemical industries of the ship channel to the east (Figures 2 and 3). The urban area source is dominated by emissions from motor vehicles, which produce substantial

quantities of CO and NO<sub>x</sub>, very little SO<sub>2</sub>, and relatively small amounts of CO<sub>2</sub> compared with industrial point sources. Compared with the large increases in particle number and volume concentration observed in the plumes from the Parish power plant and the ship channel petrochemical industries, only relatively modest enhancements in particle volume and number above background were found within the Houston urban plume on either day (Table 1). There was no detectable systematic change in particle volume with age of the plume from the Houston urban center, suggesting that a large fraction of the particle mass was directly emitted and that rates of gas-to-particle conversion were low. Mean particle volume concentrations were 3–5 μm<sup>3</sup> cm<sup>-3</sup> higher in the urban plume compared with background concentrations. On 27 August, a Sunday, particle volume enhancements above background were slightly lower (Table 1), perhaps reflecting a decrease in particle generation from vehicular traffic compared with the following workday. Mean particle number concentrations measured just downwind of the downtown core were a factor of ~2 lower than those measured immediately downwind of the ship channel industries and the Parish power plant.

### 3.4. Geographically Isolated Refineries

[20] On both 27 and 28 August, the Electra sampled plumes from individual petrochemical complexes located on the coastal plain south of Houston near the town of Freeport, Texas (Figure 4). These industries are similar to those found along the Houston ship channel. However, because the Freeport-area plants are geographically isolated, with no significant upwind anthropogenic particle sources, they afford the opportunity to examine particle formation and growth in the absence of emissions from other nearby point, area, and mobile sources. Two discrete plumes have been identified as originating from two specific clusters of facilities: near the Dow Chemical Freeport B plant (Dow) and near the Gulf Chemical and Metallurgical plant (Gulf). The Dow facility, a group of plastics, epoxy, and hydrocarbon processing plants, combined with the nearby BASF Corp. plant, emit  $13 \times 10^6$  kg yr<sup>-1</sup> of NO<sub>x</sub> and  $2.4 \times 10^5$  kg yr<sup>-1</sup> of SO<sub>2</sub>, while the Gulf plant, a catalyst manufacturing facility, together with two nearby facilities operated by Dow, emit less than half as much NO<sub>x</sub> and about 10 times more SO<sub>2</sub>. These differences in NO<sub>x</sub> and SO<sub>2</sub> emissions and the >6 km spatial separation of the plants allow unambiguous identification of the plumes from the clusters of facilities during the flight transects (Figure 4).

[21] The plumes from these and other nearby plants were sampled during two downwind transects on 28 August, corresponding to approximate times since emission of 0.6 and 2.0 hours for the Dow plant and 0.8 and 2.2 hours for the Gulf plant (Figure 4). The further transect showed increases in particle volume concentration of ~2 μm<sup>3</sup> cm<sup>-3</sup> above the surrounding background only in the plume of the Gulf plant, which is relatively rich in SO<sub>2</sub>. Particle number concentration was also substantially enhanced above background in the relatively SO<sub>2</sub>-rich Gulf plume, and not in the SO<sub>2</sub>-poor Dow plume. These findings are very similar to those reported in industrial and power plant plumes in the south central United States, in which substantial increases in particle mass concentration above background are found only in plumes from large sources of SO<sub>2</sub> [Brock *et al.*, 2002].

[22] The gas-phase photochemical reactivity of these isolated petrochemical plumes has been documented by Ryerson *et al.* (submitted manuscript, 2002). The plumes have substantial and similar OH reactivity due in large part to the coemission of reactive alkenes with NO<sub>x</sub>. Thus, if SO<sub>2</sub> is present, the oxidation of SO<sub>2</sub> by OH and the subsequent formation of condensable sulfate compounds is expected to proceed readily [Meng *et al.*, 1997; Hoppel *et al.*, 2001]. Measurements of the concentration of VOCs in the Dow and Gulf plumes indicate that both contain concentrations of aromatics and other VOC compounds well above background values (Table 2). Smog chamber studies using NO<sub>x</sub>-VOC mixtures and concentrations atypical of those found in these petrochemical plumes have demonstrated that aromatic compounds can oxidize in photochemically active environments to produce particulate organic material [e.g., Odum *et al.*, 1996, 1997a, 1997b]. However, among plumes from the isolated petrochemical facilities studied here, particle volume growth above background was detected in only the Gulf plume, which contained SO<sub>2</sub>. Oxidation and condensation of organic material in the SO<sub>2</sub>-poor Dow plume was insufficient to produce detectable enhancements in particle volume in the conditions measured.

## 4. Analysis

### 4.1. Particle Fluxes

[23] The relative contribution of each of the major sources of particle volume in the Houston area cannot be determined from the observed concentrations alone because of the different spatial extent of the plumes. To account for varying plume dispersion, the observed enhancements above background were integrated across the width of the plume following the study of Ryerson *et al.* [1998]. Background values were determined for each transect from measurements west of the Parish power plant plume and east of the ship channel plume. The horizontal fluxes of particle volume and number were then calculated for the plumes from Parish power plant, the Houston urban core, and the ship channel industries, using an average wind velocity of  $4.5 \pm 1$  m s<sup>-1</sup>. To estimate the fluxes, the plume is assumed to be vertically well mixed throughout the PBL. The PBL height has been estimated as a function of geographic position and time of day based on vertical profiles made by the Electra aircraft at the termini of some of the transects, on data from a network of meteorological microwave profilers, and on vertical profiles of aerosol backscatter from a lidar system [Senff *et al.*, 1998] operated aboard a DC-3 aircraft in the same region on 28 August. The height of the PBL increased significantly northward and westward of the coastline on both days as the marine air was advected toward the north and became modified by surface heat fluxes. The PBL heights used in the flux estimates ranged from 1.3 to 2.5 km.

[24] Aerosol particles produced from the Houston ship channel industries dominated the particle number and volume mass fluxes downwind of the Houston metropolitan area (Figure 5). At the furthest downwind distances, the particle volume flux from the ship channel industries exceeded that from the Parish power plant by a factor of ~4. The particle volume fluxes within the plume from the Houston urban core are difficult to estimate because there were only modest enhancements in particle volume above

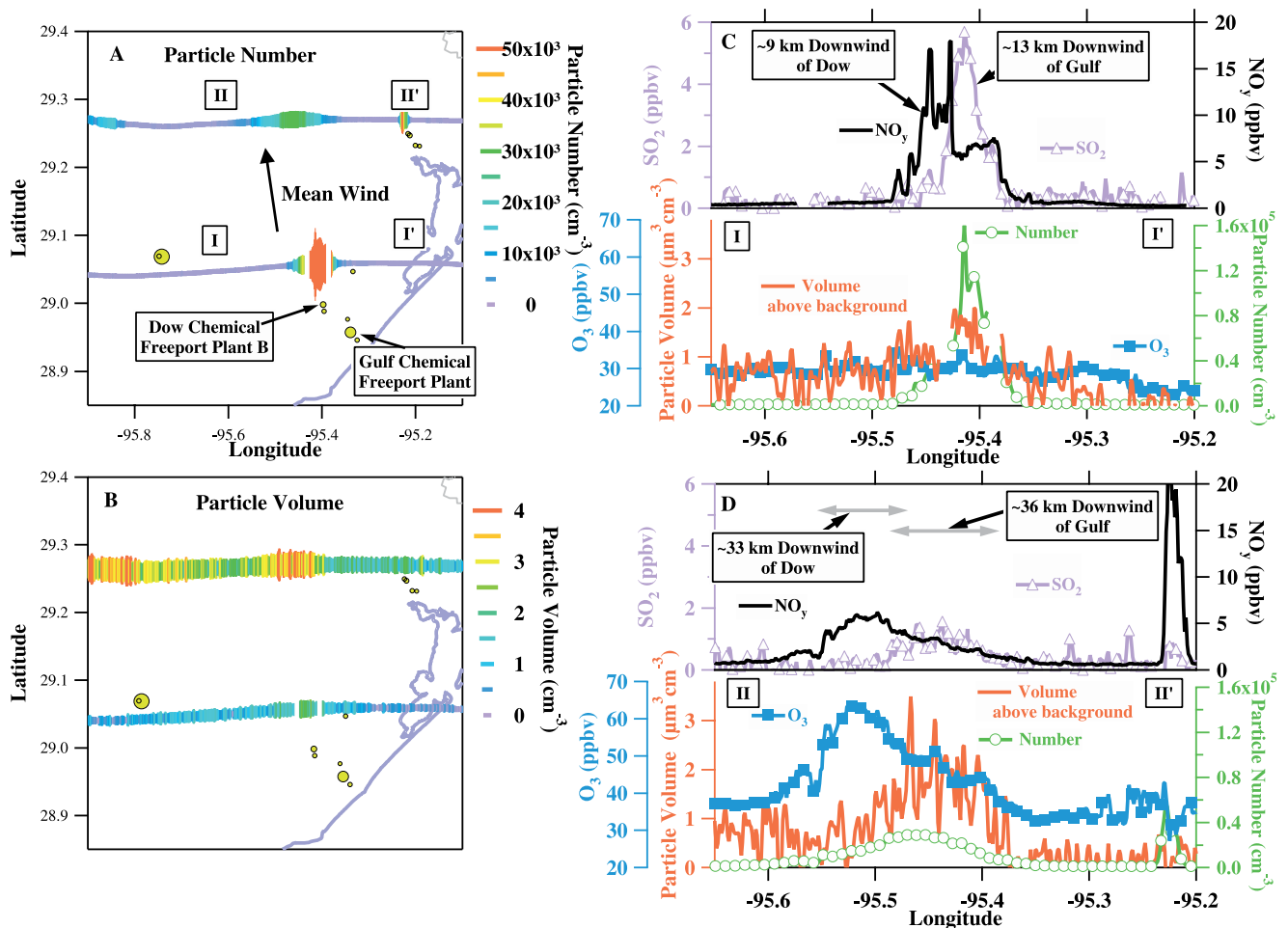


**Figure 4.** (a) Map of the coastal area south of Houston with flight track of the NCAR Electra aircraft during longitudinal transects (approximately perpendicular to the wind) within the PBL on 28 August 2000. The transects are color and size coded by particle number concentration. Portions of the flight track indicated by I-I' and II-II' are shown in (c) and (d). Significant sources of SO<sub>2</sub> are indicated by the circles, sized by annual emissions. The Texas coastline is in blue. (b) As in (a), but color and size coded by particle volume above background. (c) NO<sub>y</sub>, SO<sub>2</sub>, and O<sub>3</sub> mixing ratios and particle volume and number concentrations as a function of longitude for the portion of the transect indicated by I-I' in (a), close to isolated industrial facilities. (d) As in (c), but for transect II-II' in (a), further downwind of the industrial facilities.

the background, and because the Parish and ship channel plumes extended into the urban plume on either side. Because of this increasing encroachment of the surrounding industrial plumes into the Houston urban plume with increasing distance, the particle number and volume fluxes reported for the urban plume are upper limit estimates. For plume ages >3 hours, the particle volume flux within the Houston urban plume was ~1/2 that from the Parish power plant. Note that the particle volume fluxes from the ship channel industries and the Parish power plant continued to increase up to the maximum measured plume age, indicating continuing particle mass growth from gas-to-particle conversion in these plumes.

#### 4.2. Sulfur Gas-to-Particle Conversion

[25] Particle volume concentration was positively correlated with SO<sub>2</sub> mixing ratio within the plume of the Parish power plant and within the plume from industries along the

Houston ship channel. These data may be used to test if the observed increase in particle volume with increasing plume age is consistent with oxidation of SO<sub>2</sub> by OH and subsequent condensation of the sulfate oxidation products. This test involves assuming a composition for the particles and then examining the derived sulfur budget of the plume compared with that calculated with a numerical model of plume chemistry. Unpublished data from the TexAQS 2000 mission (R. Weber, personal communication, 2001) indicate that the sulfate aerosol within the Houston area during afternoons was usually fully neutralized by ammonium. If all of the enhancement in dry particle volume observed within a transect of a plume were caused by formation of (NH<sub>4</sub>)<sub>2</sub>SO<sub>4</sub>, the fraction of total plume sulfur (particulate sulfur + SO<sub>2</sub>) within the particles can be calculated from the measurements. With increasing plume age, and dependent upon the plume NO<sub>x</sub> and VOC concentrations and insolation, the slope of the regression between particulate and

**Table 2.** Measured Concentrations of Nonmethane Hydrocarbons (NMHCs) and Aromatics in Selected Petrochemical Plumets

Source	Distance Downwind (km)	Plume Age (hours)	$\Sigma$ NMHCs (ppbv)	$\Sigma$ aromatics (ppbv)
27 August 1999				
Gulf of Mexico (background)	NA <sup>a</sup>	NA	0.98	0.025
Gulf Plant	13	0.8	4.81	0.27
Gulf + Dow	~34	~2	3.09	0.13
Gulf + Dow	~34	~2	4.44	0.15
Ship Channel (west side)	~8	~0.5	5.97	0.54
Ship Channel (east side)	~8	~0.5	29.8	1.59
Ship Channel (west side)	27	1.7	22.6	0.96
28 August 1999				
Gulf of Mexico (background)	NA	NA	1.12	0.028
Gulf Plant	13	0.8	5.02	0.43
Dow Plant	9	0.6	9.20	0.37
Dow Plant	33	2.0	5.67	0.099
Ship Channel (west side)	~8	~0.5	45.9	1.79
Ship Channel (east side)	~8	~0.5	28.7	0.51
Ship Channel (west side)	24	1.5	23.6	1.09
Ship Channel (east side)	24	1.5	19.2	1.01

<sup>a</sup>NA: Not applicable.

total plume sulfur should increase as a larger fraction of the SO<sub>2</sub> is oxidized by OH and the resulting sulfuric acid condenses on the particles and is neutralized to form (NH<sub>4</sub>)<sub>2</sub>SO<sub>4</sub> (Figure 6). This analysis is dependent upon the assumption that the particles are composed of (NH<sub>4</sub>)<sub>2</sub>SO<sub>4</sub>, and the absence of substantial loss of plume sulfur through aqueous oxidation and dry deposition. In-cloud oxidation of SO<sub>2</sub> is believed to have been negligible because there were only scattered cumulus clouds on 27 and 28 August in the study region, and because, as discussed later, the ratio of SO<sub>2</sub> to NO<sub>y</sub> within the plumes did not vary substantially as a function of plume age. Loss of SO<sub>2</sub> due to dry deposition is not negligible, but will be ignored for the moment since it is incorporated in the numerical model of plume chemistry with which these data will be compared.

[26] Under these assumptions, the fraction of plume sulfur observed in the particulate phase (the slopes in Figure 6) should increase with increasing integrated exposure of emitted SO<sub>2</sub> to OH. If the assumptions regarding particle composition and losses of SO<sub>2</sub> are correct, the fraction should reach one when all of the SO<sub>2</sub> in the plume has oxidized and been converted to particulate (NH<sub>4</sub>)<sub>2</sub>SO<sub>4</sub>. For the greatest plume age, 5.7 hours, the particulate sulfur fraction derived from the observations is 0.76 (Figure 6). However, based on plume flux estimates, only a small fraction (less than ~30%) of the SO<sub>2</sub> within the plume had been oxidized at this plume age. If a less neutralized sulfate composition, such as (NH<sub>4</sub>)HSO<sub>4</sub> or H<sub>2</sub>SO<sub>4</sub>, is assumed, an even higher fraction of plume sulfur would be calculated to reside in the particulate phase. These discrepancies strongly suggest that the assumed predominantly sulfate composition is incorrect, and that compounds other than (NH<sub>4</sub>)<sub>2</sub>SO<sub>4</sub>, such as nitrates or organics, contributed to most of the observed particle growth in the plume from the petrochemical industries along the Houston ship channel.

[27] This regression approach can be used to compare particle growth as a function of plume age among plumes from different sources with different emission characteristics. However, the oxidation rate of SO<sub>2</sub> is strongly affected by the concentration of OH, which in turn is highly depend-

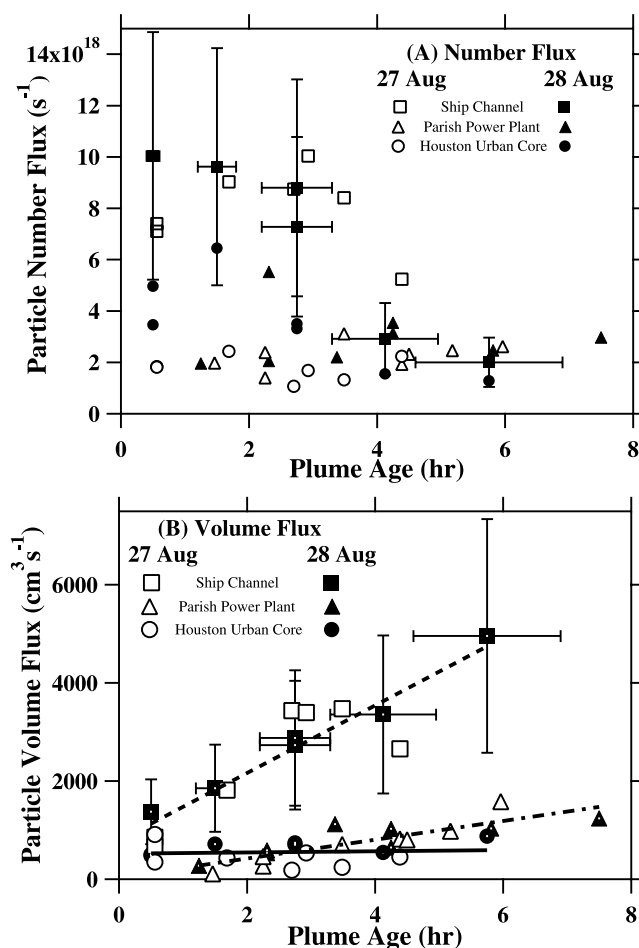


**Figure 5.** Horizontal flux of particle number (a) and volume (b) within the PBL from three different sources in the vicinity of the Houston metropolitan area as measured on 27 and 28 August 2000. Error bars (shown for a subset of the data for clarity) are calculated in quadrature from measurement uncertainties and estimated uncertainties in determining wind speed and boundary layer height.

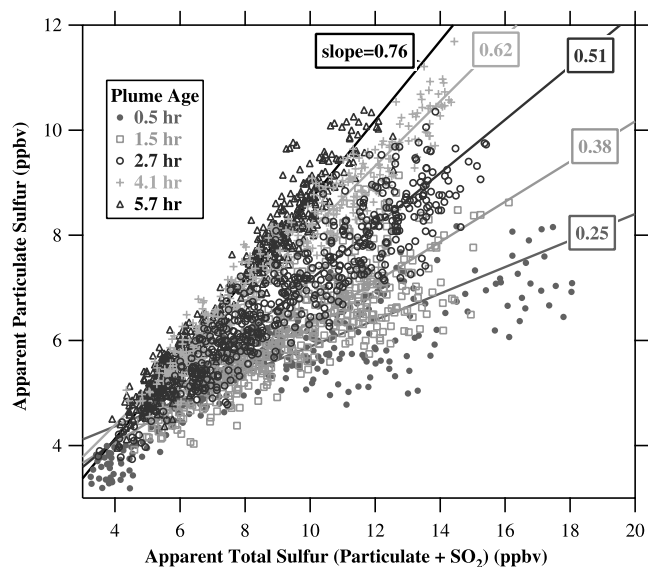


**Figure 6.** Apparent mixing ratio of sulfur in particles within the plume from the Houston ship channel industries calculated from observed particle volume assuming a composition of  $(\text{NH}_4)_2\text{SO}_4$ , plotted as a function of total plume sulfur (measured  $\text{SO}_2$  + apparent particulate sulfur). Lines are least squares univariate linear regressions from data obtained on 28 August 2000 in the merged plumes of the industries located along the Houston ship channel during five different transects downwind. Since depositional and aqueous losses of  $\text{SO}_2$  are small over the time period of the observations, the increase in slopes of the regression lines with increasing plume age is attributed to gas-to-particle conversion within the plume.

ent upon  $\text{NO}_x$  and insolation, and will also differ between plumes depending on hydrocarbon concentrations and reactivity. Therefore, time since emission (plume age) does not effectively represent the photochemical oxidation history of a given plume parcel. Because  $\text{HNO}_3$  is produced by oxidation of  $\text{NO}_2$  by OH, the fraction of total odd nitrogen ( $\text{NO}_y$ ) converted to  $\text{HNO}_3$  is a better proxy for the integrated exposure of the plume to OH. The calculated fraction of total plume sulfur found in the particulate phase increases with increasing  $\text{HNO}_3/\text{NO}_y$  for both the Parish and ship channel plumes on both 27 and 28 August (Figure 7). The apparent particulate sulfur fraction at a given value of  $\text{HNO}_3/\text{NO}_y$  is substantially greater in the plume from the Houston ship channel than in that from the Parish power plant. Because particle volume, rather than mass, was measured, this difference between the plumes is critically dependent upon the assumption of a particle composition of  $(\text{NH}_4)_2\text{SO}_4$ . For example, if the particles in the ship channel plume are composed of a mixture of 30% by mass of organics (with a density of  $\sim 1 \text{ g cm}^{-3}$ ) and 70%  $(\text{NH}_4)_2\text{SO}_4$  (with a density of  $\sim 1.8 \text{ g cm}^{-3}$ ), the actual particulate sulfur mass is lower by almost a factor of 2 compared with that calculated assuming a composition of pure  $(\text{NH}_4)_2\text{SO}_4$ . This analysis also assumes that the only substantial loss of  $\text{SO}_2$  is due to oxidation and conversion to aerosol sulfate. Because the ratio of  $\text{SO}_2$  to  $\text{NO}_y$  remained approximately constant with increasing plume age (Figure 8), there do not appear to have

been substantial sinks (such as aqueous reactions) that preferentially removed  $\text{SO}_2$ .

[28] The particulate sulfur fraction derived from the observations can be compared with the results from a numerical model of plume mixing and photochemistry that includes  $\text{SO}_2$  oxidation processes. A Lagrangian model [Trainer *et al.*, 1991; Wert *et al.*, 2003; Brock *et al.*, 2002] was initialized with inventoried emissions of  $\text{NO}_x$  and  $\text{SO}_2$  in the Parish plume and inventoried  $\text{NO}_x$  and observed  $\text{SO}_2$  in the ship channel plume. Emissions of VOCs were estimated using their measured mixing ratios relative to  $\text{NO}_y$  (for which demonstrably accurate emission rates are known), after accounting for the expected oxidation of the VOCs by OH since emission. The Gaussian dispersion of the plume was prescribed to match the observed plume dimensions. The model successfully simulates observed  $\text{O}_3$  formation rates and yields (Ryerson *et al.*, submitted manuscript, 2002),  $\text{NO}_y$  partitioning [Neuman *et al.*, 2002], and formaldehyde production [Wert *et al.*, 2003] in the ship channel and Parish plume. The model includes  $\text{SO}_2$  loss via reaction by OH and by dry deposition. Sulfur molecules oxidized by OH in the model are presumed to rapidly form condensable products and transfer to the particulate phase.

[29] The model predicts a conversion of  $\text{SO}_2$  to condensable sulfate as a function of  $\text{HNO}_3/\text{NO}_y$  that is approximately half of the central values calculated from observed particle growth in the  $\text{SO}_2$ -rich plume from the Parish power plant as it advected over terrain with low isoprene emissions and rural and suburban land use patterns (Figure 7). However, the modeled sulfur conversion fraction is still within the uncertainty estimate for the particulate sulfur fraction calculated from the observations using a compositional assumption of  $(\text{NH}_4)_2\text{SO}_4$ . In contrast to this relatively good agreement between model and measurement within the power plant plume, the model underpredicts particle growth in the VOC-rich and  $\text{SO}_2$ -rich plume from the combined industries located along the Houston ship channel by a factor ranging between 2 and 10 compared with the uncertainty range of the observations. The model accurately replicates observed gas-phase speciation and mixing ratios within the plume of the ship channel industries, implying that modeled OH concentrations are substantially correct. Also, the model faithfully simulates the observed  $\text{SO}_2/\text{NO}_y$  ratios with increasing plume age (Figure 8), indicating that the heterogeneous  $\text{SO}_2$  oxidation is not important in this data set and that the dry deposition parameterization in the model is appropriate. Therefore, the difference in particulate sulfur fraction between the model and measurements is probably caused by the assumption that the observed particle volume growth is due solely to the condensation of sulfate compounds and the subsequent formation of aerosol  $(\text{NH}_4)_2\text{SO}_4$ . The most likely explanation for the discrepancy (one supported by ground-based observations of submicron particle chemistry made a few km south of the ship channel during the TexAQS 2000 project (D. Worsnop, personal communication, 2002)) is that gas-to-particle conversion of organic matter produces a substantial fraction of the observed particle volume growth within the oxidized ship channel plume. Condensation of smaller quantities of organic matter, as well as area-source contributions to the particle loading, may explain why the model results for the Parish power plant plume are at the

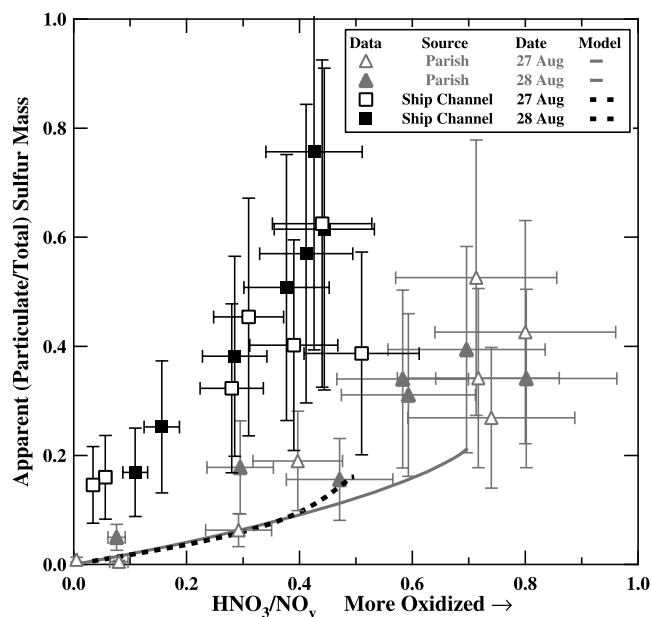


**Figure 7.** Apparent fraction of total plume sulfur in the particulate phase, determined as in Figure 6, plotted as a function of measured fraction of  $\text{NO}_y$  converted to  $\text{HNO}_3$  (an indicator of total OH exposure). Particles are assumed to be composed of  $(\text{NH}_4)_2\text{SO}_4$ . Lines give the same parameters determined from a Lagrangian model of plume chemistry (see text). Measured data and model calculations are for the plume of the Parish power plant (triangles and solid curve) and the merged ship channel industries (squares and dashed curve).

bottom limit of agreement with the observations within experimental uncertainties.

## 5. Discussion and Summary

[30] There are three principal findings to this work: (1) the petrochemical industries located along the Houston ship channel are the predominant source of particle number and volume (mass) flux downwind of the Houston metropolitan area, followed in importance by the Parish power plant and the urban core of Houston; (2) substantial increases in particle volume concentration with increasing plume age, indicating conversion of gas-phase compounds to the particulate phase, were found in only those plumes with detectable enhancements in  $\text{SO}_2$ ; and (3) the particle growth in the plume of the Parish power plant was generally consistent with the condensation of the oxidation products of  $\text{SO}_2$  alone, while particle growth within the VOC-rich ship channel plume exceeded that expected solely from  $\text{SO}_2$  oxidation.

[31] Prior research [e.g., Hewitt, 2001; Brock et al., 2002] has shown that particle mass fluxes from urban areas are often smaller than those within oxidized plumes from nearby, large point sources of  $\text{SO}_2$ . Similarly, the data presented here show that the particle volume flux within the oxidized plume from the Parish power plant exceeds that from the Houston urban core. What is more surprising is the observed association between  $\text{SO}_2$  and particle volume in oxidized plumes downwind of petrochemical industries. One might expect particle growth in such plumes even in the

absence of  $\text{SO}_2$ , since smog chamber and field studies in heavily urbanized areas such as Los Angeles show substantial organic particle formation and growth in environments rich in  $\text{NO}_x$  and VOCs even in the absence of much  $\text{SO}_2$  [e.g., Collins et al., 2000; Jacobson et al., 2000; Turpin and Huntzicker, 1991; Odum et al., 1996, 1997a, 1997b]. However, these studies were accomplished with VOC mixtures and concentrations that may not be representative of those found in the plumes from the Houston petrochemical industries. In Houston, recent new particle formation and volume growth due to vapor condensation was evident in only those plumes characterized by detectable enhancements in  $\text{SO}_2$ . Yet, the amount of growth observed in the combined plume from the industries along the Houston ship channel was substantially greater than could be accounted for by condensation of the oxidation products of  $\text{SO}_2$  alone, suggesting a linkage between sulfate and organic gas-to-particle conversion. Ground-based observations of particle composition at the LaPorte municipal airport a few km south of the ship channel support this speculation. Organic matter, which contributed >30% of the total volatile submicron particle mass during afternoon, photochemically active periods during the TexAQS 2000 project, was positively correlated with ammonium and sulfate, which contributed ~30–50% of the total volatile submicron mass during the same periods (D. Worsnop, personal communication, 2002).

[32] The partitioning of the semivolatile products of VOC oxidation between the gas and particulate phase is an area of active research. There are few data available on particle formation in VOC-rich mixtures at concentrations representative of actual atmospheric conditions. However, smog

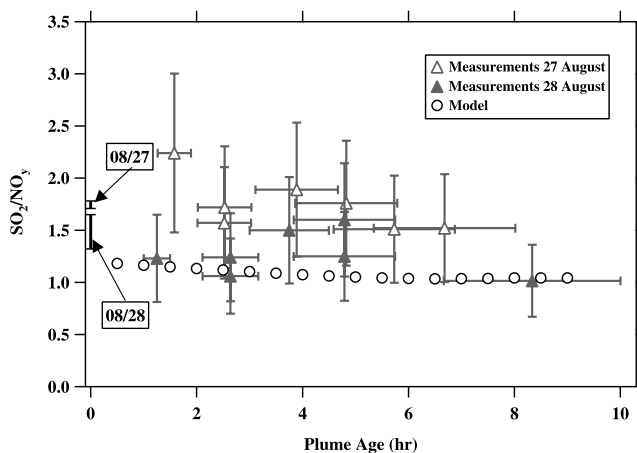


**Figure 8.** Ratios of  $\text{SO}_2/\text{NO}_y$  observed as a function of the age of the Parish power plant plume on 27 and 28 August 2000 (triangles) and calculated from the photochemical plume model (circles). The vertical bars at a plume age of 0 hour show the range of  $\text{SO}_2/\text{NO}_x$  (virtually all  $\text{NO}_y$  emissions initially are in the form of  $\text{NO}_x$ ) reported hourly from chemical emissions monitoring equipment at the power plant for the times corresponding to the emission times of the sampled plumes. There is no substantial change in the  $\text{SO}_2/\text{NO}_y$  ratio with increasing plume age in either the model or the measurements, indicating that there is little heterogeneous oxidation of  $\text{SO}_2$  and that the gas-phase oxidation and dry deposition processes within the model adequately represent the actual  $\text{SO}_2$  losses.

chamber measurements of the fraction of organic matter forming in the particulate phase are in general agreement with absorptive partitioning theory for high concentrations of relatively simple mixtures of aromatic compounds [e.g., Odum *et al.*, 1996, 1997a, 1997b]. This theory indicates only a few to several percent of the total aromatic mass should oxidize, form semivolatile products, and partition to the particulate phase. Analysis of air samples collected during transects ~8 km downwind of the ship channel industries on both 27 and 28 August 2000 show mixing ratios of aromatic compounds (the only VOC aerosol precursors sampled) summing to <2 ppbv (Table 2). These mixing ratios are insufficient to explain the observed aerosol mass growth using absorptive partitioning theory in the absence of other unmeasured condensable organic species. Substantial quantities of unmeasured VOC compounds, such as organic acids, could have been present and served as the parent material for the formation of condensable organic mass. Alternately, heterogeneous mechanisms for the formation of secondary organic particle mass, such as acid-catalyzed reactions [e.g., Jang and Kamens, 2001], may have contributed the apparent organic particle formation within the plume of the Houston ship channel, and might explain the observed association of the particle growth with enhanced SO<sub>2</sub> concentrations.

[33] Flagan *et al.* [1991] and Hoppel *et al.* [2001] found that, in initially particle-free air rich in NO<sub>x</sub> and reactive VOCs in smog chambers, very rapid particle nucleation and growth occurred when SO<sub>2</sub> was added to the system. Without SO<sub>2</sub>, the onset of detectable particle formation and condensational growth was substantially delayed and the initial rates of growth were smaller. Flagan *et al.* did not quantitatively determine whether the observed particle formation and volume growth was consistent with the mass budget of organic matter and SO<sub>2</sub> within the smog chamber. Hoppel *et al.* found that there was no detectable change in particulate organic yield whether SO<sub>2</sub> was present or absent. In neither experiment was the mix or concentration of reactive VOCs within the smog chamber representative of that found in the plumes of the petrochemical plants studied during TexAQS 2000. Further laboratory studies of particle mass growth and composition using SO<sub>2</sub>, NO<sub>x</sub>, and reactive VOC compounds at mixing ratios and timescales similar to those reported here may help elucidate the processes leading to particle formation and growth within the Houston metropolitan area.

[34] **Acknowledgments.** We thank the management, staff, and flight crew from the NCAR Research Aviation Facility for their exceptional support during this field mission and the preceding instrument integration. We also thank F. Brechtel, M. Canagaratna, J. Jimenez, R. Weber, and D. Worsnop for their contributions and comments. This work was supported in part by the TNRC and the NOAA Health of the Atmosphere and Climate and Global Change Programs.

## References

- Brock, C. A., F. Schröder, B. Kärcher, A. Petzold, R. Busen, and M. Fiebig, Ultrafine particle size distributions measured in aircraft exhaust plumes, *J. Geophys. Res.*, *105*, 26,555–26,567, 2000.
- Brock, C. A., *et al.*, Particle growth in the plumes of coal-fired power plants, *J. Geophys. Res.*, *107*, 4155, doi:10.1029/2001JD001062, 2002.
- Collins, D. R., H. H. Jonsson, H. Liao, R. C. Flagan, J. H. Seinfeld, K. J. Noone, and S. V. Hering, Airborne analysis of the Los Angeles aerosol, *Atmos. Environ.*, *34*, 3155–3173, 2000.
- Dreher, D. B., and R. A. Harley, A fuel-based inventory for heavy-duty diesel truck emissions, *J. Air Waste Manage. Assoc.*, *48*, 352–358, 1998.
- Flagan, R. C., S.-C. Wang, F. Yin, J. H. Seinfeld, G. Reischl, W. Winklmayr, and R. Karch, Electrical mobility measurements of fine-particle formation during chamber studies of atmospheric photochemical reactions, *Environ. Sci. Technol.*, *25*, 883–890, 1991.
- Heidt, L. E., J. F. Vedder, W. H. Pollock, R. A. Lueb, and B. E. Henry, Trace gases in the Antarctic atmosphere, *J. Geophys. Res.*, *94*, 11,599–11,611, 1989.
- Hewitt, C. N., The atmospheric chemistry of sulphur and nitrogen in power station plumes, *Atmos. Environ.*, *35*, 1155–1170, 2001.
- Hoppel, W., *et al.*, Particle formation and growth from ozonolysis of  $\alpha$ -pinene, *J. Geophys. Res.*, *106*, 27,603–27,618, 2001.
- Jacobson, M. C., H.-C. Hansson, K. J. Noone, and R. J. Charlson, Organic atmospheric aerosols: Review and state of the science, *Rev. Geophys.*, *38*, 267–294, 2000.
- Jang, M., and R. M. Kamens, Atmospheric secondary aerosol formation by heterogeneous reactions of aldehydes in the presence of a sulfuric acid aerosol catalyst, *Environ. Sci. Technol.*, *35*, 4758–4766, 2001.
- Jonsson, H. H., *et al.*, Performance of a focused-cavity aerosol spectrometer for measurements in the stratosphere of particle size in the 0.06–2.0  $\mu$ m diameter range, *J. Atmos. Oceanic Technol.*, *12*, 115–129, 1995.
- Kleinman, L. I., P. H. Daum, D. Imre, Y.-N. Lee, L. J. Nunnermacker, S. R. Springston, J. Weinstein-Lloyd, and J. Rudolph, Ozone production rate and hydrocarbon reactivity in 5 urban areas: A cause of high ozone concentration in Houston, *Geophys. Res. Lett.*, *29*, 10.1029–10.1033, 2002.
- Marr, L. C., D. R. Black, and R. A. Harley, Formation of photochemical air pollution in central California, I, Development of a revised motor vehicle emission inventory, *J. Geophys. Res.*, *107*, doi:10.1029/2001JD000689, 2002.
- Meng, Z., D. Dabdub, and J. H. Seinfeld, Chemical coupling between atmospheric ozone and particulate matter, *Science*, *277*, 116–119, 1997.
- Neuman, J. A., *et al.*, Fast-response airborne in situ measurements of HNO<sub>3</sub> during the Texas 2000 Air Quality Study, *J. Geophys. Res.*, *107*, doi:10.1029/2001JD001437, 2002.
- Odum, J. R., T. Hoffmann, F. Bowman, D. Collins, R. C. Flagan, and J. H. Seinfeld, Gas/particle partitioning and secondary organic aerosol yields, *Environ. Sci. Technol.*, *30*, 2580–2585, 1996.
- Odum, J. R., T. P. W. Jungkamp, R. J. Griffin, H. J. L. Forstner, R. C. Flagan, and J. H. Seinfeld, Aromatics, reformulated gasoline, and atmospheric organic aerosol formation, *Environ. Sci. Technol.*, *31*, 1890–1897, 1997a.
- Odum, J. R., T. P. W. Jungkamp, R. J. Griffin, R. C. Flagan, and J. H. Seinfeld, The atmospheric aerosol-forming potential of whole gasoline vapor, *Science*, *276*, 96–99, 1997b.
- Ryerson, T. B., *et al.*, Emissions lifetimes and ozone formation in power plant plumes, *J. Geophys. Res.*, *103*, 22,569–22,583, 1998.
- Ryerson, T. B., *et al.*, Observations of ozone formation in power plant plumes and implications for ozone control strategies, *Science*, *292*, 719–723, 2001.
- Schauffler, S., E. Atlas, D. Blake, F. Flocke, R. Lueb, J. Lee-Taylor, V. Stroud, and W. Travnicek, Distributions of brominated organic compounds in the troposphere and lower stratosphere, *J. Geophys. Res.*, *104*, 21,513–21,535, 1999.
- Senff, C. J., R. M. Hardesty, R. J. Alvarez II, and S. D. Mayor, Airborne lidar characterization of power plant plumes during the Southern Oxidants Study, *J. Geophys. Res.*, *103*, 31,173–31,189, 1998.
- Trainer, M., M. P. Buhr, C. M. Curran, F. C. Fehsenfeld, E. Y. Hsie, S. C. Liu, R. B. Norton, D. D. Parrish, and E. J. Williams, Observations and modeling of the reactive nitrogen photochemistry at a rural site, *J. Geophys. Res.*, *96*, 3045–3063, 1991.
- Turpin, B. J., and J. J. Huntzicker, Secondary formation of organic aerosol in the Los Angeles Basin: A descriptive analysis of organic and elemental carbon concentrations, *Atmos. Environ.*, *25A*, 207–215, 1991.
- Wert, B. P., *et al.*, Signatures of terminal alkene oxidation in airborne formaldehyde measurements during TexAQS 2000, *J. Geophys. Res.*, *108*, doi:10.1029/2002JD002502, in press, 2003.

E. L. Atlas, S. G. Donnelly, S. M. Schauffler, V. R. Stroud, and C. Wiedinmyer, Atmospheric Chemistry Division, National Center for Atmospheric Research, Boulder, CO 80307, USA.

C. A. Brock, F. C. Fehsenfeld, G. J. Frost, J. S. Holloway, G. Hübler, J. A. Neuman, D. K. Nicks Jr., D. D. Parrish, T. B. Ryerson, and M. Trainer, Aeronomy Laboratory, National Oceanic and Atmospheric Administration, Boulder, CO 80306, USA. (cbrock@al.noaa.gov)

H. Hilbert, B. G. Lafleur, J. M. Reeves, and J. C. Wilson, Department of Engineering, University of Denver, Denver, CO 80208, USA.

**Effect of petrochemical industrial emissions of reactive alkenes  
and NO<sub>x</sub> on tropospheric ozone formation in Houston, TX**

**by**

T.B. Ryerson, M. Trainer, W.M. Angevine, C.A. Brock, R.W. Dissly, F.C. Fehsenfeld,  
G.J. Frost, P.D. Goldan, J.S. Holloway, G. Hübler, R.O. Jakoubek, W.C. Kuster, J.A.  
Neuman, D.K. Nicks Jr., D.D. Parrish, J.M. Roberts, and D.T. Sueper



1 **Effect of petrochemical industrial emissions of reactive alkenes and NO<sub>x</sub> on tropospheric**  
2 **ozone formation in Houston, TX**

3

4 T.B. Ryerson, M. Trainer, W.M. Angevine<sup>1</sup>, C.A. Brock<sup>1</sup>, R.W. Dissly<sup>1\*</sup>, F.C. Fehsenfeld<sup>1</sup>, G.J.  
5 Frost<sup>1</sup>, P.D. Goldan, J.S. Holloway<sup>1</sup>, G. Hübler<sup>1</sup>, R.O. Jakoubek, W.C. Kuster, J.A. Neuman<sup>1</sup>,  
6 D.K. Nicks Jr.<sup>1</sup>, D.D. Parrish, J.M. Roberts, and D.T. Sueper<sup>1</sup>

7 Aeronomy Laboratory, National Oceanic and Atmospheric Administration, Boulder, CO

8

9 E.L. Atlas, S.G. Donnelly, F. Flocke, A. Fried, W.T. Potter, S. Schauffler, V. Stroud, A.J.

10 Weinheimer, B.P. Wert, and C. Wiedinmyer

11 Atmospheric Chemistry Division, National Center for Atmospheric Research, Boulder, CO

12

13 R.J. Alvarez<sup>1</sup>, R.M. Banta, L.S. Darby<sup>1</sup>, and C.J. Senff<sup>1</sup>

14 Environmental Technology Laboratory, National Oceanic and Atmospheric Administration,

15 Boulder, CO

16

17 <sup>1</sup>also with Cooperative Institute for Research in Environmental Sciences, University of Colorado,

18 Boulder, CO

19 \*now at Ball Aerospace Corporation, Boulder, CO

20

21 **Abstract.** Petrochemical industrial facilities can emit large amounts of highly reactive  
22 hydrocarbons and NO<sub>x</sub> to the atmosphere; in the summertime, such co-located emissions are shown  
23 to consistently result in rapid and efficient ozone formation downwind. Airborne measurements  
24 show initial hydrocarbon reactivity in petrochemical source plumes in the Houston, TX metropolitan  
25 area is primarily due to routine emissions of the alkenes propene (C<sub>3</sub>H<sub>6</sub>) and ethene (C<sub>2</sub>H<sub>4</sub>).

26 Reported emissions of these highly reactive compounds are substantially lower than emissions

27 inferred from measurements in the plumes from these sources. Net ozone formation rates and

1 yields per  $\text{NO}_x$  molecule oxidized in these petrochemical industrial source plumes are substantially  
2 higher than rates and yields observed in urban or rural power plant plumes. These observations  
3 suggest that reductions in reactive alkene emissions from petrochemical industrial sources are  
4 required to effectively address the most extreme ozone exceedences in the Houston metropolitan  
5 area.

6

## 7 **1. Introduction**

8 Ozone ( $\text{O}_3$ ) is formed in the troposphere by photochemical reactions involving the oxides of  
9 nitrogen  $\text{NO}$  and  $\text{NO}_2$  (summed as  $\text{NO}_x$ ) and reactive volatile organic compounds (VOCs)  
10 [Crutzen, 1979; Haagen-Smit, 1952; Leighton, 1961; Levy, 1971]. Model studies have shown that  
11 ozone formation rates and yields are dependent upon both the absolute concentrations of  $\text{NO}_x$  and  
12 VOCs and upon the ratios of these species (e.g., [Derwent and Davies, 1994; Liu *et al.*, 1987;  
13 Sillman, 2000]). Results from ambient measurements have confirmed that substantial differences in  
14 the rate and magnitude of ozone production consistently occur in plumes downwind of different  
15 anthropogenic source types, characterized by different  $\text{NO}_x$  and VOC emissions rates and the  
16 VOC/ $\text{NO}_x$  ratios that result (e.g., [Daum *et al.*, 2000a; Gillani *et al.*, 1998; Luria *et al.*, 2000;  
17 Neuman *et al.*, 2002; Nunnermacker *et al.*, 2000; Ryerson *et al.*, 1998; Ryerson *et al.*, 2001]).

18 Three anthropogenic source types with contrasting emissions rates and VOC/ $\text{NO}_x$  ratios are  
19 fossil-fueled electric power plants, the transportation sources typical of urban areas, and the  
20 petrochemical industry. The first two combined account for approximately 75% of total U.S.  
21 anthropogenic  $\text{NO}_x$  emissions annually [EPA, 2001]. Fossil-fueled electric power plants are very  
22 concentrated point sources of  $\text{NO}_x$  but do not emit appreciable amounts of VOCs. Thus, ozone  
23 production observed in plumes downwind of isolated, rural power plants in the U.S. (e.g., [Davis *et*  
24 *al.*, 1974]) occurs as a result of mixing plume  $\text{NO}_x$  with primarily biogenic reactive VOCs,  
25 especially with isoprene [Chameides *et al.*, 1988; Trainer *et al.*, 1987a; Trainer *et al.*, 1987b], over  
26 time during plume transport. Measurements confirm the strong dependence of ozone production

1 on NO<sub>x</sub> concentration [Gillani *et al.*, 1998; Nunnermacker *et al.*, 2000; Ryerson *et al.*, 1998] and  
2 on ambient VOC concentration and reactivity [Luria *et al.*, 2000; Ryerson *et al.*, 2001].

3 Power plant plume VOC/NO<sub>x</sub> ratios can be sufficiently low that ozone formation is initially  
4 suppressed in favor of efficient nitric acid (HNO<sub>3</sub>) production, removing NO<sub>x</sub> from further  
5 participation in ozone formation cycles [Neuman *et al.*, 2002; Ryerson *et al.*, 2001]. In contrast, the  
6 tailpipe emissions that dominate urban areas are sources of both NO<sub>x</sub> and VOCs. The many small  
7 individual sources contributing to urban emissions are usually considered together as an area  
8 source dispersed over tens to hundreds of square kilometers. As a result, urban plumes are  
9 relatively dilute, with total NO<sub>x</sub> emissions rates comparable to those from power plants but  
10 dispersed over a much larger area. Co-emission in this manner results in initial VOC/NO<sub>x</sub> ratios  
11 that favor ozone formation immediately upon emission, typically leading to faster ozone production  
12 rates and higher yields in urban plumes than in concentrated power plant plumes [Daum *et al.*,  
13 2000a; Luria *et al.*, 1999; Nunnermacker *et al.*, 2000].

14 The fastest rates of ozone formation, and the highest yields per NO<sub>x</sub> molecule emitted, are  
15 predicted for conditions where strongly elevated concentrations of NO<sub>x</sub> and reactive VOCs are  
16 simultaneously present. These conditions can be routinely found in the NO<sub>x</sub>- and VOC-rich  
17 plumes from petrochemical industrial facilities (e.g., [Sexton and Westberg, 1983]). Petrochemical  
18 NO<sub>x</sub> emissions are a byproduct of fossil-fuel combustion for electric power generation, for heat  
19 generation, and from flaring of unwanted volatile materials; NO<sub>x</sub> emission from a large  
20 petrochemical facility can approach that from a large electric utility power plant. While a given  
21 facility may have hundreds of combustion sources, spread over many square kilometers, the  
22 majority of petrochemical NO<sub>x</sub> emissions typically come from only a few of the largest sources.  
23 Thus, concentrations of NO<sub>x</sub> in plumes from large petrochemical facilities are typically much higher  
24 than in those from urban areas. Sources of VOC emissions from a petrochemical industrial facility  
25 are thought to be much more numerous than sources of NO<sub>x</sub>. VOCs can be emitted via continuous  
26 emissions from stacks, episodic emissions specific to individual processes, and leaks from pipes  
27 and valving. The wide variety of VOC compounds typically emitted from petrochemical facilities,

1 with differing reactivities toward the hydroxyl radical (OH), must be considered to understand the  
2 ozone-forming potential of these sources [*Carter, 1994; Derwent, 2000; Watson et al., 2001*].

3 The greater Houston, TX metropolitan area is distinguished by the largest concentration of  
4 petrochemical industrial facilities in the United States (Plate 1). Further, Houston is noted for some  
5 of the highest ozone mixing ratios routinely encountered in the continental U.S. in the present day.  
6 As a result, photochemical ozone and aerosol production in the Houston area was the focus of the  
7 Texas Air Quality Study 2000 field project [*Brock et al., 2002; Kleinman et al., 2002; Neuman et*  
8 *al., 2002; Wert et al., 2002*]. We report measurements taken from an instrumented aircraft during  
9 that project to evaluate the effects of petrochemical industrial emissions on tropospheric ozone  
10 formation. First, we analyze ozone production in spatially-resolved plumes from the geographically  
11 isolated complexes at Sweeny, Freeport, and Chocolate Bayou (Plate 1). We then extend this  
12 analysis to include data from coalesced plumes downwind of multiple petrochemical complexes in  
13 the heavily industrialized Houston Ship Channel and Texas City areas. Finally, ozone production  
14 in petrochemical industrial plumes is compared to that observed downwind of urban areas and rural,  
15 fossil-fueled electric utility power plants.

16

## 17 **2. Experimental procedure**

18 The National Center for Atmospheric Research L-188C Electra aircraft leased by the  
19 National Oceanic and Atmospheric Administration (NOAA) was based at Ellington Field, Houston,  
20 TX as part of the Texas Air Quality Study in August and September 2000. Instrumentation aboard  
21 the Electra included 1-Hz measurements of ozone ( $O_3$ ), nitric oxide (NO), nitrogen dioxide ( $NO_2$ ),  
22  $HNO_3$ , total reactive nitrogen ( $NO_y$ ), carbon monoxide (CO), carbon dioxide ( $CO_2$ ), sulfur dioxide  
23 ( $SO_2$ ), and spectrally-resolved actinic flux [*Holloway et al., 2000; Neuman et al., 2002; Nicks et al.,*  
24 *2002; Ryerson et al., 1998; Ryerson et al., 1999; Ryerson et al., 2000*]. Formaldehyde ( $CH_2O$ ) was  
25 measured by tunable diode laser absorption spectrometry [*Fried et al., 1998; Wert et al., 2002*] at  
26 10-s resolution for August 27 and 28, the two flights reported here. Peroxyacyl nitrate compounds  
27 (e.g., peroxyacetyl nitrate (PAN)) were measured once every 3.5 minutes by gas chromatography

1 (GC) using electron capture detection. GC measurements, either performed *in situ* [Goldan *et al.*,  
2 2000] or as a whole-air sample (WAS) from canisters [Schauffler *et al.*, 1999], provided speciated  
3 data on an extensive set of VOCs (Table 1). 39 WAS canisters were sampled on each flight; in  
4 addition to the VOCs, the WAS instrument provided data on CO, methane (CH<sub>4</sub>), C<sub>1</sub> through C<sub>5</sub>  
5 monofunctional alkyl nitrate compounds (RONO<sub>2</sub>), and a variety of other halogenated species.

6 *Measurement uncertainties.* Here we briefly assess uncertainties in the chemical  
7 measurements most relevant to the following analyses. Calibrations of the reactive nitrogen (NO,  
8 NO<sub>2</sub>, HNO<sub>3</sub>, PAN compounds, and total NO<sub>y</sub>) measurements are conservatively estimated to be  
9 accurate to better than ±10% based on in-flight standard addition calibration data, multiple internal  
10 consistency checks, and extensive intercomparison with other aircraft and ground measurements of  
11 these species [Neuman *et al.*, 2002]. In addition to uncertainties in calibration, estimated  
12 imprecision for the 1-Hz reactive nitrogen measurements at low mixing ratios varied between ±20  
13 parts per trillion by volume (pptv) for NO to ±150 pptv for NO<sub>y</sub>. Both the NO<sub>y</sub>  
14 chemiluminescence instrument and the HNO<sub>3</sub> chemical ionization mass spectrometer have been  
15 shown to sample atmospheric HNO<sub>3</sub> rapidly and quantitatively during flight [Neuman *et al.*, 2002;  
16 Ryerson *et al.*, 2000]. Tight correlation ( $r^2 = 0.962$ ), a linear-least-squares fitted slope of  $0.96 \pm$   
17  $0.05$ , and an intercept of 22 pptv suggests that no systematic bias existed between the sum of (NO  
18 + NO<sub>2</sub> + HNO<sub>3</sub> + PAN compounds) and the total NO<sub>y</sub> measurement over the course of the field  
19 mission (e.g., [Neuman *et al.*, 2002]). The fractional contribution of C<sub>1</sub>-C<sub>5</sub> monofunctional alkyl  
20 nitrate (RONO<sub>2</sub>) compounds (measured in the whole-air canister samples) ranged between 0.01 to  
21 0.02 of total NO<sub>y</sub>, similar to or slightly lower than previous studies [Bertman *et al.*, 1995; Flocke *et*  
22 *al.*, 1991; Ridley *et al.*, 1997]. Although coincident alkyl nitrate and PAN data are very sparse,  
23 inclusion of the average RONO<sub>2</sub> fraction of 0.015 in the above NO<sub>y</sub> budget brings the sum very  
24 close to 1, indicating that all the major components of the reactive nitrogen family were measured  
25 accurately.

26 Comparison of the two independent CO measurements aboard the Electra (GC analysis of  
27 whole-air canister samples [Schauffler *et al.*, 1999] and vacuum-ultraviolet resonance fluorescence

1 [Holloway *et al.*, 2000]) showed tight correlation ( $r^2 = 0.989$ ), a fitted linear-least-squares slope of  
2 1.03, and an intercept of 4 ppbv, suggesting that both instruments measured ambient CO to within  
3 the stated uncertainties of the two techniques [Nicks *et al.*, 2002]. The CH<sub>2</sub>O measurement has  
4 been critically evaluated to characterize its time response, precision, and accuracy, and the data were  
5 compared to a ground-based long-path measurement using differential optical absorption  
6 spectroscopy (DOAS) [Stutz and Platt, 1997]. These tests suggest the 10-s CH<sub>2</sub>O data on board  
7 the Electra are accurate to better than  $\pm(120 \text{ pptv} + 10\%)$  [Wert *et al.*, 2002]. The 1-s ozone  
8 measurement by NO-induced chemiluminescence was compared to a UV-absorption measurement  
9 aboard the Electra, and to a separate UV-absorption measurement during overflights of an  
10 instrumented ground site, and shown to be accurate within the stated uncertainty of  $\pm(0.3 \text{ ppbv} +$   
11  $3\%)$ . VOC data were compared between the WAS measurements and the in-situ GC and found to  
12 be accurate, within stated experimental uncertainties of  $\pm 10\%$  or less, for the compounds reported  
13 here at the elevated mixing ratios relevant to this report. Generally the uncertainty of the SO<sub>2</sub>  
14 measurement was within  $\pm 10\%$  for SO<sub>2</sub> levels well above the detection limit of approximately 0.5  
15 ppbv. However, for the data on the two flights presented here this accuracy was sporadically  
16 degraded by short-term transients, of up to several ppbv, due to operational difficulties with the in-  
17 flight calibration system. The SO<sub>2</sub> data are used here only in a relative sense, e.g., to distinguish  
18 between different anthropogenic source types by noting the presence or absence of elevated SO<sub>2</sub> in  
19 a given plume.

20 *Meteorological and emissions data.* Information on wind speed and direction, mixed layer  
21 heights, and vertical mixing within and above the mixed layer is derived from on-board chemical  
22 and meteorological measurements [Ryerson *et al.*, 1998] and observations from other airborne  
23 [Senff *et al.*, 1998] and ground-based [Angevine *et al.*, 1994] remote-sensing instrumentation  
24 deployed throughout the area for the Texas 2000 study. Uncertainties in wind speeds of  $\pm 1 \text{ m/s}$   
25 and in boundary layer heights of  $\pm 10\%$  are estimated by comparing derived values from the various  
26 aircraft- and ground-based data sets. Tabulated information on source emissions was obtained  
27 from and, where possible, cross-checked between various inventory databases. These included the

1 U.S. Environmental Protection Agency (EPA) AIRS, TRI, and E-Grid databases  
2 ([www.epa.gov/ttn/chief](http://www.epa.gov/ttn/chief)), as well as from information provided by plant operators to the Texas  
3 Natural Resource Conservation Commission (TNRCC) for the 2000 reporting year  
4 ([www.tnrcc.state.tx.us/air/aqp/psei.html](http://www.tnrcc.state.tx.us/air/aqp/psei.html)). We use the TNRCC point source database (PSDB) for  
5 2000 as the primary reference in this report. Hourly-averaged emissions data, from continuous  
6 emission monitoring systems (CEMS) and from estimates provided by facility operators, were also  
7 examined for the time periods of the present study. The timing and nature of non-routine emission  
8 events, or upsets, at many facilities was also reported to TNRCC and are taken into account in the  
9 present analysis.

10 *Plume identification.* Plumes from different sources are distinguished by markedly  
11 different enhancements above background of many of the chemical species measured aboard the  
12 Electra aircraft, reflecting the different emissions profiles from each source type. Fossil-fueled  
13 electric utility power plant plumes show relatively strong enhancements in NO<sub>y</sub> species and CO<sub>2</sub>.  
14 SO<sub>2</sub> can also be strongly enhanced in power plant plumes if sulfur-rich fuels are used and  
15 emissions are not treated to remove it; typically, coal- and oil-fired units emit substantial amounts of  
16 SO<sub>2</sub>, while natural-gas-fired turbine units do not. CO enhancements are typically negligible in  
17 power plant plumes, with some exceptions [*Nicks et al.*, 2002]. Substantial VOC enhancements in  
18 power plant plumes are never detected. Urban plumes are characterized by substantial  
19 enhancements in CO and VOCs, typical of tailpipe combustion sources [*Harley et al.*, 2001]; NO<sub>y</sub>  
20 species and CO<sub>2</sub> are also enhanced, but to a lesser degree than in power plant plumes. SO<sub>2</sub> is  
21 typically not substantially enhanced in urban plumes. Plumes from petrochemical complexes have  
22 varied chemical composition, but typically have enhanced NO<sub>x</sub> and CO<sub>2</sub> characteristic of the  
23 embedded power plants required to supply electricity and heat to the facilities. Petrochemical  
24 plumes can also be characterized by elevated CO levels, and elevated SO<sub>2</sub> depending on the fuel  
25 source. Enhanced VOC levels specific to individual processes and facilities are also characteristic  
26 of petrochemical source plumes [*Watson et al.*, 2001]. Thus, examination of the chemical data in  
27 conjunction with aircraft position, wind speed, and wind direction information permits identification

1 of plumes from different sources until they are nearly fully mixed with each other or with  
2 background air.

3 Plume chemical and dynamic evolution was tracked from the Electra aircraft by performing  
4 crosswind transects within the mixed layer at successive distances downwind of individual sources  
5 and source complexes (e.g., [Brock *et al.*, 2002; Ryerson *et al.*, 1998]). These data were taken  
6 between noon and 5 PM local standard time, at times of day when mixing was most rapid, so that  
7 compounds emitted from a source were rapidly and extensively mixed within the boundary layer.  
8 Emissions from an individual petrochemical complex are treated as coming from a single or at most  
9 a few point emitters for transects performed >10 km or a few source diameters downwind [Wert *et*  
10 *al.*, 2002]. This is justified by downwind observations of multiple Ship Channel point source  
11 plumes on these two flight days; originally separated plumes became mutually indistinguishable  
12 between successive afternoon transects 15 km apart, or roughly an hour of transport time  
13 downwind.

14

### 15 **3. Results**

16 Hourly-averaged ozone mixing ratios measured at surface sites can exceed 200 parts per  
17 billion by volume (ppbv) during severe summertime pollution episodes in the Houston metropolitan  
18 area. Previous studies in Houston have suggested these extreme ozone exceedences are more  
19 common on days characterized by relatively complex meteorological conditions, and can be  
20 frequent during stagnation episodes [Davis *et al.*, 1998]. For Sunday, August 27, and Monday,  
21 August 28, 2000, however, no exceedence of the 1-hour, 120-ppbv Federal air quality standard was  
22 recorded in the Houston metropolitan area, in part due to steady ventilation by relatively clean  
23 southerly winds from the Gulf of Mexico. Despite relatively low ozone mixing ratio enhancements,  
24 Electra research flights on these two days provided data from which ozone formation rates and  
25 yields downwind of different anthropogenic source types are determined under relatively uniform-  
26 flow conditions. We analyze data from these days specifically because the prevailing wind  
27 direction provided spatially separated and relatively well-resolved plumes from several isolated

1 petrochemical industrial facilities, the W.A. Parish power plant, the multiple petrochemical  
2 complexes along the Ship Channel, and the urban core of Houston itself.

3 We present data on photochemical ozone production from emissions released during the  
4 morning and early afternoon hours and observed within 15 min. to ca. 8 hours following release.  
5 These findings are most relevant to typical Houston summertime conditions characterized by low to  
6 moderate background ozone levels (40-60 ppbv) coupled with substantial and rapid ozone  
7 production (within 4 hrs of release) in a single day. This characteristic is unique to Houston and is  
8 in contrast to other urban areas in the U.S., in which the highest ozone mixing ratios typically result  
9 from slower accumulation of ozone over the period of several days (e.g., [*Banta et al.*, 1998; *Daum*  
10 *et al.*, 2000b; *Kleinman et al.*, 2000; *Winner and Cass*, 1999]).

11

### 12 **3.1. Isolated petrochemical industrial complexes**

13 Aircraft flights on August 27 and 28, 2000, sampled the spatially resolved plumes from  
14 several isolated petrochemical complexes south of the Houston metropolitan area (Plate 2). These  
15 plumes were composed of the aggregated emissions from groupings of chemical plants in well-  
16 segregated areas several kilometers in extent. On both days, emissions plumes from complexes at  
17 Sweeny, Freeport, and Chocolate Bayou were carried inland by steady winds at  $4.5 \pm 1.0$  m/s at  
18  $160 \pm 16^\circ$  from the Gulf of Mexico. Measurements upwind over the Gulf on both days  
19 characterized the inflow as relatively clean, devoid of appreciable amounts of reactive VOCs or  $\text{NO}_x$ ,  
20 with CO levels below 100 ppbv and ozone roughly 35 ppbv. For the isolated sources, we establish  
21 that the source of enhanced plume levels of  $\text{NO}_x$  and VOCs, and the ozone and other photoproduct  
22 formation, are due to emissions from the petrochemical facilities themselves. The plume transect  
23 data are then used to estimate VOC/ $\text{NO}_x$  emissions ratios,  $\text{NO}_x$  oxidation rates,  $\text{HNO}_3$  production  
24 rates, net ozone production rates and yields, and to determine the primary species contributing to  
25 OH reactivity in these petrochemical emissions plumes.

26 **3.1.1. Emissions sources.** Enhancements of  $\text{NO}_x$ , CO,  $\text{CO}_2$ , and VOCs, and secondary  
27 photoproducts including ozone,  $\text{CH}_2\text{O}$ ,  $\text{CH}_3\text{CHO}$ , and PAN compounds, observed in these isolated

1 plumes can be unambiguously attributed to emissions from the petrochemical facilities at each  
2 location. Potential emissions of NO<sub>x</sub> and reactive hydrocarbons from co-located automobile, truck,  
3 ship, and rail traffic in the area are ruled out as significant contributors to the totals emitted from  
4 these three complexes. The fraction of on-road transportation, or tailpipe, emissions from  
5 automobiles and trucks is expected to have been minimal owing to the location of these complexes,  
6 which are remote from city or town centers and are characterized by low roadway densities in all  
7 three source areas (Plate 1). Recent reports suggest that such tailpipe emissions result in tightly  
8 correlated enhancements in CO and NO<sub>x</sub>, with characteristic morning emissions ratios in 2000 of  
9 roughly 5 - 6 (mol CO/mol NO<sub>x</sub>) [Harley *et al.*, 2001; Parrish *et al.*, 2002]. These values are in  
10 good agreement with tailpipe CO/NO<sub>x</sub> emissions ratios of  $6 \pm 1$ , estimated from Electra data taken  
11 in late-morning transects of the Houston urban core. In contrast, for transects flown very close to  
12 the isolated petrochemical facilities, observed enhancements of these species were often poorly  
13 correlated, suggesting physically separate emissions of CO and NO<sub>x</sub> uncharacteristic of tailpipe  
14 sources. CO/NO<sub>x</sub> ratios measured in plume transects within 10 km of the three isolated  
15 petrochemical complexes varied, ranging from 0.1 to nearly 1, further illustrating that the NO<sub>x</sub> was  
16 not emitted from tailpipe sources.

17 Ratios of hydrocarbons to ethyne (acetylene; C<sub>2</sub>H<sub>2</sub>) measured in plume transects also rule  
18 out tailpipe sources as substantial contributors to the observed enhancements in the isolated  
19 petrochemical facility plumes. Tailpipe emissions have characteristic ratios of (ethene/ethyne)  
20 ranging from 1 to 3 and (propene/ethyne) from 0.5 to 1.5, determined from airborne VOC  
21 measurements above the urban cores of Nashville, TN and Atlanta, GA in 1999, and in Houston and  
22 Dallas, TX, in 2000. Atmospheric oxidation processes decrease these two ratios over time between  
23 emission and measurement, primarily due to the substantially faster OH reaction rate coefficients of  
24 ethene and propene compared to ethyne (Table 1). Nonetheless, the ratios in the urban plumes  
25 observed from aircraft are in good agreement with recent tunnel measurements in both Houston  
26 (W. Lonneman, unpublished data, 2000) and in Nashville [Harley *et al.*, 2001]). In contrast,  
27 observed molar ratios in near-field transects of the plumes from a variety of petrochemical facilities

1 in the Houston study region for (ethene/ethyne) ranged from 10 to 30 and for (propene/ethyne)  
2 from 5 to 40. These values are substantially higher than ratios from tailpipe sources, confirming  
3 that the contribution of alkenes from tailpipe sources was negligible in these plumes.

4 For the isolated facilities, the absence of substantially elevated  $\text{SO}_2$  in these plumes is  
5 characteristic of gas-fired turbine exhaust and suggests that locomotive and marine diesel  
6 emissions, which are typically rich in  $\text{SO}_2$  [Corbett and Fischbeck, 1997], are not significant  
7 sources of  $\text{NO}_x$  in the plumes studied here. Small enhancements of  $\text{SO}_2$  observed in the Freeport  
8 plume are qualitatively consistent with emissions from the Gulf Chemical and Metallurgical Plant, a  
9 known  $\text{SO}_2$  source within the Freeport complex [Brock *et al.*, 2002]. We conclude the observed  
10 plume enhancements are due to emissions of reactive VOC and  $\text{NO}_x$  directly from the  
11 petrochemical facilities themselves.

12 While other co-located sources are ruled out as substantial contributors to the isolated  
13 petrochemical plumes, these plumes may have entrained emissions from other sources during  
14 transport. For example, the wind direction on the two days considered here advected the Sweeny  
15 plume over a wooded area to the north-northwest, which is a known weak biogenic source of  
16 isoprene [Wiedinmyer *et al.*, 2001]. This acted to continually replenish the Sweeny plume with low  
17 but non-negligible amounts of isoprene during transport. Plumes from the petrochemical  
18 complexes south of Houston, as well as that from the W.A. Parish power plant, eventually were  
19 transported over the western and southern edges of the Houston urban area, with additional mixing  
20 of urban tailpipe emissions into the aged plumes. The overall impact of entrainment during  
21 transport on derived  $\text{NO}_x$  oxidation rates, and plume production rates of ozone and other secondary  
22 products, is shown below to be relatively minor.

23 **3.1.2. VOC reactivity.** Whole-air canister samples taken in resolved plumes from the  
24 three isolated petrochemical complexes show elevated mixing ratios of many of the measured  
25 hydrocarbons (Table 1), including substantial enhancements in alkanes, alkenes, aromatics, and  
26 ethyne. In general, the compounds ethane ( $\text{C}_2\text{H}_6$ ), ethene ( $\text{C}_2\text{H}_4$ ), propane ( $\text{C}_3\text{H}_8$ ), propene ( $\text{C}_3\text{H}_6$ ),  
27 and isomers of butane and pentane were the most abundant, with differing relative abundances

1 characteristic of the three source complexes. However, the contribution of an individual  
2 hydrocarbon species to prompt ozone formation is determined both by its concentration and by  
3 how rapidly that compound can react with OH, which is the rate-limiting step in ozone formation  
4 (e.g., [Atkinson, 1994; Atkinson, 1997; DeMore *et al.*, 1997]). Alkenes and larger aromatic  
5 compounds typically have relatively large OH rate coefficients (Table 1); thus, these compounds  
6 will contribute more to prompt ozone production at a given concentration than will alkanes or  
7 alkynes. To elucidate the directly-emitted VOCs primarily responsible for plume ozone formation,  
8 the hydrocarbon data are presented in Plate 3 by multiplying the concentration of each measured  
9 species by the appropriate OH rate coefficient at the measured ambient temperature and pressure.  
10 The black horizontal bars in Plates 3a and 3c show total OH reactivity calculated from the measured  
11 VOCs, excluding the photoproducts  $\text{CH}_2\text{O}$  and acetaldehyde ( $\text{CH}_3\text{CHO}$ ). While plume OH  
12 reactivities due to  $\text{NO}_2$ ,  $\text{CH}_4$ , and  $\text{CO}$  are not negligible (Plate 3a and 3c), the large increases over  
13 reactivities calculated from samples taken outside the plumes are almost entirely due to  
14 petrochemical VOC emissions. Further examination of the individually speciated VOC data shows  
15 that of the many compounds emitted and measured, two compounds alone account for the majority  
16 of the plume reactivity above the background. The data in Plates 3b and 3d from both days show  
17 that the principal reaction partners for OH in all three plumes were the directly emitted alkenes  
18 ethene and propene and their oxidation products. Mixing ratios of ethene and propene observed  
19 within 5 km of these sources exceeded background levels by factors ranging from 20 to over 200.  
20 Elevated plume levels of the reactive alkenes ethene and propene and their photooxidation products  
21  $\text{CH}_2\text{O}$  and  $\text{CH}_3\text{CHO}$  are sufficient to dominate OH reactivity for some time after emission. For  
22 example, in the ~20-min.-old Chocolate Bayou plume sampled at 19:02 GMT (1:02 PM local time)  
23 on August 27 (Plate 3a), ethene and propene account for >80% of the OH reactivity calculated from  
24 the measured hydrocarbons (Table 1). Even in the ~45-min.-old Freeport plume, ethene and  
25 propene still account for 75% of OH reactivity.

26 As these alkenes are rapidly consumed, their photoproducts  $\text{CH}_2\text{O}$  and  $\text{CH}_3\text{CHO}$  increase  
27 in relative importance as OH partners, acting to further propagate the radical chain leading to ozone

1 formation. Measurements of plume  $\text{CH}_2\text{O}$  show that direct emissions of this compound are  
2 negligibly small compared to  $\text{CH}_2\text{O}$  formed during transport from the OH-induced oxidation of the  
3 directly-emitted VOCs, primarily ethene and propene [Wert *et al.*, 2002]. The  $\text{CH}_2\text{O}$  derived from  
4 alkene oxidation, once formed, constitutes a major reaction partner for OH in all these plumes, and  
5 photolysis of  $\text{CH}_2\text{O}$  becomes an important free radical source.  $\text{CH}_2\text{O}$  and  $\text{CH}_3\text{CHO}$  are  
6 themselves relatively short-lived, and within hours the longer-lived alkane compounds are observed  
7 to dominate plume reactivity downwind. However, by then, the shorter-lived  $\text{NO}_x$  had already been  
8 extensively oxidized.

9         The presence of elevated mixing ratios of longer-lived alkanes suggests that ozone  
10 formation may have continued beyond the final aircraft transect downwind ( $\sim 60$  km), catalyzed by  
11 the  $\text{NO}_x$  remaining, additional  $\text{NO}_x$  from other downwind sources, and that recycled from thermal  
12 decomposition of PAN-type compounds. However, the remaining alkanes will oxidize relatively  
13 slowly thereafter, and alkane reaction products are predominantly the less-reactive ketones  
14 [Atkinson, 1997]. Given the low observed mixing ratios of  $\text{NO}_x$  and reactive VOC remaining at  
15 these distances, and the observed decrease in ozone production rates between successive transects,  
16 the rate at which ozone would be formed is also expected to be substantially lower downwind. The  
17 evolution over time of plume  $\text{CH}_2\text{O}$  mixing ratios [Wert *et al.*, 2002] further suggests that  
18 reservoirs of compounds serving as precursors to peroxy radical formation in the plumes were also  
19 relatively depleted at these distances. Thus, ozone formation downwind of the final Electra transects  
20 (plume ages  $>4$  hours) in the isolated petrochemical plumes is expected to have been relatively  
21 minor compared to that observed on the timescales considered here. The majority of ozone  
22 produced in these plumes is therefore ascribed to co-located emission of large amounts of ethene  
23 and propene with  $\text{NO}_x$  from the isolated petrochemical facilities.

24         Equally important in designing an effective ozone control strategy is the identification of  
25 VOC compounds that did not contribute significantly to OH reactivity, and thus prompt ozone  
26 formation, in the isolated plumes. While mixing ratios of many alkane compounds were enhanced,  
27 sometimes strongly, these contributed negligibly to ozone formation in the Freeport and Sweeny

1 plumes on these timescales due to their substantially lower OH reaction rates. An exception is  
2 noted for the Chocolate Bayou plume, in which isobutane mixing ratios exceeding 20 ppbv were  
3 measured 5 km downwind, accounting for 11% of OH reactivity with the measured VOC  
4 compounds at this distance. Alkenes other than ethene and propene contributed little to initial OH  
5 reactivity. While the OH rate coefficient for 1,3-butadiene is a factor of ~3 larger than that for  
6 propene (Table 1), emissions of 1,3-butadiene contributed relatively little to OH reactivity in these  
7 plumes, even after accounting for differential loss in samples taken within 10 km of the Freeport  
8 and Chocolate Bayou facilities. All other directly emitted and individually measured VOCs  
9 contributed less than  $0.2 \text{ s}^{-1}$  to the OH loss rate, and, to first approximation, can be neglected in  
10 terms of prompt ozone formation. This finding includes the suite of higher aromatic compounds  
11 measured (Table 1), which, like 1,3-butadiene, are very reactive but were present at sufficiently low  
12 levels to be minor contributors to rapid ozone formation in the plumes presented here. Thus,  
13 relatively few compounds were responsible for the bulk of initial VOC reactivity of these  
14 petrochemical plumes, which were dominated for the first 50 km of transport (first 2-3 hours after  
15 emission) by anthropogenic emissions of ethene and propene and by the aldehyde photoproducts  
16 derived from these species. Enhancements in initial plume OH reactivity due to CO and NO<sub>2</sub>  
17 emissions were negligible compared to the enhancements resulting from alkene emissions (Plate 3).  
18 Considering the wide variety of VOCs emitted from petrochemical industrial sources [Derwent,  
19 2000], this finding suggests a relatively straightforward ozone control strategy. Reducing emission  
20 of these two alkenes is clearly indicated as the most effective VOC-reduction strategy to minimize  
21 prompt ozone formation downwind of these sources.

22

23 **3.1.3. (Alkene/NO<sub>x</sub>) emission ratios.** Ratios of co-emitted species from a single large  
24 source are, to first order, independent of dilution over time during transport downwind and are given  
25 by the slope of a linear fit to measured data. Ratios measured downwind in plumes will differ from  
26 the emissions ratio if chemical reaction or physical removal rates differ for the two species in  
27 question. We use plume transect data to estimate the emissions ratios of (ethene/NO<sub>x</sub>) and

1 (propene/ $\text{NO}_x$ ) for the Sweeny, Freeport, and Chocolate Bayou facilities, account for differential  
2 chemical loss with respect to OH, and compare to emissions ratios calculated from the 2000  
3 TNRCC point source database (PSDB) inventory. We note that some differences exist between the  
4 1999 inventory used by Wert et al. [2002], and the 2000 inventory used in the present work, which  
5 has only recently become available, for the Texas 2000 study period. These inventory tabulations  
6 are not static over time, reflecting changes in operating conditions, plant activity, and addition of new  
7 facilities or shutting down older units. Changes from the 1999 to the 2000 inventory are also due  
8 to a substantially smaller fraction of VOC emissions reported as “unspeciated” in 2000. The  
9 PSDB inventory is the basis for the predictive and regulatory modeling by TNRCC and EPA.

10 (Ethene/ $\text{NO}_x$ ) ratios measured in transects within 5 km of the Freeport and Chocolate  
11 Bayou facilities were not significantly affected by differential chemical or physical removal; the  
12 inferred emissions ratios are therefore judged to be accurate to within the combined measurement  
13 uncertainties of  $\pm 17\%$ . The closest Sweeny plume transects took place ca. 22 km or 1.4 hr  
14 downwind; given the larger OH reaction rate for propene relative to  $\text{NO}_x$  (Table 1) the resulting  
15 estimated (propene/ $\text{NO}_x$ ) emission ratio is subject to the largest uncertainty. We judge the  
16 estimated (propene/ $\text{NO}_x$ ) emissions ratio for Sweeny is only accurate to within a factor of two.  
17 These estimated emissions data are presented in Table 2 along with the ratios calculated from  
18 annual emissions rates listed in the 2000 PSDB inventory for the geographic source areas given by  
19 the rectangles in Plate 1. The data in Table 2 show that substantial discrepancies, many times larger  
20 than the measurement uncertainty, exist between the measurement-inferred emission ratios and  
21 those calculated from the 2000 inventory values. Small differences in the inventory (alkene/ $\text{NO}_x$ )  
22 ratios between Table 2 in this report and those in Table 4 of Wert et al. [2002] are due to the  
23 different inventory reporting years.

24 Such large discrepancies could arise from inaccuracy either in the tabulated inventory values  
25 of  $\text{NO}_x$ , of alkenes, or of both, for the petrochemical complexes in question. The discrepancy could  
26 also arise if the actual  $\text{NO}_x$  emissions were extremely low, or the alkene emissions extremely high,  
27 from all three facilities simultaneously during both the August 27 and 28 plume studies compared

1 to the annual averages. In the following section we show that the  $\text{NO}_x$  emissions were relatively  
2 constant over time and are reasonably well estimated in the inventory.

3 *NO<sub>x</sub> emissions were constant over time.* The  $\text{NO}_x$  emissions information is derived from  
4 continuous emission monitoring systems (CEMS) data for many of the largest  $\text{NO}_x$  sources at each  
5 complex; these data are believed to be accurate to better than  $\pm 30\%$  on average [Placet *et al.*, 2000;  
6 Ryerson *et al.*, 1998]. Petrochemical facilities are typically operated continuously, so that variation  
7 in their  $\text{NO}_x$  output over time can be minimal (C. Wyman, personal communication, 2001). As an  
8 example, total hourly-averaged  $\text{NO}_x$  emissions rates reported by the largest of the four facilities in  
9 the Chocolate Bayou area differed by less than 5% for the August 27 and 28 plume study periods  
10 reported here. Further, very little variation is apparent over the eleven days of hourly-averaged  
11 emission rates for  $\text{NO}_x$  (264 consecutive hours,  $\text{average} \pm \text{sigma} = (7.9 \pm 0.2)$ ,  $\text{max} = 8.5$ ,  $\text{min} = 7.5$ , with  
12 units of  $10^{23}$  molec/s) reported by this facility (August 22-September 1, 2000, including the plume  
13 study periods). The 2000 PSDB annually-averaged  $\text{NO}_x$  emission rate is further consistent within  
14 15% with that derived from the hourly averages from this facility. In addition, the available daily-  
15 averaged  $\text{NO}_x$  emissions data from the second-largest facility show variations of less than 10%  
16 (eleven consecutive days,  $\text{average} \pm \text{sigma} = (2.7 \pm 0.2)$ ,  $\text{max} = 3.0$ ,  $\text{min} = 2.5$ , with units of  $10^{23}$   
17 molec/s). Annual averages suggest these two facilities account for 91% of the total  $\text{NO}_x$  emissions  
18 from the Chocolate Bayou source region. Similar arguments can be constructed for the facilities in  
19 the Sweeny and Freeport source regions (Plate 1). These findings suggest that for the August 27  
20 and 28 plume studies the emissions rates derived from hourly-, daily-, and annually-averaged  $\text{NO}_x$   
21 inventories are comparable, and that  $\text{NO}_x$  emissions from the three isolated petrochemical source  
22 regions were quite constant and representative of normal operating conditions of these complexes.

23 *NO<sub>x</sub> emissions are well represented by the available inventories.* The overall accuracy of  
24 the  $\text{NO}_x$  emissions rates for these three complexes is evaluated by comparing to emissions rates  
25 inferred from plume mass flux of  $\text{NO}_y$ , calculated from near-field aircraft transect data [Brock *et al.*,  
26 2002; Ryerson *et al.*, 1998; Ryerson *et al.*, 2001; Trainer *et al.*, 1995; White *et al.*, 1976], to the  
27 available inventory values. Mass flux estimates from aircraft data taken in well-resolved plumes are

1 subject to several sources of uncertainty, including depositional losses, venting to the free  
2 troposphere, incomplete mixing within the boundary layer, and variability in wind speeds. These  
3 uncertainties and their evaluation are discussed extensively in Ryerson *et al.* [1998]. Examination  
4 of the multiple plume transect data on these two days suggests that the  $\text{NO}_y$  mass flux was  
5 relatively well conserved over time. Plume  $\text{NO}_y/\text{SO}_2$  ratios remained constant, within  $\pm 30\%$ ,  
6 between successive transects on these two days (e.g., see Figure 8 in Brock *et al.* [2002] for the  
7 analysis of the W.A. Parish plume), suggesting minimal differential loss of  $\text{NO}_y$  relative to  $\text{SO}_2$   
8 and/or  $\text{CO}_2$ . Further, the total estimated mass of  $\text{NO}_y$  in each petrochemical plume remained  
9 constant within  $\pm 30\%$  over time downwind of each complex, in turn suggesting that depositional  
10 loss of  $\text{HNO}_3$  was relatively small compared to the total  $\text{NO}_y$  on the timescales considered here.  
11 Thus,  $\text{NO}_y$  appears to have been approximately conserved during the course of these plume studies.  
12 Given additional uncertainties in wind speed histories and boundary layer heights, for the isolated  
13 petrochemical plumes studied here, we conservatively estimate the uncertainty in derived  $\text{NO}_y$  mass  
14 flux to be a factor of two. Comparison of the aircraft-derived  $\text{NO}_y$  flux estimates to the annually-  
15 averaged  $\text{NO}_x$  inventory emissions values shows agreement within  $\pm 50\%$ , well within the  
16 uncertainty in deriving mass fluxes for these isolated facilities for these two days. This level of  
17 agreement rules out the inventory  $\text{NO}_x$  values as the primary source of inventory-measurement  
18 (alkene/ $\text{NO}_x$ ) ratio discrepancies of factors of 20 to nearly 70, mentioned above. These  
19 discrepancies are roughly a factor of 2 smaller than those noted in Wert *et al.* [2002] using the  
20 1999 PSDB inventory; while the total VOC emissions numbers remained approximately constant,  
21 more complete speciation in the 2000 inventory accounted for much of the change.

22 *Alkene emissions are consistently underestimated.* Inventory values of alkene emissions  
23 are therefore implicated as the primary cause of the large discrepancies in (alkene/ $\text{NO}_x$ ) emissions  
24 ratios. Hourly and daily ethene, propene, and butadiene emissions data from facilities in, e.g., the  
25 Chocolate Bayou source region suggest that total emissions of these alkenes showed minimal  
26 variability, within  $\pm 20\%$  of the average value over the August 22-September 1 time period,  
27 encompassing the two plume study days. Similarities observed between plumes sampled on

1 August 27 and 28, further consistent with the larger Electra data set from the month-long Texas  
2 2000 project, suggest that the instantaneous VOC emissions were representative of normal  
3 operations on both days and generally consistent with the annual average. No substantial upsets, or  
4 non-routine emission events, were recorded for these facilities for the plume intercepts studied here.  
5 We conclude that consistently large discrepancies between measurement-derived and tabulated  
6 (alkene/NO<sub>x</sub>) ratios are due to consistently and substantially underestimated VOC emissions from  
7 the petrochemical facilities [Wert *et al.*, 2002].

8 **3.1.4. NO<sub>x</sub> oxidation rate.** As discussed above, within  $\pm 30\%$  the measured NO<sub>y</sub> was a  
9 reasonably conserved tracer of the NO<sub>x</sub> originally emitted in these plumes. Any NO<sub>y</sub> loss from the  
10 plumes would have biased derived NO<sub>x</sub> oxidation rates to smaller-than-actual values, and ozone  
11 production rates and yields to larger-than-actual values. We assume that NO<sub>y</sub> was conserved but  
12 present the derived NO<sub>x</sub> oxidation rates as lower limits, and ozone rates and yields as upper limits,  
13 for plumes from the isolated petrochemical complexes.

14 Slopes of linear-least-squares fits to measured NO<sub>x</sub> versus NO<sub>y</sub> from successive transects  
15 downwind are plotted in Figure 1a as a function of estimated transport time after emission [Ryerson  
16 *et al.*, 1998]. An average NO<sub>x</sub> oxidation lifetime of  $1.5 \pm 0.5$  hours is derived from an exponential  
17 fit to the transect slope data, illustrating rapid photochemical processing of NO<sub>x</sub> during transport  
18 downwind from all three sources on both days. Measured (NO<sub>x</sub>/NO<sub>y</sub>) ratios >2.5 hours downwind  
19 were slightly elevated, relative to background ratios outside these plumes, likely due to entrainment  
20 of fresh emissions during transport over the edges of the Houston urban area. While this effect  
21 increases the derived lifetime, a fit excluding these last points indicates a lifetime only 5% shorter.

22 This derived lifetime of  $1.5 \pm 0.5$  hours reflects both NO<sub>x</sub> oxidation via peroxy radical  
23 reaction, primarily leading to formation of PAN-type compounds with a minor fraction forming  
24 alkyl nitrates, and NO<sub>x</sub> oxidation via OH + NO<sub>2</sub> leading to formation of HNO<sub>3</sub>. HNO<sub>3</sub> accounted  
25 for roughly 50% of NO<sub>y</sub> after several hours of transport (Figure 1b), with an approximately  
26 exponential rise time of 6 hours. In general, enhancements in PAN-type compounds, inferred from

1 1-Hz ( $\text{NO}_y - (\text{NO}_x + \text{HNO}_3)$ ) data, were substantial within the plumes, with peak contributions  
2 occurring sooner than for  $\text{HNO}_3$  and accounting for roughly 50% of plume  $\text{NO}_y$  at the peak.

3 Previous studies of isolated, rural power plant plumes under midsummer afternoon, high-  
4 sun conditions with steady winds have reported  $\text{NO}_x$  lifetimes ranging generally from 2 to 5 hours  
5 [Nunnermacker *et al.*, 2000; Ryerson *et al.*, 1998; Ryerson *et al.*, 2001]. The range arises from  
6 differences in  $\text{NO}_x$  emissions rate (40 to 600 kmole/hr; Table 3), variability in meteorological  
7 conditions determining plume dispersion rates, and availability of ambient reactive VOCs,  
8 principally isoprene. Together these factors have been shown to modulate the  $\text{NO}_x$  lifetime by over  
9 a factor of two, with the shortest (2-hour) derived lifetimes observed in plumes from mid-sized (~50  
10 to 100 kmole/hr) power plants emitted into a high isoprene background. The petrochemical plume  
11  $\text{NO}_x$  oxidation reported here is presumed to proceed more rapidly due to initially-mixed conditions  
12 arising from co-emission of  $\text{NO}_x$  simultaneously with reactive VOCs.

13 **3.1.5. Ozone production rate and yield.** Prompt ozone formation downwind of these  
14 petrochemical facilities was observed on both days (Plate 2 and Figure 1c). For example,  
15 enhancements of 20 ppbv in ozone were observed on the transects flown west-to-east at 29.3  
16 latitude at 35 km downwind, or roughly 2 hours transport time, from the Freeport complex. These  
17 enhancements in mixing ratio are relatively modest, comparable to the increases in ozone observed  
18 in power plant plumes reported by Ryerson *et al.* [1998; 2001] and Nunnermacker *et al.* [2000],  
19 despite the generally lower  $\text{NO}_x$  emissions rates for the petrochemical sources. The modest mixing  
20 ratio increases were in part due to dilution of the plumes into a rapidly deepening mixed layer, from  
21 400 m at the coast to over 1500 m at 25 km inland, as determined from airborne lidar measurements  
22 [Senff *et al.*, 1998] during the plume transects reported here. Given that  $\text{NO}_y$  appears to have been  
23 relatively well conserved in these plumes, we calculate a net ozone production efficiency, or yield,  
24 from the plume transect data [Trainer *et al.*, 1993].

25 This calculation shows that while ozone mixing ratio enhancements were relatively small,  
26 ozone production rates and yields were high. Estimates of ozone yields per molecule of  $\text{NO}_x$   
27 oxidized, derived from slopes of linear-least-squares fits to plume ozone versus ( $\text{NO}_y - \text{NO}_x$ ) data

1 [Trainer *et al.*, 1993], are plotted in Figure 1c as a function of time downwind for these three  
2 plumes for both days. Derived ozone yields ranged from 10 to 18 molecules of ozone produced  
3 per  $\text{NO}_x$  molecule oxidized. Similar ozone yield values are derived using plume-integrated amounts  
4 of ozone and  $(\text{NO}_y - \text{NO}_x)$  according to a mass balance approach (e.g., [Brock *et al.*, 2002; Ryerson  
5 *et al.*, 1998; Trainer *et al.*, 1995; White *et al.*, 1976]). These derived values were achieved very  
6 rapidly after emission, within roughly 2 hours for the isolated petrochemical plumes in Fig. 1. The  
7 slow increases in derived yield after 2.5 hours in Figure 1c may be real, due to real ozone  
8 production from entrainment of fresh urban  $\text{NO}_x$  or to slower ozone production rates from longer-  
9 lived VOCs in the plume, or spurious, from non-negligible depositional losses of  $\text{HNO}_3$  during  
10 transport. In any case, this effect is relatively minor for the short timescales and small changes in  
11 derived ozone yield after 2.5 hours observed here.

12 While all plumes were consistent in producing ozone in high yield, differences between the  
13 Freeport and Sweeny plumes (Fig. 1) are noted, with derived yields about 50% lower for Freeport.  
14 These differences are qualitatively consistent with different emissions rates of propene and ethene,  
15 and  $(\text{alkene}/\text{NO}_x)$  ratios, explored in the VOC reactivity section, above. In general, similarity  
16 between measured mixing ratios and derived plume formation rates and yields for each complex on  
17 Sunday and Monday, with no upsets reported to TNRCC by the facility operators, implies the  
18 observed ozone production is representative of the effects of these facilities' routine emissions on  
19 tropospheric ozone mixing ratios downwind under these meteorological conditions.

20 *Uncertainties in derived ozone yield (resolved plumes).* Interpretation of ozone-to- $(\text{NO}_y -$   
21  $\text{NO}_x)$  relationships in isolated, resolved plumes as a net ozone production yield is subject to several  
22 uncertainties, which are extensively discussed by Trainer *et al.* [1993] and Ryerson *et al.* [1998].  
23 Of these,  $\text{NO}_y$  loss from these particular plumes during transport was a minor contributor, as  
24 discussed above. For the isolated and well-resolved petrochemical plumes from Sweeny, Freeport,  
25 and Chocolate Bayou, defining background mixing ratios immediately outside of the plumes is  
26 easily accomplished and introduces relatively little uncertainty in the derived ozone yields. Vertical  
27 profiles of chemical and meteorological data further support the assumption that the boundary layer

1 was vertically well mixed, and that detrainment into the free troposphere was minimal, for these  
2 plumes within 5 hours of release.

3 The most likely bias to the interpretation of the isolated petrochemical plume ozone and  
4 ( $\text{NO}_y$ - $\text{NO}_x$ ) data as an apparent ozone production yield involves the use of a linear fit to inherently  
5 non-linear relationships in the data (e.g., [Liu *et al.*, 1987; Ryerson *et al.*, 1998; Ryerson *et al.*,  
6 2001; Sillman, 2000]). However, the ratio of plume-integrated ozone to plume-integrated ( $\text{NO}_y$ -  
7  $\text{NO}_x$ ) assumes no particular relationship between the two data sets. Apparent ozone production  
8 yields for the isolated petrochemical plumes agree to better than  $\pm 50\%$  whether they are calculated  
9 from the slope of a linear fit, or from integrations, of the plume transect data (e.g., [Ryerson *et al.*,  
10 1998]). We therefore assign approximate but conservative uncertainties of  $\pm 50\%$  to the derived  
11 ozone yields for the isolated petrochemical plumes for these two days.

12 *Comparison to power plant and urban plumes.* Derived ozone yields are significantly  
13 higher and are attained more rapidly after emission in these resolved petrochemical plumes than are  
14 typically observed in rural power plant plumes (e.g., [Gillani *et al.*, 1998; Nunnermacker *et al.*,  
15 2000; Ryerson *et al.*, 1998; Ryerson *et al.*, 2001]). This is attributed in part to the co-location of  
16 sources of anthropogenic  $\text{NO}_x$  with anthropogenic reactive VOCs, in distinct contrast to rural power  
17 plant plumes into which reactive VOCs must be entrained over time during transport [Luria *et al.*,  
18 2000; Miller *et al.*, 1978; Ryerson *et al.*, 2001].

19 For comparison purposes, the data in Plate 4a and 4b show ozone production rates and  
20 yields for several rural, isolated power plant plumes and for the Nashville, TN urban plume, taken  
21 from multiple NOAA WP-3D aircraft research flights during the Southern Oxidants Study 1995  
22 and 1999 field projects. Table 3 gives the  $\text{NO}_x$  emissions rates for the power plants included in  
23 Plate 4a. Petrochemical ozone yield data from Figure 1c are reproduced in Plate 4c. These data  
24 were all taken under approximately similar summertime afternoon high-sun conditions with  
25 relatively constant wind speeds between 4 and 5 m/s; all plumes were extensively oxidized at the  
26 final transects, with measured ( $\text{NO}_x/\text{NO}_y$ ) ratios of 0.25 or smaller. The data show scatter from day  
27 to day for a given plume, within the range expected from time-varying emissions rates, solar

1 insolation, and meteorological conditions. Differences in  $\text{NO}_x$  emissions rates (Table 3) also affect  
2 ozone yields in these plumes. In general, however, the  $\text{NO}_x$ -rich power plant plumes take longer to  
3 fully oxidize, and produce less ozone per unit  $\text{NO}_x$  oxidized, than do the urban plumes from  
4 Nashville [Daum *et al.*, 2000a; Nunnermacker *et al.*, 2000]. An exception is found in the  
5 Johnsonville plume, a mid-sized power plant located in a wooded area characterized by strong  
6 biogenic isoprene emissions. The Johnsonville plume typically experiences the highest  $\text{VOC}/\text{NO}_x$   
7 ratios of the power plant plumes shown, with corresponding relative increases in ozone production  
8 rates and yields [Ryerson *et al.*, 1998; Ryerson *et al.*, 2001]. The Nashville urban plume data were  
9 calculated from the slopes of linear fits to plume ozone vs. CO, multiplied by an assumed urban  
10  $\text{CO}/\text{NO}_x$  emissions ratio [Kleinman *et al.*, 1998; Parrish *et al.*, 2002]. The Nashville urban plume  
11 achieves a somewhat higher yield and does so more rapidly than most power plants studied to date.  
12 The petrochemical plumes, however, produce substantially more ozone per unit  $\text{NO}_x$ , and produce  
13 that ozone far more rapidly, than plumes from the other two anthropogenic source types compared  
14 here. Both the rapidity of formation and the eventual yield of ozone in these petrochemical plumes  
15 are qualitatively consistent with elevated mixing ratios of reactive VOCs and  $\text{NO}_x$  being initially  
16 present upon emission.

17         Systematic differences in derived ozone yields between plumes from the three isolated  
18 petrochemical facilities are consistent with differences in source VOC profiles. The Sweeny plume  
19 was characterized by the highest initial (ethene/ $\text{NO}_x$ ) ratio and showed the highest ozone yields of  
20 the three plumes studied here. The additional entrainment of biogenic isoprene into the Sweeny  
21 plume during transport also tends to increase the ozone yield. The Freeport plume exhibited the  
22 lowest (alkene/ $\text{NO}_x$ ) ratios and consequently showed slightly lower ozone yields than plumes from  
23 the other two facilities. Real differences exist in petrochemical source emissions profiles, so that  
24 generalization from this study to all petrochemical industrial emissions is not warranted. Plumes  
25 from gasoline refineries, for example, are primarily composed of alkanes and are low in reactive  
26 alkenes (e.g., [Kalabokas *et al.*, 2001; Sexton and Westberg, 1979; Sexton and Westberg, 1983;  
27 Watson *et al.*, 2001]; these typically do not produce ozone as rapidly or in as high a yield.

1           **3.1.6. Contrast to initial OH reactivity in a power plant plume.** The OH + alkene  
2 reactions described above initiate radical chain propagation steps that result in substantial net ozone  
3 formation downwind. The radical chain termination step of  $\text{NO}_2 + \text{OH}$  is seen to be of lesser  
4 importance soon after emission (Plates 3b and 3d), confirming that overall radical chain lengths are  
5 relatively long at the high (VOC/ $\text{NO}_x$ ) ratios characteristic of these petrochemical industrial plumes.  
6 The apparent yield of 10-18 molecules of ozone per  $\text{NO}_x$  molecule oxidized from these complexes  
7 is qualitatively consistent with the extended radical chain length deduced from initial hydrocarbon  
8 reactivity (e.g., Plate 3; [Derwent and Davies, 1994]). In contrast, in the  $\text{NO}_x$ -rich and VOC-poor  
9 plume from the W.A. Parish electric utility power plant,  $\text{NO}_2$  is the primary OH reaction partner  
10 immediately downwind (Plate 5), favoring  $\text{HNO}_3$  formation in the early stages of plume transport  
11 [Neuman et al., 2002; Ryerson et al., 2001]. Slower rates of ozone formation and lower eventual  
12 ozone yields are predicted for the Parish plume on the basis of the data shown in Plate 5. We  
13 present the derived ozone yield in the aged Parish plume along with those from the Ship Channel  
14 petrochemical industrial sources and the Houston urban area in the Comparison section, below.

15

## 16 **3.2. Comparison of anthropogenic source types: petrochemical, urban, and power plant.**

17           The Electra flights of August 27 and 28 also sampled the coalesced plume from multiple  
18 petrochemical complexes to the southeast and east of Houston, the plume from the Houston urban  
19 core, and that from the W.A. Parish gas- and coal-fired power plant (Plate 1). Steady southerly  
20 winds on both days led to transport of anthropogenic  $\text{NO}_x$  and VOC emissions from facilities in  
21 Texas City towards and over other substantial petrochemical sources located in LaPorte, Deer Park,  
22 Pasadena, Channelview, and Baytown, all generally adjacent to the Houston Ship Channel roughly  
23 40 km north of Texas City (Plate 1). Each complex encompasses a large number of individual  
24 facilities in close proximity, each with potentially unique emissions with differing ratios of VOCs to  
25  $\text{NO}_x$ , complicating transect-by-transect analysis of individual source emissions plumes. Transport  
26 times on the order of hours over this extended grouping of petrochemical sources further  
27 complicates process analysis similar to that employed for the isolated petrochemical plumes, above,

1 which requires knowledge of transport time. In contrast to the isolated plumes, photochemical  
2 processing in the coalesced Texas City/Ship Channel plume air parcels on these two days was  
3 repeatedly affected by substantial injections of fresh emissions during transport over source  
4 locations downwind. While near-field transect data are sufficient to distinguish individual sources,  
5 mixing during transport quickly acted to diminish individual plume signatures.

6 We focus on data taken in photochemically-aged plumes downwind of the respective source  
7 regions to illustrate the net cumulative effect of multiple upwind sources on ozone formation rate  
8 and yield. The northernmost transects were flown east-to-west at 30.3° latitude or 70 km north of  
9 the Ship Channel on August 27 (30.6° or 90 km on August 28) and were characterized by a plume  
10  $\text{NO}_x/\text{NO}_y$  ratio of roughly 0.20, indicating that ~80% of the original  $\text{NO}_x$  emissions had been  
11 oxidized at this distance downwind. During these transects, no single petrochemical point source  
12 was clearly distinguishable in the time series, while broad enhancements in oxidized nitrogen  
13 species, ozone, CO,  $\text{CO}_2$ , and  $\text{SO}_2$  were all well correlated due to extensive mixing and reaction of  
14 plume constituents from multiple petrochemical point sources upwind. We analyze data from two  
15 transects, one at ~2.7 hours and the other ~5.6 hours downwind of the Ship Channel, to extract  
16 information on differences in ozone formation rates and yields between the three source types.

17

### 18 **3.2.1. Coalesced petrochemical plumes.**

#### 19 **3.2.1.1. Contribution of petrochemical emissions to observed $\text{NO}_x$ mixing ratios.**

20 Comparisons of the observed petrochemical source region  $\text{CO}/\text{NO}_x$  ratios to those from other  
21 urban areas (e.g., [Harley *et al.*, 2001; Kleinman *et al.*, 1998; Parrish *et al.*, 1991; Parrish *et al.*,  
22 2002]) and to that in the Houston urban core imply that petrochemical  $\text{NO}_x$  emissions contributed  
23 substantially to the elevated  $\text{NO}_x$  mixing ratios typically observed in the Ship Channel plume. The  
24 magnitudes of the largest enhancements in  $\text{NO}_x$ ,  $\text{CO}_2$ , and  $\text{SO}_2$ , as well as their tight correlations,  
25 are characteristic of natural gas- or oil-fired point sources and are quite different than those  
26 typically observed as a result of tailpipe emissions alone. However, the contribution of  $\text{NO}_x$  emitted  
27 from typically urban mobile sources in this area was not negligible in terms of ozone formation in

1 these coalesced plumes. Observed ozone downwind of the Ship Channel on the 27th and 28th is  
2 therefore interpreted as the net effect of photochemical processing of  $\text{NO}_x$  emissions from both  
3 petrochemical and urban  $\text{NO}_x$  sources.

#### 4 **3.2.1.2. Contribution of petrochemical emissions to observed VOC mixing ratios.**

5 (Propene/ethyne) and (ethene/ethyne) ratios above and immediately downwind of the Ship Channel  
6 and Texas City source areas ranged from 5 to 40 and from 3 to 40, respectively. These ratios are  
7 consistent with those in resolved plumes from geographically-isolated petrochemical sources south  
8 of Houston, discussed above, suggesting that elevated mixing ratios of reactive alkenes in the  
9 coalesced Ship Channel plume are primarily due to emissions from the petrochemical industry. We  
10 conclude that on-road tailpipe emissions were insignificant contributors to the observed alkene  
11 mixing ratio enhancements, and thus the bulk of VOC reactivity determining ozone formation,  
12 despite the general location of petrochemical sources within the extended Houston metropolitan  
13 area. The resulting prompt ozone formation is primarily ascribed to emissions of propene and  
14 ethene from Ship Channel petrochemical industrial sources, with relatively minor contributions  
15 from urban VOCs on the timescales considered here.

16 **3.2.1.3. Initial VOC reactivity.** Aircraft measurements on August 27 and 28 show that  
17 the primary OH reactivity in the coalesced petrochemical plume beginning north of Texas City and  
18 extending downwind over and past the Ship Channel was due to reaction with petrochemical  
19 emissions of reactive alkenes and their photoproducts  $\text{CH}_2\text{O}$  and  $\text{CH}_3\text{CHO}$ . Because of the limited  
20 number of VOC samples on any single flight, this conclusion is best illustrated using the full data  
21 set from all 14 Electra research flights in the Houston area (Plate 6). Derived total OH loss rates to  
22 measured VOC compounds from *in-situ* and canister measurements within the boundary layer  
23 during the 2000 Houston study are plotted (circles) as a function of sampling location in Plate 6.  
24 The symbols in Plate 6 are sized by the magnitude of OH reactivity with measured VOCs and  
25 colored by the fractional contribution of alkenes to the total reactivity.

26 The data shown in Plate 6 demonstrate that OH reactivity from the measured VOC  
27 compounds was substantially enhanced above the petrochemical source regions relative to the urban

1 area or the surrounding rural areas. Emissions plumes were encountered in different directions  
2 downwind depending on the prevailing wind direction on a particular day; for example, in Plate 6  
3 the Texas City plume enhancements can be found both east over Galveston Bay, or west and inland.  
4 Independent of wind direction, the maximum reactivity on every flight was clearly localized over the  
5 Ship Channel. The samples in the Sweeny, Freeport, and Chocolate Bayou plumes on August 27  
6 and 28, discussed above, are included in Plate 6 but show relatively low reactivity compared to the  
7 Ship Channel region. Alkenes strongly dominated the total reactivity. Above the Ship Channel the  
8 contribution from alkenes was typically >80% (Plate 6). The contribution from elevated mixing  
9 ratios of propene and ethene dominated, with the two compounds constituting >70% of the  
10 measured total directly over the source areas. Generally, propene contributed a factor of  
11 approximately 2 more than did ethene, and all other alkenes contributed substantially less, to derived  
12 OH reactivity in the Ship Channel source region.

13 The remainder of alkene reactivity was primarily due to isoprene, likely from a combination  
14 of anthropogenic and biogenic sources, and 1,3-butadiene; however, on average these dienes  
15 contributed less than 10% of the Ship Channel total. Samples taken immediately downwind of the  
16 Texas City petrochemical complexes suggest proportionally greater contributions from the  
17 branched alkanes 2-methylpropane and 2-methylbutane, but these did not exceed 10% of the total  
18 calculated OH reactivity close to the source region. Given the varied nature of the petrochemical  
19 industrial facilities in the Houston area, other compounds were occasionally substantially enhanced,  
20 presumably when a VOC sample was taken very close to an individual source of that particular  
21 compound. With few exceptions, however, propene and ethene dominated the reactivity toward OH  
22 of the emissions mix from the petrochemical industry in this area.

23 In contrast to the Ship Channel area, measurements taken in the Houston urban core  
24 exhibited substantially lower OH reactivity, with values typically  $<2.0 \text{ s}^{-1}$  and similar to that of other  
25 major urban areas studied to date. While a major fraction of reactivity in the urban core is due to  
26 alkenes emitted from transportation sources, the resulting mixing ratios were sufficiently low that

1 the total OH reactivity was small compared to air masses sampled directly over petrochemical  
2 source regions in the Ship Channel.

3 Enhancements in propene and ethene dominated OH reactivity above the petrochemical  
4 source regions, but these compounds are sufficiently reactive that daytime atmospheric mixing  
5 ratios decay rapidly with distance downwind (Plate 6). Photooxidation of these reactive alkenes  
6 produces  $\text{CH}_2\text{O}$  and  $\text{CH}_3\text{CHO}$ , which are themselves quite reactive and are also subject to  
7 photolysis, further propagating the  $\text{HO}_x$  radical chain.  $\text{CH}_2\text{O}$  data measured aboard the Electra on  
8 the August 27 and 28 flights are shown as a function of aircraft location in Plate 7. Minimal  
9 enhancements above petrochemical source regions suggest that while some direct emissions are  
10 possible, the bulk of the observed  $\text{CH}_2\text{O}$  on August 27 and 28 was formed as a secondary product  
11 of alkene oxidation downwind of petrochemical complexes [Wert *et al.*, 2002]. The enhancements  
12 of  $\text{CH}_2\text{O}$  at intermediate distances downwind of the Sweeny and Freeport facilities shown in the  
13 time series of Plates 3b and 3d are also apparent in Plate 6b. Decreases in  $\text{CH}_2\text{O}$  mixing ratios  
14 observed further downwind are also consistent with very short-lived alkene species as the primary  
15  $\text{CH}_2\text{O}$  source. As source alkenes were rapidly reacted away (Plate 6),  $\text{CH}_2\text{O}$  mixing ratios first  
16 increased, then decreased with distance downwind (Plate 7) as the alkene source was consumed, and  
17  $\text{CH}_2\text{O}$  loss and plume dilution acted to decrease atmospheric mixing ratios thereafter [Wert *et al.*,  
18 2002]. On-board measurements of  $\text{CH}_3\text{CHO}$  (P. Goldan, manuscript in preparation, 2002), while  
19 more limited in coverage, are generally consistent with the interpretation of VOC and  $\text{CH}_2\text{O}$  data  
20 presented above. Thus, on the flights of the 27th and 28th of August, the bulk of the measured  
21 VOC reactivity in coalesced plumes from Texas City and the Houston Ship Channel was due to  
22 substantial petrochemical emissions of propene and ethene and their photoproducts  $\text{CH}_2\text{O}$  and  
23  $\text{CH}_3\text{CHO}$ . Again, no substantial upsets involving propene or ethene releases coincident with the  
24 aircraft transects were reported to TNRCC on either of these two days, suggesting that the  
25 observations are representative of the averaged impact of routine petrochemical industrial operations  
26 in this area.

#### 1           **3.2.1.4. Ozone formation rate and yield in the coalesced petrochemical plume.**

2 Ozone production takes place rapidly in the coalesced plume downwind of the Ship Channel  
3 industrial facilities, consistent with the findings from the isolated petrochemical plumes discussed  
4 above. This is illustrated by a time series of ozone data taken along the E-W transect at 30.1°  
5 latitude within the boundary layer (Plate 8). Plume locations from sources in the Ship Channel  
6 (blue line, in inset map in Plate 8), the Houston urban area (red line), and the W.A. Parish power  
7 plant (black circle) are shown as heavy overlays along the flight track (dotted line). The upper time  
8 series in Plate 8 shows the directly emitted compounds  $\text{NO}_y$ ,  $\text{CO}_2$ , and  $\text{CO}$ ; these tracers and  $\text{SO}_2$   
9 (not shown) were used to differentiate between the various plumes, whose edges are approximately  
10 defined by the vertical dashed lines. The lower time series shows the photoproducts ozone and  
11  $\text{CH}_2\text{O}$  measured along this transect, which was flown approximately 43 km north, or 2.7 hours  
12 transport time, downwind of the Ship Channel and the I-10 corridor just north of downtown  
13 Houston.

14           Differences are apparent between the three plumes in the amount of ozone produced by this  
15 time downwind. Petrochemical plume mixing ratios of ozone approaching 140 ppbv were  
16 coincident with  $\text{CH}_2\text{O}$  of 14 ppbv, which were the highest values for either species encountered  
17 during this flight; much smaller enhancements are found in the urban and power plant plumes.  
18 Differences in  $\text{NO}_y$  mixing ratios between the three plumes were much less pronounced (Plate 8,  
19 top panel), suggesting that the rapidity of ozone formation was primarily due to the enhanced VOC  
20 reactivity characteristic of Houston-area petrochemical emissions. Rapid ozone production leading  
21 to the accumulation of very high, spatially localized surface ozone mixing ratios has been a unique  
22 feature of the Houston area; these findings point toward petrochemical industrial emissions as the  
23 primary cause of the observed high ozone events.

24           Ozone formation yield is inferred from data taken in the most fully oxidized transects  
25 downwind. The geographical extent of the photochemically processed Ship Channel/Texas City  
26 plume on August 28 is defined by substantial enhancements in  $\text{CO}_2$  and  $\text{SO}_2$ , with relatively smaller  
27 enhancements in  $\text{CO}$ , observed on the northernmost transect downwind (Plate 9 inset). At this

1 transect, ~5.6 hours downwind of the Ship Channel, the coalesced petrochemical plume ( $\text{NO}_x/\text{NO}_y$ )  
2 ratio was  $0.19 \pm 0.02$ , indicating extensive photooxidation of primary NO emissions had occurred  
3 during transport. Coalesced petrochemical plume ozone data from this transect are plotted in Plate  
4 8a versus measured ( $\text{NO}_y - \text{NO}_x$ ). These data are highly correlated ( $r^2 = 0.978$ ) with a linear-least-  
5 squares fitted slope suggesting that, neglecting depositional loss of  $\text{HNO}_3$  during transport, roughly  
6 12 molecules of ozone had been generated per  $\text{NO}_x$  molecule oxidized [*Trainer et al.*, 1993] at this  
7 distance downwind on August 28. For comparison, a slope of 11 is derived from ozone plotted vs.  
8 ( $\text{NO}_y - \text{NO}_x$ ) using the August 27 flight data from the northernmost transect, showing consistency  
9 from day to day. These high apparent yields are consistent with the range of ozone yields derived  
10 using data from the isolated and resolved plumes from the petrochemical complexes at Sweeny,  
11 Freeport, and Chocolate Bayou, described above. Again, these derived yields are substantially  
12 larger than recent measurements suggest for both urban and power plant plumes, reflecting the  
13 extremely reactive mix of VOC and the elevated ( $\text{VOC}/\text{NO}_x$ ) ratios in plumes from petrochemical  
14 industrial complexes in the Houston area. Similarity in derived ozone yields between the two days,  
15 with no substantial emission upsets reported to TNRCC, indicates these values are representative  
16 for emissions during normal operation of the multiple Ship Channel and Texas City petrochemical  
17 complexes under the meteorological conditions of those two days.

18 We note that the derived yields exceeding 10 mol/mol for the petrochemical plumes  
19 encountered on August 27 and 28 are some of the highest values calculated from the Electra data set  
20 during the Texas 2000 project. Lower ozone yields are derived in the more concentrated plumes  
21 that lead to the highest ozone mixing ratios, from 150 to over 200 ppbv of ozone, during the  
22 extreme ozone exceedence episodes observed from the Electra aircraft. More rapid plume dilution,  
23 under the meteorological conditions of the 27th and 28th of August, likely increased the ozone  
24 formation yield in the plumes considered in this report; this is qualitatively consistent with the  
25 expected dependence of ozone formation yield on plume  $\text{NO}_x$  concentration (e.g., [*Derwent and*  
26 *Davies*, 1994; *Liu et al.*, 1987; *Ryerson et al.*, 2001]). Slower rates of dilution are expected to both  
27 decrease ozone yield and permit higher ozone mixing ratios to accumulate. In addition, the

1 prevailing wind direction has a substantial effect on atmospheric concentrations resulting from Ship  
2 Channel petrochemical emissions. N-S winds perpendicular to the Ship Channel axis, such as on  
3 August 27<sup>th</sup> and 28<sup>th</sup>, 2000, will advect a given air parcel much more rapidly over the petrochemical  
4 source region than will E-W winds blowing along the long axis of the Ship Channel (Plate 1).  
5 Other things being equal, different atmospheric mixing ratios due to different prevailing wind  
6 directions will therefore modulate ozone formation rates and yields downwind.

7 **3.2.2. Ozone yields in the Houston urban plume.** The relatively undisturbed Houston  
8 urban plume is defined by a maximum in CO, the relative minimum in CO<sub>2</sub>, and the absence of  
9 measurable SO<sub>2</sub> found between the coalesced Ship Channel/TX City plume and the Parish power  
10 plant plume on transects from both days. While these segments do not encompass the entire urban  
11 plume, they are sufficient to define an approximately linear trend in ozone versus measured (NO<sub>y</sub> -  
12 NO<sub>x</sub>), plotted in Plate 9a from the northernmost transect on August 28. These urban plume data  
13 were characterized by a NO<sub>x</sub>/NO<sub>y</sub> ratio of  $0.19 \pm 0.03$ , virtually identical to that observed in the  
14 Ship Channel plume, suggesting a roughly similar extent of photochemical processing and  
15 facilitating direct comparison of derived ozone yields at this transect. The ozone yield of  $5.4 \pm 0.2$   
16 derived from a fitted slope to the Houston urban plume data in Plate 9a is consistent with the range  
17 of reported yields for other urban areas (e.g., [Daum *et al.*, 2000a; Nunnermacker *et al.*, 2000;  
18 Trainer *et al.*, 1995]; see also Plate 4b). The yield in the Houston urban plume is found to be a  
19 factor of ~2 lower than that derived for the Ship Channel plume along the same transect at similar  
20 levels of NO<sub>x</sub> oxidized. The difference resulted from substantially different proportions of NO<sub>x</sub>  
21 oxidation by OH relative to oxidation by peroxy radicals integrated over the transport history of  
22 each plume.

23 **3.2.3. Ozone yields in the W.A. Parish power plant plume.** The Parish plume  
24 transect characterized by a NO<sub>x</sub>/NO<sub>y</sub> ratio of  $0.24 \pm 0.04$  was sampled at 30.1° latitude on August  
25 28, or two transects south of that used to derive Ship Channel and Houston urban plume ozone  
26 yields. The derived ozone yield from the slope of the power plant plume transect data in Plate 9a is  
27  $2.2 \pm 0.2$ . The Parish plume had been emitted into the aged plume from the Freeport complex

1 upwind and was later advected over the western edge of the Houston metropolitan area. Despite  
2 these external sources of hydrocarbons, the Parish plume (VOC/NO<sub>x</sub>) ratio (Plate 5) during  
3 transport was apparently sufficiently low that relatively little ozone had been formed by the transect  
4 shown in Plate 9a. This finding is consistent with the prediction of low ozone yield from the low  
5 (VOC/NO<sub>x</sub>) ratio observed just after emission, noted above (Plate 5). The factor of ~2 difference in  
6 observed ozone yields between the Parish power plant and the Houston urban plumes at similar  
7 (NO<sub>x</sub>/NO<sub>y</sub>) on the 28th, and a factor of over ~5 between the Parish and the Ship Channel plumes, is  
8 ascribed to the combined effects of substantial source differences in NO<sub>x</sub> and VOC emissions rates,  
9 the resulting plume mixing ratios, and (VOC/NO<sub>x</sub>) ratios between plumes from these three  
10 anthropogenic source types.

11 Ozone production rates and yields are dependent on a number of factors, including rates of  
12 dispersion and mixing determined by the meteorological situation on a particular day. Aircraft  
13 observations on other days during the Texas 2000 study show different derived rates and yields in  
14 plumes from the sources considered here. Thus, while the relative differences between ozone  
15 production in plumes from different sources remain, absolute values of ozone production rate and  
16 yield reported here will vary with insolation or meteorology.

17 *Uncertainties in derived ozone yields (overlapping plumes).* While HNO<sub>3</sub> loss has been  
18 shown to be relatively modest (<20% in 4 hrs) for the isolated petrochemical facilities and the W.A.  
19 Parish plumes on August 27<sup>th</sup> and 28<sup>th</sup>, the extent to which this process affected measured NO<sub>y</sub>  
20 mixing ratios in the overlapping Ship Channel and urban plumes is not known. However, at the  
21 earlier transects (e.g., at 30.1° latitude, 2.7 hours old, Plate 8) when potential NO<sub>y</sub> loss is thought to  
22 be less significant, the apparent ozone production efficiency had already reached 9 mol/mol in the  
23 Ship Channel plume. Another confounding factor in interpreting fitted slopes to measured ozone  
24 and (NO<sub>y</sub>-NO<sub>x</sub>) data solely in terms of photochemical ozone production comes from variability in  
25 the background due to partially overlapping plumes. Given the uncertainties in estimating ozone  
26 yields from measured data in partially overlapping plumes, the apparent ozone production yields  
27 derived here for the Parish, urban, and coalesced Ship Channel plumes are estimated to be accurate

1 to within a factor of two. However, the primary conclusion drawn from the large differences  
2 observed between plumes from the three different source types (Plate 9a) is more robust. The  
3 fractional contribution of  $\text{HNO}_3$  to the products of  $\text{NO}_x$  oxidation in each plume is a function of the  
4 ratio of OH to peroxy radicals occurring during transport. Substantial differences in ( $\text{HNO}_3/(\text{NO}_y -$   
5  $\text{NO}_x)$ ) ratios are apparent in Plate 9b between the Ship Channel and the urban and power plant  
6 plumes. The Ship Channel plume was composed of roughly equal amounts of PAN-type  
7 compounds and  $\text{HNO}_3$ , while essentially all of the Parish  $\text{NO}_x$  had been oxidized to  $\text{HNO}_3$ , at this  
8 distance downwind (Plate 9b; [Neuman *et al.*, 2002]). If  $\text{HNO}_3$  loss had been substantial,  
9 accounting for this effect would decrease the ozone yields derived from the slope data plotted in  
10 Plate 8a. Given the relative amounts of PAN formed, potential losses of  $\text{HNO}_3$  are expected to have  
11 been greater in the W.A. Parish plume than for the petrochemical or urban plumes. Any correction  
12 to derived ozone yields would therefore increase the differences in ozone production derived from  
13 the plume data in Plate 9a. Similarly, additional ozone formation downwind of the northernmost  
14 transect is expected to be relatively slow and contribute minimally to derived ozone yields, as  
15 discussed above. Taking into account observed differences in PAN-type compound abundance  
16 relative to total  $\text{NO}_y$ , further ozone production would be expected to only increase the differences in  
17 yields between these three source types.

18

#### 19 **4. Discussion**

20 A distinguishing feature of petrochemical plumes is that a substantial amount of reactive  
21 hydrocarbons can be co-emitted with  $\text{NO}_x$ , in contrast to power plant plumes into which reactive  
22 hydrocarbons must be entrained from the surrounding atmosphere. For power plants, then, their  
23 location relative to external sources of reactive hydrocarbons is critical in determining the rate and  
24 yield of ozone formed in plumes downwind [Ryerson *et al.*, 2001]. In contrast, large petrochemical  
25 industrial co-emission of reactive VOC and  $\text{NO}_x$  is expected to result in appreciable ozone  
26 formation in the summertime regardless of the geographic location. Despite the hundreds of VOC  
27 compounds known to be emitted from petrochemical facilities, VOC measurements aboard the

1 Electra in 2000 suggest that only two alkenes make the largest contribution to prompt ozone  
2 production in the greater Houston metropolitan area. This finding is not unique to the month-long  
3 Texas 2000 study period. Elevated alkene levels appear to have been characteristic of this area ever  
4 since the first measurement campaigns were motivated by passage of the Clean Air Act in 1970, as  
5 discussed below.

6 **4.1. Elevated alkenes in Houston, 1976 - 2002.** Substantially elevated mixing ratios of  
7 highly reactive alkenes have been a persistent feature of the Houston area for an extended period of  
8 time. Previous studies in the Houston area in 1976 (Gulf Coast Oxidant Study [*Decker et al.*,  
9 1976]), 1977 (Houston Area Oxidants Study [*HACC*, 1979]), and in 1993 (Coastal Oxidant  
10 Assessment for Southeast Texas [*Lawson et al.*, 1995] and Gulf of Mexico Air Quality Study  
11 [*Kearney*, 1995] have all found very high median mixing ratios of alkenes at sampling sites in the  
12 Ship Channel area. These studies suggest that mixing ratios of propene and ethene in particular  
13 have been strongly elevated in the Ship Channel region for over twenty years, beginning with some  
14 of the first measurements showing a Houston ozone exceedence problem. More recently, 24-hour-  
15 integrated canister VOC samples taken twice a week since 1997 at various locations along the Ship  
16 Channel have shown median mixing ratios of propene (ca. 4 ppbv) and ethene (ca. 12 ppbv)  
17 sufficient to dominate VOC reactivity, qualitatively consistent with the findings reported here (W.  
18 Crow, personal communication, 2001).

19 Most recently, on April 22, 2002 the instrumented NOAA WP-3D aircraft sampled the  
20 emissions plumes from facilities in Texas City, Chocolate Bayou, Freeport, and Sweeny, as well as  
21 that from the Seadrift petrochemical complex near Victoria, TX. Multiple VOC canister samples  
22 were acquired in the near-field plume transects (Plate 10) to provide additional data on the  
23 (alkene/ $\text{NO}_x$ ) emissions ratios observed during the Texas 2000 study from the Electra aircraft.  
24 Measured ethene, propene, and  $\text{NO}_x$  are plotted as a function of aircraft longitude to facilitate  
25 comparison. In general, while measured (alkene/ $\text{NO}_x$ ) ratios were different than in the same plumes  
26 observed in 2000, all were substantially higher than inventories suggest. The Seadrift complex is  
27 the largest ethene point source in Texas, according to TNRCC and EPA inventories; however, the

1 measured plume (ethene/ $\text{NO}_x$ ) ratio of 4-5 (Plate 9) is still much higher than the annual average  
2 emissions ratio of ~ 0.5 derived from these inventories.

3

#### 4 **Conclusions.**

5 The principal reactions leading to the rapid ozone formation characteristic of the Houston  
6 area are shown to involve oxidation of petrochemical emissions of propene and ethene. This is  
7 encouraging for successfully simulating Houston-area petrochemical plume ozone production in 3-  
8 D atmospheric models that rely on simplified, or lumped, VOC reaction schemes [Dodge, 2000].  
9 The chemical solvers in most 3-D models treat oxidation of the light alkenes explicitly and should  
10 be entirely appropriate for modeling prompt ozone formation in the Houston area. The principal  
11 shortcoming in successful model simulations of prompt ozone formation appears to be the  
12 substantial underestimate of petrochemical alkene emissions in inventory tabulations. It will be  
13 difficult for chemically explicit 3-D models of appropriate spatial resolution to reproduce ozone  
14 observations in the Houston area until routine petrochemical VOC emissions rates are more  
15 realistically included in inventories.

16 Apparent ozone formation rates and yields derived on these two days for the isolated  
17 complexes and the coalesced Ship Channel plumes are qualitatively similar and are ascribed to  
18 similarly elevated (alkene/ $\text{NO}_x$ ) emissions ratios from the aggregated petrochemical facilities at each  
19 complex. These rates and yields are substantially higher than those derived on the same day under  
20 similar meteorological conditions for the Houston urban plume and that from the W.A. Parish  
21 power plant. Further, the urban and power plant yields are qualitatively similar to those reported for  
22 other urban areas and rural power plants. Finally, the hourly-, daily-, and annually-averaged  
23 emissions suggest that these observations are the result of typical operation of the power plants and  
24 petrochemical industrial facilities in the area. Such consistency suggests that the Texas 2000  
25 mission data are representative of the normal effects of various anthropogenic emissions sources on  
26 tropospheric ozone in the Houston area. We emphasize that while derived values reported here are  
27 subject to substantial day-to-day variability according to meteorological conditions, the differences

1 in ozone formation rates and yields between the three anthropogenic source types are expected to  
2 remain.

3         The chemistry required to capture the important features of prompt ozone production in  
4 Houston is thus dependent on a limited set of all possible VOCs known to be emitted from  
5 petrochemical sources [Derwent, 2000; Watson *et al.*, 2001]. These findings ultimately suggest  
6 that correctly estimating emissions of reactive light alkenes should be emphasized in constructing  
7 accurate VOC emissions inventories for Houston-area petrochemical industrial sources. Finally,  
8 these reactive light alkenes should represent the primary focus of current and future VOC  
9 emissions control measures designed to reduce tropospheric ozone formation from these individual  
10 facilities. Reduction in emissions of ethene and propene alone would account for over 75% of  
11 initial VOC reactivity and by inference the majority of the prompt ozone formed in the  
12 petrochemical plumes studied here. Reductions in emissions of alkanes, other alkenes, and  
13 aromatic compounds would be substantially less effective in mitigating rapid ozone formation in  
14 high yield downwind of these sources.

15

#### 16 **Acknowledgments.**

17         We thank the staff and flight crew of the NCAR Research Aviation Facility for their support  
18 during the Texas 2000 project. Thanks are also due to T. Martin and R. Coulter for providing wind  
19 profiler data, to J. Mellberg and J. Neece for compiling the special emissions inventory for the  
20 Texas 2000 study, and to J. Meagher for suggestions on the draft manuscript. Participation,  
21 suggestions, and cooperation from many companies and individuals from the Houston area  
22 petrochemical industry are gratefully acknowledged. This work was funded in part by TNRCC and  
23 the NOAA Health of the Atmosphere and Climate and Global Change programs.

1 **Table 1.** Names and OH rate coefficients ( $k_{OH}$ ) for hydrocarbon compounds and selected other  
 2 species measured aboard the Electra used in this report<sup>1</sup>.  
 3

Alkanes	$k_{OH}$	Alkenes	$k_{OH}$	Aromatics	$k_{OH}$	Alkynes	$k_{OH}$	Others	$k_{OH}$
ethane	0.3	ethene	9	benzene	1.2	ethyne	0.9	CO	<b>0.2</b>
propane	1.1	propene	26	methylbenzene (toluene)	6.0	propyne	5.9	CH <sub>4</sub>	0.007
n-butane	2.4	1-butene	31	ethylbenzene	7.1			CH <sub>3</sub> CHO	17
2-methylpropane	2.2	cis-2-butene	56	1,2-dimethylbenzene	13.7			CH <sub>2</sub> O	8
n-pentane	4.0	trans-2-butene	64	1,3- and 1,4- dimethylbenzene	20			NO <sub>2</sub>	9
2-methylbutane	3.7	1,3-butadiene	67	phenylethene (styrene)	58				
cyclopentane	5.0	1-pentene	31	2-methylethylbenzene	12.3				
n-hexane	5.5	2-methyl-2-butene	87	n-propylbenzene	6.0				
2-methylpentane	5.3	3-methyl-1-butene	32	1,3,5- trimethylbenzene	58				
2,2-dimethylbutane	2.3	trans-2-pentene	67	1,2,4- trimethylbenzene	33				
2,3-dimethylbutane	6.0	cis-2-pentene	65	1,2,3- trimethylbenzene	33				
3-methylpentane	5.4	cyclopentene	67						
methylcyclopentane	5.7	<b>2-methyl-1,3- butadiene (isoprene)</b>	101						
cyclohexane	7.2								
n-heptane	7.0								
2-methylhexane	7.0								
3-methylhexane	7.5								
2,3-dimethylpentane	7.1								
2,4-dimethylpentane	5.0								
methylcyclohexane	10.0								
n-octane	8.7								
2,2,4- trimethylpentane	3.6								
cis- and trans-1,3- dimethylcyclohexane	9.5								
n-nonane	10.0								
n-decane	11.2								

4  
 5 <sup>1</sup>Normal type indicates compounds measured only in the whole-air canister samples, italicized type  
 6 indicates those measured only in the *in-situ* GC, and bold type indicates those measured in both  
 7 systems. Rate coefficients ( $k_{OH}$ , in units of  $10^{-12}$  cm<sup>3</sup> molecule<sup>-1</sup> s<sup>-1</sup>) calculated for 298 K and 1013  
 8 mb from data in Atkinson [1994, 1997] and DeMore et al. [1997]. CO, CH<sub>4</sub>, NO<sub>2</sub>, CH<sub>2</sub>O, and  
 9 CH<sub>3</sub>CHO are included for comparison.

1 **Table 2.** Tabulated NO<sub>x</sub> and alkene emission rates and ratios, and measurement-inferred emission  
 2 ratios, for selected petrochemical complexes and an electric utility power plant.  
 3

Complex	E <sub>NO<sub>x</sub></sub> <sup>1</sup>	E <sub>ethene</sub> <sup>1</sup>	tabulated ethene/NO <sub>x</sub>	measured ethene/NO <sub>x</sub>	E <sub>propene</sub> <sup>1</sup>	tabulated propene/NO <sub>x</sub>	measured propene/NO <sub>x</sub>
Sweeny	12.6	0.6	0.05	3.6	0.4	0.03	2.0
Freeport	34.8	1.8	0.05	1.5	0.4	0.01	0.5
Chocolate Bayou	7.2	0.6	0.08	2.0	0.7	0.10	4.0
W.A. Parish	66.5	-	-	-	-	-	-

4  
 5 <sup>1</sup>Sum of annually-averaged emissions (kmoles/hr) listed in the 2000 TNRCC PSDB for the boxes in Plate 1.  
 6  
 7  
 8  
 9

10  
 11  
 12 **Table 3.** Tabulated NO<sub>x</sub> emission  
 13 rates for electric utility power plants  
 14 in Plate 4.  
 15

Power plant	E <sub>NO<sub>x</sub></sub> <sup>1</sup>
Johnsonville, TN	40-65
Thomas Hill, MO	78
Cumberland, TN	300-600
Paradise, KY	350

16  
 17 <sup>1</sup>Data from continuous emissions  
 18 monitoring systems at each plant,  
 19 expressed as an annual average in  
 20 kmoles NO<sub>2</sub>/hour.

1 **Figure captions.**

2

3 **Plate 1.** A 200 x 200 km map centered on the greater Houston metropolitan area (red line),  
4 showing the study region for Electra research flights of August 27 and 28, 2000. Locations of  
5 point emission sources are shown sized according to VOC emission source strengths (“E<sub>VOC</sub>”,  
6 filled green circles) and NO<sub>x</sub> emission source strengths (“E<sub>NOx</sub>”, open black circles) according to  
7 the legends provided. Emissions data are taken from the 2000 TNRCC PSDB; only sources  
8 greater than 100 tons per year are shown. The Houston Ship Channel is east of the Houston urban  
9 center, surrounded by numerous petrochemical facilities at 29.7° latitude; other major petrochemical  
10 complexes and power plants are labeled.

11

12 **Plate 2.** 90 x 90 km detail views of the map shown in Plate 1, showing measured ozone and NO<sub>y</sub>  
13 values plotted relative to aircraft position along the SW portions of the flight tracks on August 27  
14 (upper panel) and August 28 (lower panel). Symbols along the flight tracks give sample locations  
15 for the whole-air canisters (WAS, open squares) and *in-situ* GC (barred squares). Winds on both  
16 days were steady from 160° at 4.5 m/s. The scale bars show a 20 ppbv equivalent enhancement in  
17 ozone.

18

19 **Plate 3.** A). Time series of chemical data from the aircraft transect at 29.3° latitude (Plate 2), which  
20 sampled plumes downwind of the Sweeny, Freeport, and Chocolate Bayou petrochemical  
21 complexes on August 27, 2000. Horizontal bars show the time, duration, and calculated value of  
22  $k_{OH} [NO_2]$  (green bars),  $k_{OH} [CO]$  (grey bars),  $k_{OH} [CH_4]$  (blue bars), and  $k_{OH} \Sigma[VOC]$  (black bars) for  
23 each hydrocarbon sample. B). Speciated hydrocarbon measurements show that the alkenes ethene,  
24 propene, and isoprene account for >80%, and the sum of all measured aromatics <3%, of total  
25 plume OH reactivities with hydrocarbons on this transect. Derived loss rates for all measured  
26 VOCs are plotted; note that most lie below the minimum y-axis value of 0.1 s<sup>-1</sup>. CH<sub>2</sub>O mixing  
27 ratios (blue circles) were sufficiently enhanced, primarily due to photoproduction from directly

1 emitted alkenes, to represent a substantial reaction partner for OH in these plumes. C) and D). As  
2 in A and B above, for the 29.3° latitude transect of the August 28 flight.

3  
4 **Plate 4.** Derived ozone yields plotted as a function of time downwind for three anthropogenic  
5 source types. A) plume data from fossil-fueled power plants in Cumberland, TN (red circles, five  
6 flights in '95 and '99), Johnsonville, TN (blue triangles, four flights, '95 and '99), Paradise, KY  
7 (black squares, two flights, '95), and Thomas Hill, MO (green diamonds, one flight, '99). B) the  
8 Nashville urban plume (five flights, '95), and C) plumes from the Sweeny (squares), Freeport  
9 (circles), and Chocolate Bayou (triangles) petrochemical complexes. The data in C) are reproduced  
10 from Figure 1c, with August 27 (filled symbols) and August 28 (open symbols) shown.

11  
12 **Plate 5.** As in Plate 3 for the August 28 flight data, from the aircraft transect at 29.5° latitude  
13 roughly 4 km downwind of the W.A. Parish power plant. The broad maximum in ozone resulted  
14 from photochemically-aged emissions from the Freeport petrochemical complex, into which the  
15 Parish plume, here defined by  $\text{NO} > 1$  ppbv, was emitted. The data show the  $\text{OH} + \text{NO}_2$  radical  
16 termination step leading to  $\text{HNO}_3$  formation was strongly favored in the Parish plume at this  
17 transect.

18  
19 **Plate 6.** 200 x 200 km map of the study area showing locations of *in-situ* and whole-air canister  
20 hydrocarbon measurements (circles) taken below 1.5 km aircraft altitude, sized by  $\Sigma(k_{\text{OH}} [\text{VOC}])$   
21 and colored by  $(\Sigma(k_{\text{OH}} [\text{alkene}]))/(\Sigma(k_{\text{OH}} [\text{VOC}])),$  the fractional contribution of alkenes to the total.

22  
23 **Plate 7.** Map showing  $\text{CH}_2\text{O}$  (bars) measured below 2 km altitude along Electra flight tracks of  
24 August 27 (upper panel) and August 28 (lower panel).  $\text{CH}_2\text{O}$  mixing ratios are given by the size  
25 and color of the vertical bars, according to the legend at top. Direct emissions of  $\text{CH}_2\text{O}$  are seen to  
26 be negligible compared to that produced from alkene + OH reactions during transport downwind.

27

1 **Plate 8.** The inset map shows the E-W transect at  $30.1^\circ$  latitude on August 28, 2000 (solid gray  
2 line) along the aircraft flight track (dotted gray line). Locations of plumes from the W.A. Parish  
3 power plant “P”, the Houston urban core “u”, and the combined Ship Channel and urban plume  
4 “SC+u” along this transect are indicated by the vertical lines in the inset map and in the time  
5 series.

6  
7 **Plate 9.** Transect data for the W.A. Parish (black,  $\text{NO}_x/\text{NO}_y = 0.24$ ), Houston urban (red,  
8  $\text{NO}_x/\text{NO}_y = 0.19$ ), and Ship Channel/Texas City petrochemical plumes (blue,  $\text{NO}_x/\text{NO}_y = 0.19$ ) for  
9 the August 28th flight. Location of these plume transects are given by the colored overlays along  
10 the flight track shown in the inset map. Markedly different enhancements in ozone as a function of  
11  $\text{NO}_x$  oxidized are apparent (A), consistent with initial  $\text{VOC}/\text{NO}_x$  ratios observed immediately  
12 downwind of the sources and with large differences in the fraction of  $\text{HNO}_3$  generated (B) at these  
13 distances downwind.

14  
15 **Plate 10.** 330 x 250 km map of the Texas Gulf Coast showing measured  $\text{NO}_y$  (red line) plotted  
16 along the aircraft track at 470 m altitude (dotted line) for the NOAA WP-3D transit flight of April  
17 22, 2002. Blue circles along the track denote sampling locations for the WAS VOC canisters.  
18 Point sources of  $\text{NO}_x$  and VOC are plotted as described in Plate 1; winds were from  $150 - 180^\circ$  for  
19 the period shown. Mixing ratios of ethene (heavy black circles), propene (heavy blue circles),  $\text{NO}_y$   
20 (red), and ozone (divided by 3, light blue), are also shown as a function of longitude. Plumes from  
21 facilities at Texas City, Chocolate Bayou, Freeport, Sweeny, and the Seadrift petrochemical complex  
22 near Victoria, TX were sampled.

23  
24 **Figure 1.** Data from isolated petrochemical plumes sampled on August 27 and 28, 2000. Plotted  
25 points are slopes derived from linear-least-squares fits to measured plume data. (A)  $\text{NO}_x$  lifetimes  
26 average 1.5 hours, suggesting rapid photochemical processing and strongly elevated plume  $\text{RO}_x$

- 1 and OH levels. (B)  $\text{HNO}_3$  formation over time. (C) Net ozone production yields of 10 to 18
- 2 molecules/molecule of  $\text{NO}_x$  oxidized are derived.

1 **Running head:**

2

3 **Ryerson et al.: Petrochemical emissions and ozone formation in Houston, TX**

1 **References.**

- 2
- 3 Angevine, W.M., A.B. White, and S.K. Avery, Boundary-layer depth and entrainment zone  
4 characterization with a boundary-layer profiler, *Boundary-Layer Meteorology*, 68, 375-385,  
5 1994.
- 6 Atkinson, R., *Gas-phase tropospheric chemistry of organic compounds*, American Institute of  
7 Physics, Gaithersburg, MD, 1994.
- 8 Atkinson, R., Gas-phase tropospheric chemistry of volatile organic compounds: 1. alkanes and  
9 alkenes, *Journal of Physical and Chemical Reference Data*, 26, 215-290, 1997.
- 10 Banta, R.M., C.J. Senff, A.B. White, M. Trainer, R.T. McNider, R.J. Valente, S.D. Mayor, R.J.I.  
11 Alvarez, R.M. Hardesty, D.D. Parrish, and F.C. Fehsenfeld, Daytime buildup and nighttime  
12 transport of urban ozone in the boundary layer during a stagnation episode, *Journal of*  
13 *Geophysical Research*, 103, 22,519-22,544, 1998.
- 14 Bertman, S.B., J.M. Roberts, D.D. Parrish, M.P. Buhr, P.D. Goldan, W.C. Kuster, F.C.  
15 Fehsenfeld, S.A. Montzka, and H. Westberg, Evolution of alkyl nitrates with air mass age,  
16 *Journal of Geophysical Research*, 100, 22,805-22,813, 1995.
- 17 Brock, C.A., M. Trainer, T.B. Ryerson, J.A. Neuman, D.D. Parrish, J.S. Holloway, D.K.J. Nicks,  
18 G.J. Frost, G. Hübler, and F.C. Fehsenfeld, Particle growth in urban and industrial plumes in  
19 Texas, *Journal of Geophysical Research (in press)*, 2002.
- 20 Carter, W.P.L., Development of ozone reactivity scales for volatile organic compounds, *Journal of*  
21 *the Air and Waste Management Association*, 44, 881-899, 1994.
- 22 Chameides, W.L., R.W. Lindsay, J. Richardson, and C.S. Kiang, The role of biogenic  
23 hydrocarbons in urban photochemical smog: Atlanta as a case study, *Science*, 241, 1473-1475,  
24 1988.
- 25 Corbett, J.J., and P. Fischbeck, Emissions from ships, *Science*, 278, 823-824, 1997.
- 26 Crutzen, P.J., The role of NO and NO<sub>2</sub> in the chemistry of the troposphere and stratosphere,  
27 *Annual Reviews of Earth and Planetary Science*, 7, 443-472, 1979.

- 1 Daum, P.H., L. Kleinman, D.G. Imre, L.J. Nunnermacker, Y.-N. Lee, S.R. Springston, L. Newman,  
2 and J. Weinstein-Lloyd, Analysis of the processing of Nashville urban emissions on July 3 and  
3 July 18, 1995, *Journal of Geophysical Research*, *105*, 9155-9164, 2000a.
- 4 Daum, P.H., L. Kleinman, D.G. Imre, L.J. Nunnermacker, Y.-N. Lee, S.R. Springston, L. Newman,  
5 J. Weinstein-Lloyd, R.J. Valente, R.E. Imhoff, R.L. Tanner, and J.F. Meagher, Analysis of O<sub>3</sub>  
6 formation during a stagnation episode in central Tennessee in summer 1995, *Journal of*  
7 *Geophysical Research*, *105*, 9107-9119, 2000b.
- 8 Davis, D.D., G. Smith, and G. Klauber, Trace gas analysis of power plant plumes via aircraft  
9 measurement: O<sub>3</sub>, NO<sub>x</sub>, and SO<sub>2</sub> chemistry, *Science*, *186*, 733-735, 1974.
- 10 Davis, J.M., B.K. Eder, D. Nychka, and Q. Yang, Modeling the effects of meteorology on ozone in  
11 Houston using cluster analysis and generalized additive models, *Atmospheric Environment*, *32*,  
12 2505-2520, 1998.
- 13 Decker, C.E., L.A. Ripperton, J.J.B. Worth, F.M. Vukovich, W.D. Bach, J.B. Tommerdahl, F.  
14 Smith, and D.E. Wagoner, Formation and transport of oxidants along Gulf Coast and in  
15 northern U.S., Research Triangle Park, NC, 1976.
- 16 DeMore, W.B., S.P. Sander, D.M. Golden, R.F. Hampson, M.J. Kurylo, C.J. Howard, A.R.  
17 Ravishankara, C.E. Kolb, and M.J. Molina, Chemical kinetics and photochemical data for use in  
18 stratospheric modeling, NASA Jet Propulsion Laboratory, Pasadena, California, 1997.
- 19 Derwent, R.G., Ozone formation downwind of an industrial source of hydrocarbons under  
20 European conditions, *Atmospheric Environment*, *34*, 3689-3700, 2000.
- 21 Derwent, R.G., and T.J. Davies, Modelling the impact of NO<sub>x</sub> or hydrocarbon control on  
22 photochemical ozone in Europe, *Atmospheric Environment*, *28*, 2039-2052, 1994.
- 23 Dodge, M.C., Chemical oxidant mechanisms for air quality modeling: critical review, *Atmospheric*  
24 *Environment*, *34*, 2103-2130, 2000.
- 25 EPA, National Air Quality and Emissions Trends Report, 1999, United States Environmental  
26 Protection Agency, Research Triangle Park, 2001.

- 1 Flocke, F., A. Volz-Thomas, and D. Kley, Measurements of alkyl nitrates in rural and polluted air  
2 masses, *Atmospheric Environment*, 25A, 1951-1960, 1991.
- 3 Fried, A., B. Henry, B. Wert, S. Sewell, and J.R. Drummond, Laboratory, ground-based, and  
4 airborne tunable diode laser systems: performance characteristics and applications in  
5 atmospheric studies, *Applied Physics B*, 67, 317-330, 1998.
- 6 Gillani, N.V., J.F. Meagher, R.J. Valente, R.E. Imhoff, R.L. Tanner, and M. Luria, Relative  
7 production of ozone and nitrates in urban and power plant plumes 1. Composite results based  
8 on data from 10 field measurement days, *Journal of Geophysical Research*, 103, 22,593-22,615,  
9 1998.
- 10 Goldan, P.D., D.D. Parrish, W.C. Kuster, M. Trainer, S.A. McKeen, J. Holloway, B.T. Jobson,  
11 D.T. Sueper, and F.C. Fehsenfeld, Airborne measurements of isoprene, CO, and anthropogenic  
12 hydrocarbons and their implications, *Journal of Geophysical Research*, 105, 9091-9105, 2000.
- 13 Haagen-Smit, A.J., Chemistry and physiology of Los Angeles smog, *Industrial and Engineering  
14 Chemistry*, 44, 1342-1346, 1952.
- 15 HACC, Houston Area Oxidants Study program summary, Houston Area Chamber of Commerce,  
16 Houston, TX, 1979.
- 17 Harley, R.A., S.A. McKeen, J. Pearson, M.O. Rodgers, and W.A. Lonneman, Analysis of motor  
18 vehicle emissions during the Nashville/Middle Tennessee Ozone Study, *Journal of Geophysical  
19 Research*, 106, 3559-3567, 2001.
- 20 Holloway, J.S., R.O. Jakoubek, D.D. Parrish, C. Gerbig, A. Volz-Thomas, S. Schmitgen, A. Fried,  
21 B. Wert, B. Henry, and J.R. Drummond, Airborne intercomparison of vacuum ultraviolet  
22 fluorescence and tunable diode laser absorption measurements of tropospheric carbon  
23 monoxide, *Journal of Geophysical Research*, 105, 24,251-24,261, 2000.
- 24 Kalabokas, P.D., J. Hatzianestis, J.G. Bartzis, and P. Papagiannakopoulos, Atmospheric  
25 concentrations of saturated and aromatic hydrocarbons around a Greek oil refinery,  
26 *Atmospheric Environment*, 35, 2545-2555, 2001.

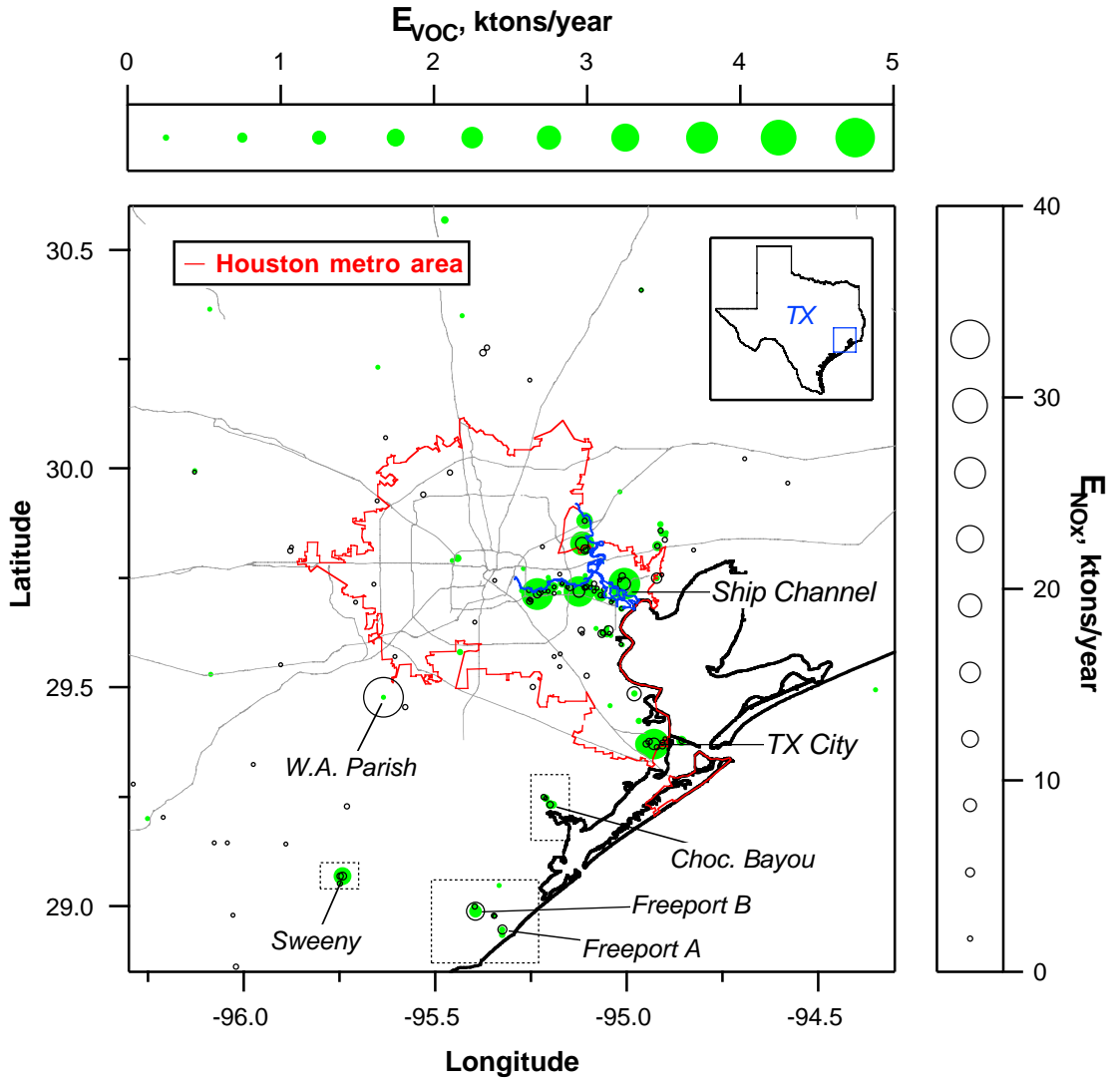
- 1 Kearney, A.T., Gulf of Mexico air quality study, final report. Volume I: Summary of data analysis  
2 and modeling, U.S. Department of the Interior, New Orleans, LA, 1995.
- 3 Kleinman, L., P.H. Daum, D.G. Imre, C. Cardelino, K.J. Olszyna, and R.G. Zika, Trace gas  
4 concentrations and emissions in downtown Nashville during the 1995 Southern Oxidants  
5 Study/Nashville Intensive, *Journal of Geophysical Research*, 20, 22,545-22,553, 1998.
- 6 Kleinman, L.I., P.H. Daum, D.G. Imre, J.H. Lee, Y.-N. Lee, L.J. Nunnermacker, S.R. Springston, J.  
7 Weinstein-Lloyd, and L. Newman, Ozone production in the New York City urban plume,  
8 *Journal of Geophysical Research*, 105, 14,495-14,512, 2000.
- 9 Kleinman, L.I., P.H. Daum, D.G. Imre, Y.-N. Lee, L.J. Nunnermacker, S.R. Springston, J.  
10 Weinstein-Lloyd, and J. Rudolph, Ozone production rate and hydrocarbon reactivity in 5 urban  
11 areas: a cause of high ozone concentration in Houston, *Geophysical Research Letters*, 29,  
12 10.1029/2001GL014569, 2002.
- 13 Lawson, D.R., N.F. Robinson, S. Diaz, J.G. Watson, E.M. Fujita, and P.T. Roberts, Coastal oxidant  
14 assessment for southeast Texas (COAST) project: final report, Desert Research Institute, Reno,  
15 NV, 1995.
- 16 Leighton, P.A., *Photochemistry of Air Pollution*, 300 pp., Academic Press, New York, 1961.
- 17 Levy, H., Normal atmosphere: large radical and formaldehyde concentrations predicted, *Science*,  
18 173, 141-143, 1971.
- 19 Liu, S.C., M. Trainer, F.C. Fehsenfeld, D.D. Parrish, E.J. Williams, D.W. Fahey, G. Hübler, and  
20 P.C. Murphy, Ozone production in the rural troposphere and the implications for regional and  
21 global ozone distributions, *Journal of Geophysical Research*, 92, 4191-4207, 1987.
- 22 Luria, M., R.L. Tanner, R.E. Imhoff, R.J. Valente, E.M. Bailey, and S.F. Mueller, Influence of  
23 natural hydrocarbons on ozone formation in an isolated power plant plume, *Journal of*  
24 *Geophysical Research*, 105, 9177-9188, 2000.
- 25 Luria, M., R.J. Valente, R.L. Tanner, N.V. Gillani, R.E. Imhoff, S.F. Mueller, K.J. Olszyna, and J.F.  
26 Meagher, The evolution of photochemical smog in a power plant plume, *Atmospheric*  
27 *Environment*, 33, 3023-3026, 1999.

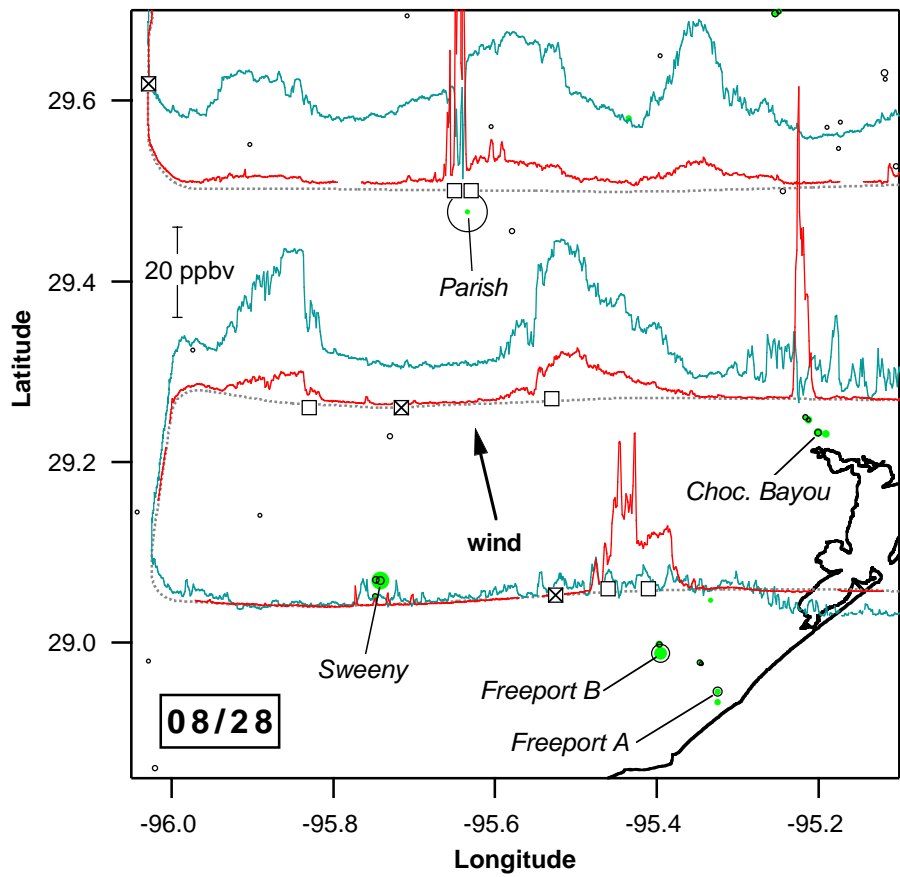
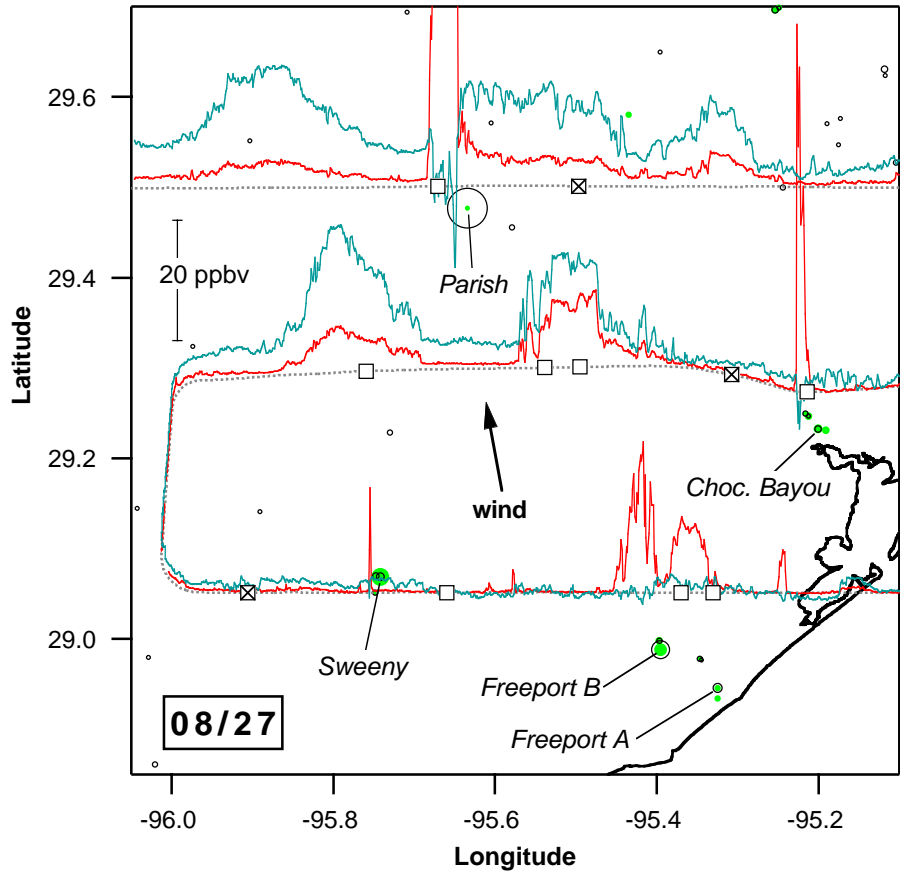
- 1 Miller, D.F., A.J. Alkezweeny, J.M. Hales, and R.N. Lee, Ozone formation related to power plant  
2 emissions, *Science*, 202, 1186-1188, 1978.
- 3 Neuman, J.A., L.G. Huey, R.W. Dissly, F.C. Fehsenfeld, F. Flocke, J.C. Holocek, J.S. Holloway,  
4 G. Hübler, R.O. Jakoubek, D.K.J. Nicks, D.D. Parrish, T.B. Ryerson, D.T. Sueper, and A.J.  
5 Weinheimer, Fast-response airborne in situ measurements of HNO<sub>3</sub> during the Texas 2000 Air  
6 Quality Study, *Journal of Geophysical Research (in press)*, 2002.
- 7 Nicks, D.K.J., J.S. Holloway, T.B. Ryerson, R.W. Dissly, D.D. Parrish, G.J. Frost, M. Trainer,  
8 S.G. Donnelly, S. Schauffler, E.L. Atlas, G. Hübler, D.T. Sueper, and F.C. Fehsenfeld, Fossil-  
9 fueled power plants as a source of atmospheric carbon monoxide, *Journal of Environmental*  
10 *Monitoring (in press)*, 2002.
- 11 Nunnermacker, L.J., L.I. Kleinman, D. Imre, P.H. Daum, Y.-N. Lee, J.H. Lee, S.R. Springston, L.  
12 Newman, and N. Gillani, NO<sub>y</sub> lifetimes and O<sub>3</sub> production efficiencies in urban and power plant  
13 plumes: analysis of field data, *Journal of Geophysical Research*, 105, 9165-9176, 2000.
- 14 Parrish, D.D., M. Trainer, M.P. Buhr, R. Watkins, and F.C. Fehsenfeld, Carbon monoxide  
15 concentrations and their relation to concentrations of total reactive oxidized nitrogen at two rural  
16 U.S. sites, *Journal of Geophysical Research*, 96, 9309-9320, 1991.
- 17 Parrish, D.D., M. Trainer, D. Hereid, E.J. Williams, K.J. Olszyna, R.A. Harley, J.F. Meagher, and  
18 F.C. Fehsenfeld, Decadal change in carbon monoxide to nitrogen oxide ratio in U.S. vehicular  
19 emissions, *Journal of Geophysical Research (in press)*, 2002.
- 20 Placet, M., C.O. Mann, R.O. Gilbert, and M.J. Niefer, Emissions of ozone precursors from  
21 stationary sources: a critical review, *Atmospheric Environment*, 34, 2183-2204, 2000.
- 22 Ridley, B.A., E.L. Atlas, J.G. Walega, G.L. Kok, T.A. Staffelbach, J.P. Greenberg, F.E. Grahek,  
23 P.G. Hess, and D.D. Montzka, Aircraft measurements made during the spring maximum of  
24 ozone over Hawaii: peroxides, CO, O<sub>3</sub>, NO<sub>y</sub>, condensation nuclei, selected hydrocarbons,  
25 halocarbons, and alkyl nitrates between 0.5 and 9 km altitude, *Journal of Geophysical Research*,  
26 102, 18,935-18,961, 1997.

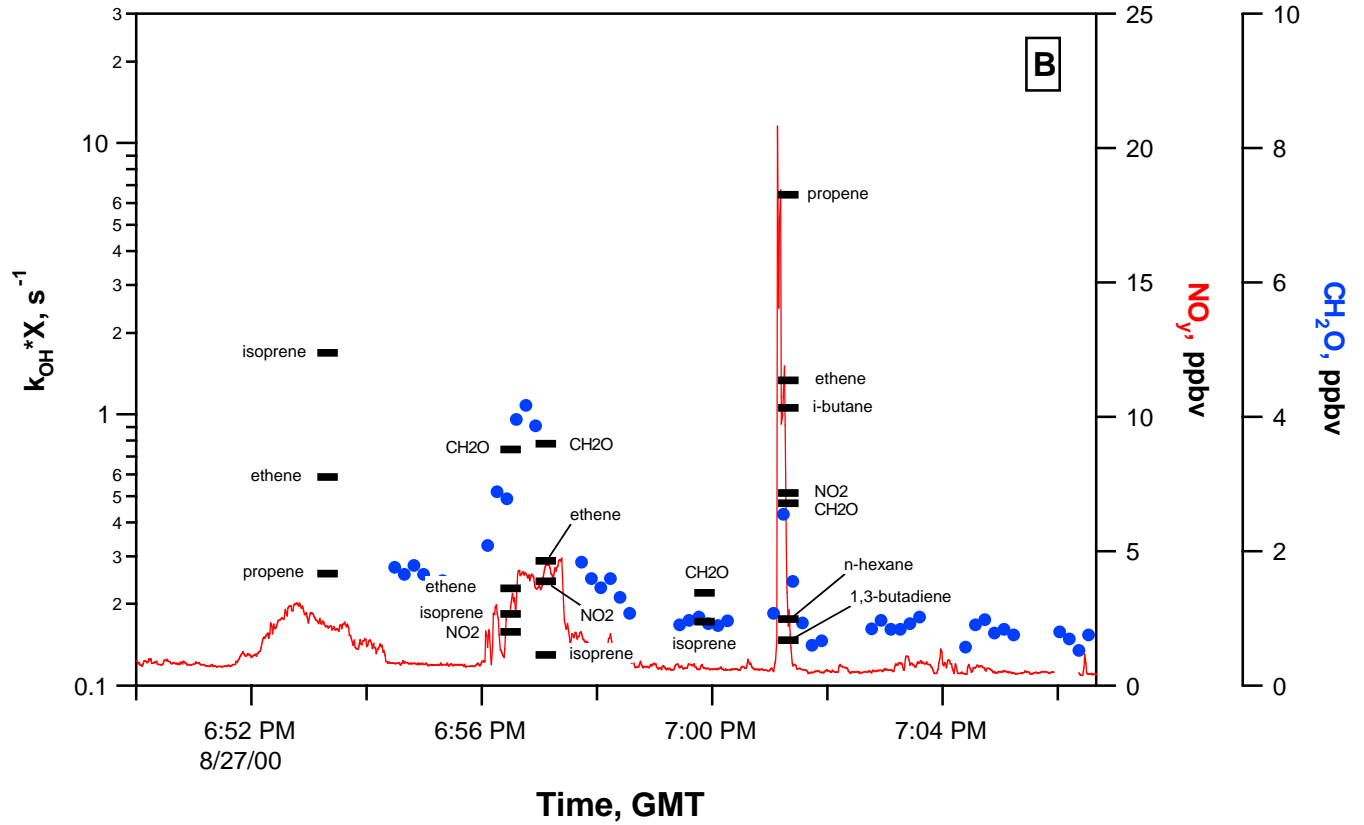
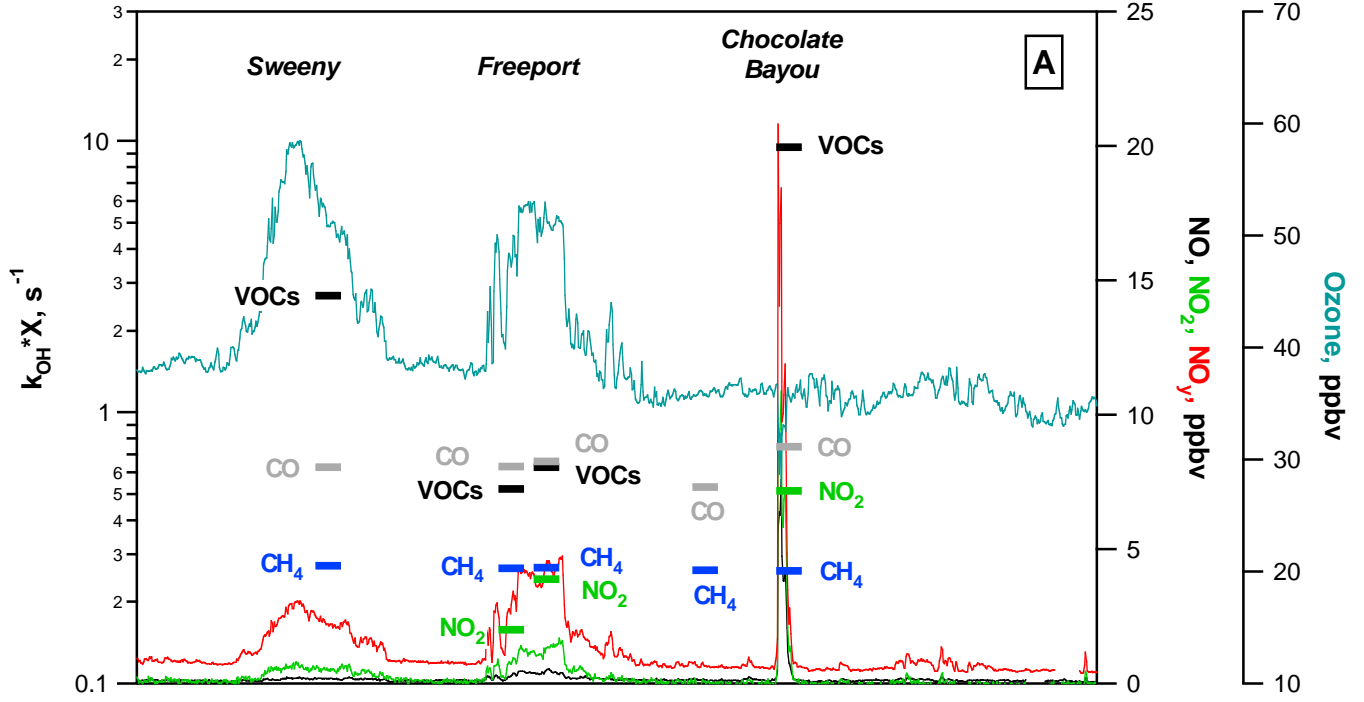
- 1 Ryerson, T.B., M.P. Buhr, G. Frost, P.D. Goldan, J.S. Holloway, G. Hübler, B.T. Jobson, W.C.  
2 Kuster, S.A. McKeen, D.D. Parrish, J.M. Roberts, D.T. Sueper, M. Trainer, J. Williams, and  
3 F.C. Fehsenfeld, Emissions lifetimes and ozone formation in power plant plumes, *Journal of*  
4 *Geophysical Research*, 103, 22,569-22,583, 1998.
- 5 Ryerson, T.B., L.G. Huey, K. Knapp, J.A. Neuman, D.D. Parrish, D.T. Sueper, and F.C.  
6 Fehsenfeld, Design and initial characterization of an inlet for gas-phase NO<sub>y</sub> measurements  
7 from aircraft, *Journal of Geophysical Research*, 104, 5483-5492, 1999.
- 8 Ryerson, T.B., M. Trainer, J.S. Holloway, D.D. Parrish, L.G. Huey, D.T. Sueper, G.J. Frost, S.G.  
9 Donnelly, S. Schauffler, E.L. Atlas, W.C. Kuster, P.D. Goldan, G. Hübler, J.M. Meagher, and  
10 F.C. Fehsenfeld, Observations of ozone formation in power plant plumes and implications for  
11 ozone control strategies, *Science*, 292, 719-723, 2001.
- 12 Ryerson, T.B., E.J. Williams, and F.C. Fehsenfeld, An efficient photolysis system for fast-response  
13 NO<sub>2</sub> measurements, *Journal of Geophysical Research*, 105, 26447-26461, 2000.
- 14 Schauffler, S., E.L. Atlas, D.R. Blake, F. Flocke, R.A. Lueb, J.M. Lee-Taylor, V. Stroud, and W.  
15 Trivicek, Distributions of brominated organic compounds in the troposphere and lower  
16 stratosphere, *Journal of Geophysical Research*, 104, 21,513-21,535, 1999.
- 17 Senff, C.J., R.M. Hardesty, R.J.I. Alvarez, and S.D. Mayor, Airborne lidar characterization of  
18 power plant plumes during the 1995 Southern Oxidants Study, *Journal of Geophysical*  
19 *Research*, 103, 31,173-31,189, 1998.
- 20 Sexton, K., and H. Westberg, Ambient air measurements of petroleum refinery emissions, *Journal*  
21 *of the Air Pollution Control Association*, 29, 1149-1152, 1979.
- 22 Sexton, K., and H. Westberg, Photochemical ozone formation from petroleum refinery emissions,  
23 *Atmospheric Environment*, 17, 467-475, 1983.
- 24 Sillman, S., Ozone production efficiency and loss of NO<sub>x</sub> in power plant plumes: Photochemical  
25 model and interpretation of measurements in Tennessee, *Journal of Geophysical Research*, 105,  
26 9189-9202, 2000.

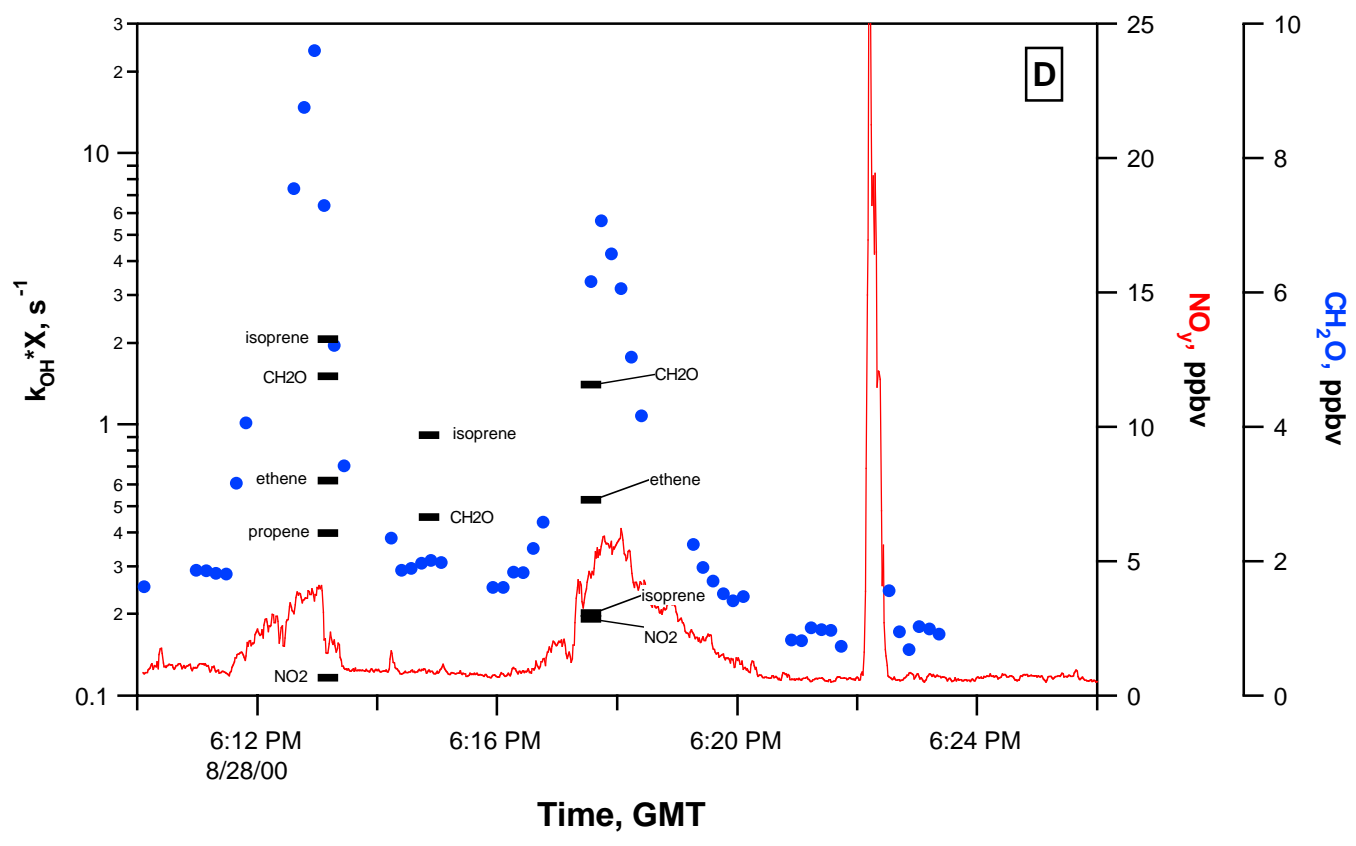
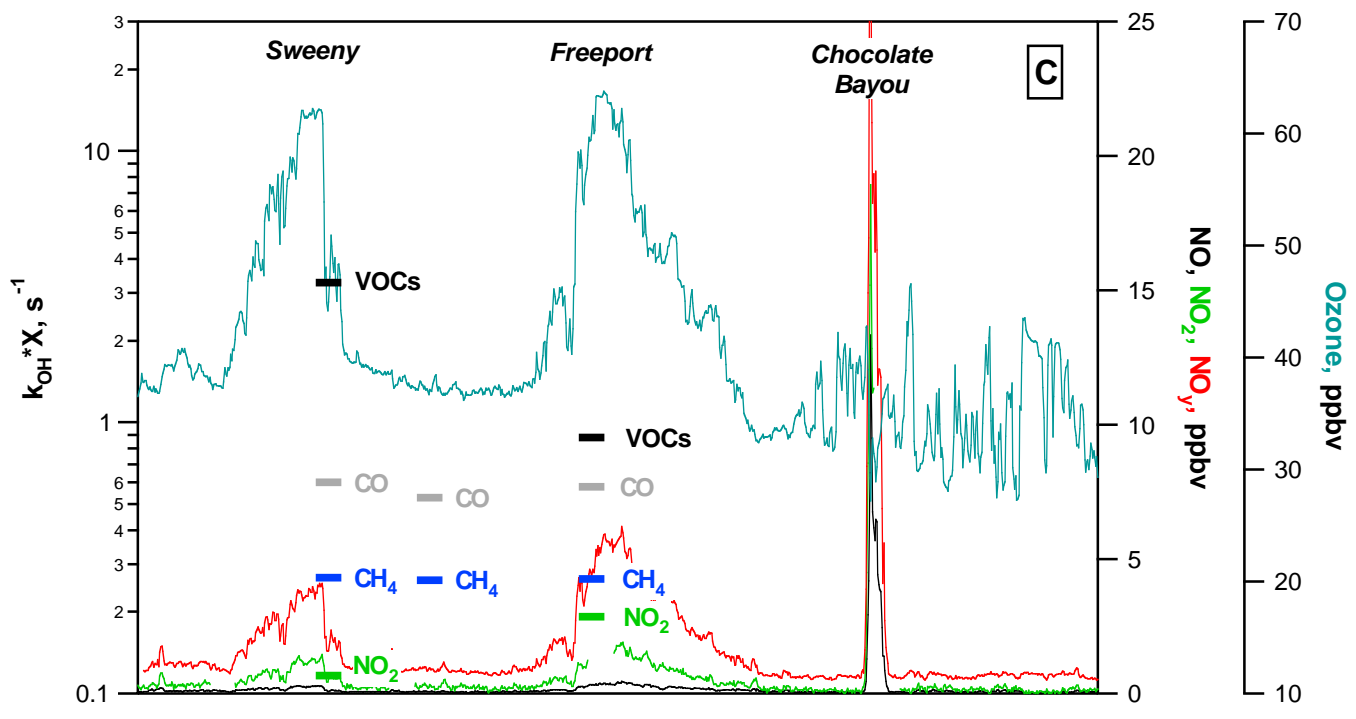
- 1 Stutz, J., and U. Platt, Improving long-path differential optical absorption spectroscopy with a  
2 quartz-fiber mode mixer, *Applied Optics*, 36, 1105-1115, 1997.
- 3 Trainer, M., E.-Y. Hsie, S.A. McKeen, R. Tallamraju, D.D. Parrish, F.C. Fehsenfeld, and S.C. Liu,  
4 Impact of natural hydrocarbons on hydroxyl and peroxy radicals at a remote site, *Journal of*  
5 *Geophysical Research*, 92, 11,879-11,894, 1987a.
- 6 Trainer, M., D.D. Parrish, M.P. Buhr, R.B. Norton, F.C. Fehsenfeld, K.G. Anlauf, J.W.  
7 Bottenheim, Y.Z. Tang, H.A. Weibe, J.M. Roberts, R.L. Tanner, L. Newman, V.C. Bowersox,  
8 J.F. Meagher, K.J. Olszyna, M.O. Rodgers, T. Wang, H. Berresheim, K.L. Demerjian, and  
9 U.K. Roychowdhury, Correlation of ozone with NO<sub>y</sub> in photochemically aged air, *Journal of*  
10 *Geophysical Research*, 98, 2917-2925, 1993.
- 11 Trainer, M., B.A. Ridley, M.P. Buhr, G. Kok, J. Walega, G. Hübler, D.D. Parrish, and F.C.  
12 Fehsenfeld, Regional ozone and urban plumes in the southeastern United States: Birmingham, a  
13 case study, *Journal of Geophysical Research*, 100, 18,823-18,834, 1995.
- 14 Trainer, M., E.J. Williams, D.D. Parrish, M.P. Buhr, E.J. Allwine, H.H. Westberg, F.C. Fehsenfeld,  
15 and S.C. Liu, Models and observations of the impact of natural hydrocarbons on rural ozone,  
16 *Nature*, 329, 705-707, 1987b.
- 17 Watson, J.G., J.C. Chow, and E.M. Fujita, Review of volatile organic compound source  
18 apportionment by chemical mass balance, *Atmospheric Environment*, 35, 1567-1584, 2001.
- 19 Wert, B.P., M. Trainer, A. Fried, T.B. Ryerson, B. Henry, W. Potter, S.G. Donnelly, S. Schauffler,  
20 E.L. Atlas, D.K.J. Nicks, P.D. Goldan, W.C. Kuster, D.D. Parrish, J.S. Holloway, J.A.  
21 Neuman, W.M. Angevine, J. Stutz, A. Hansel, A. Wisthaler, C. Weidinmyer, G.J. Frost, G.  
22 Hübler, D.T. Sueper, and F.C. Fehsenfeld, Signatures of alkene oxidation in airborne  
23 formaldehyde measurements during TexAQS 2000, *Journal of Geophysical Research*  
24 *(submitted)*, 2002.
- 25 White, W.H., J.A. Anderson, D.L. Blumenthal, R.B. Husar, N.V. Gillani, J.D. Husar, and W.E.J.  
26 Wilson, Formation and transport of secondary air pollutants: ozone and aerosols in the St.  
27 Louis urban plume, *Science*, 194, 187-189, 1976.

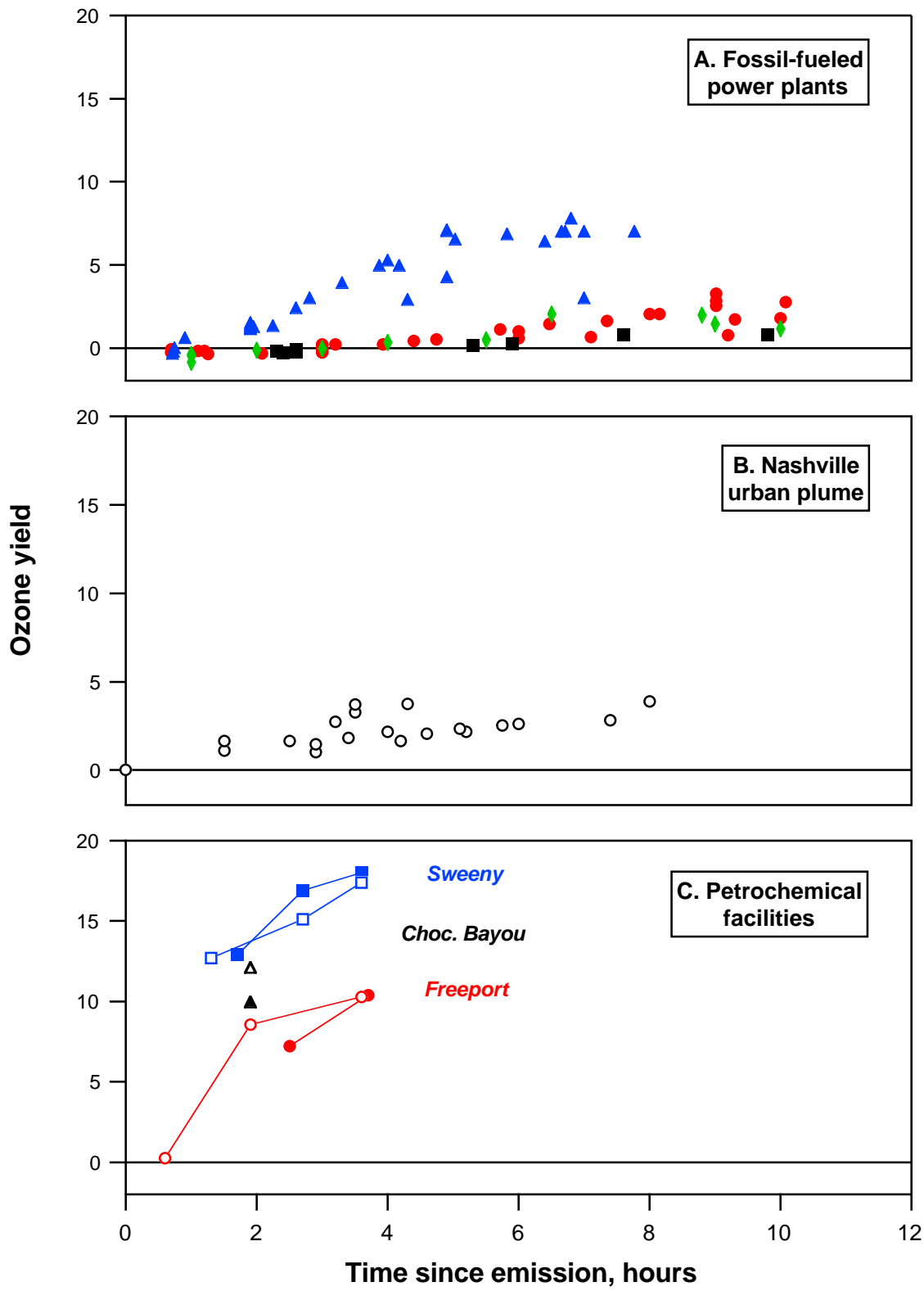
- 1 Wiedinmyer, C., A. Guenther, M. Estes, I.W. Strange, G. Yarwood, and D.T. Allen, A land-use  
2 database and examples of biogenic isoprene emission estimates for the state of Texas, USA,  
3 *Atmospheric Environment*, 35, 6465-6477, 2001.
- 4 Winner, D.A., and G.R. Cass, Modeling the long-term frequency distribution of regional ozone  
5 concentrations, *Atmospheric Environment*, 33, 431-461, 1999.
- 6

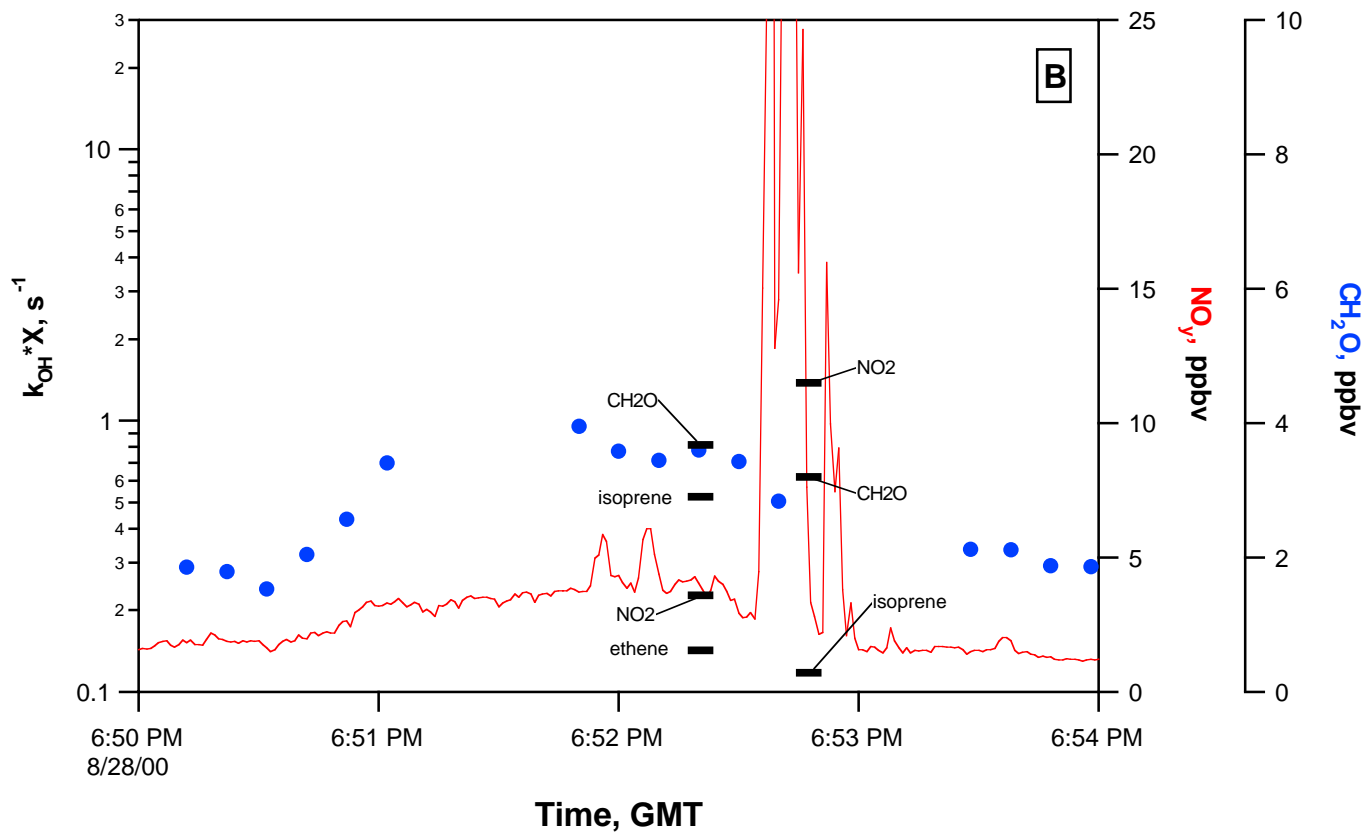
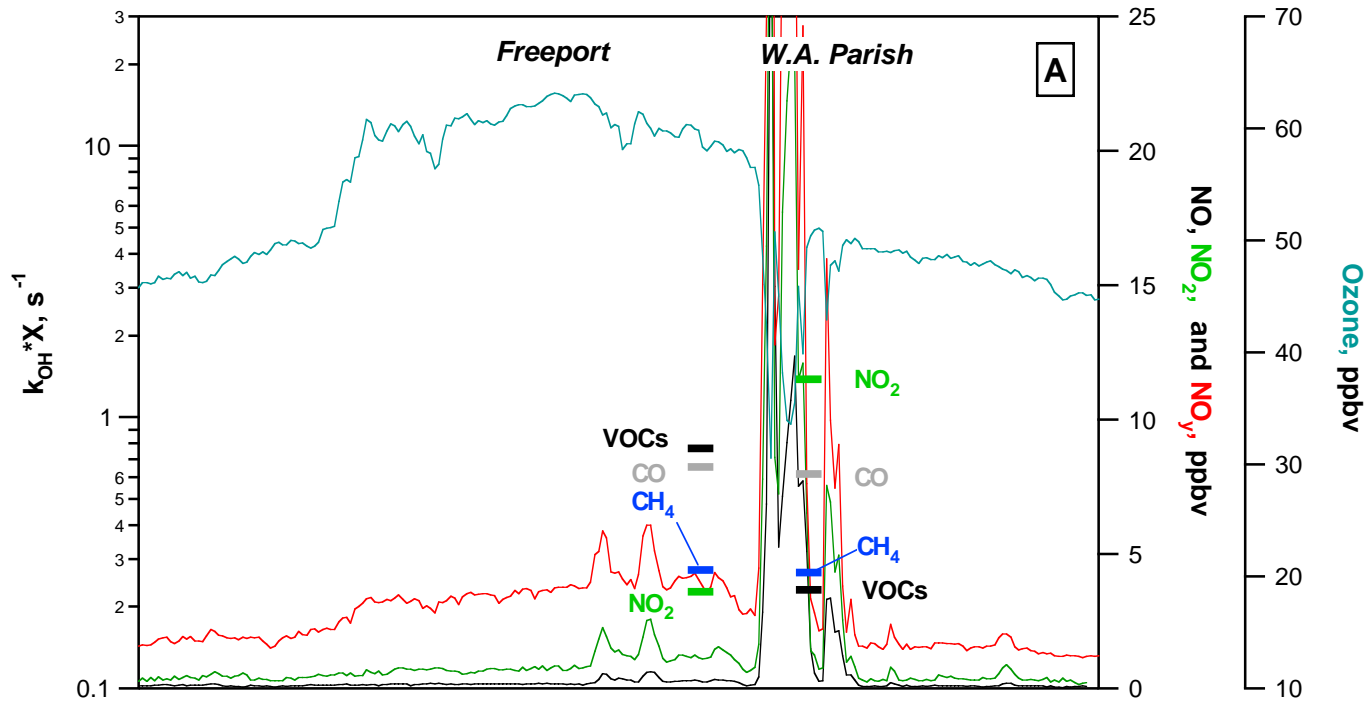


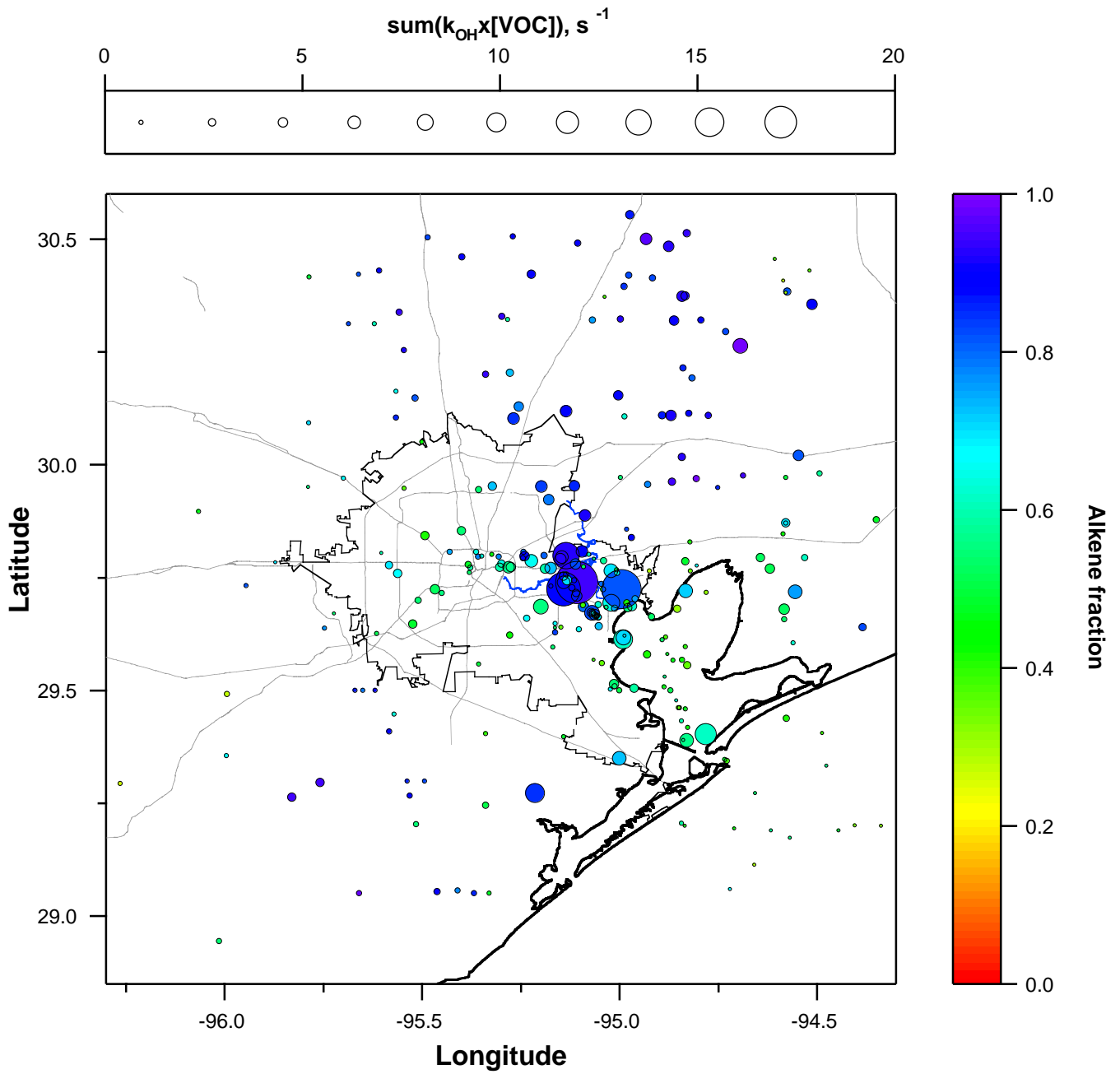


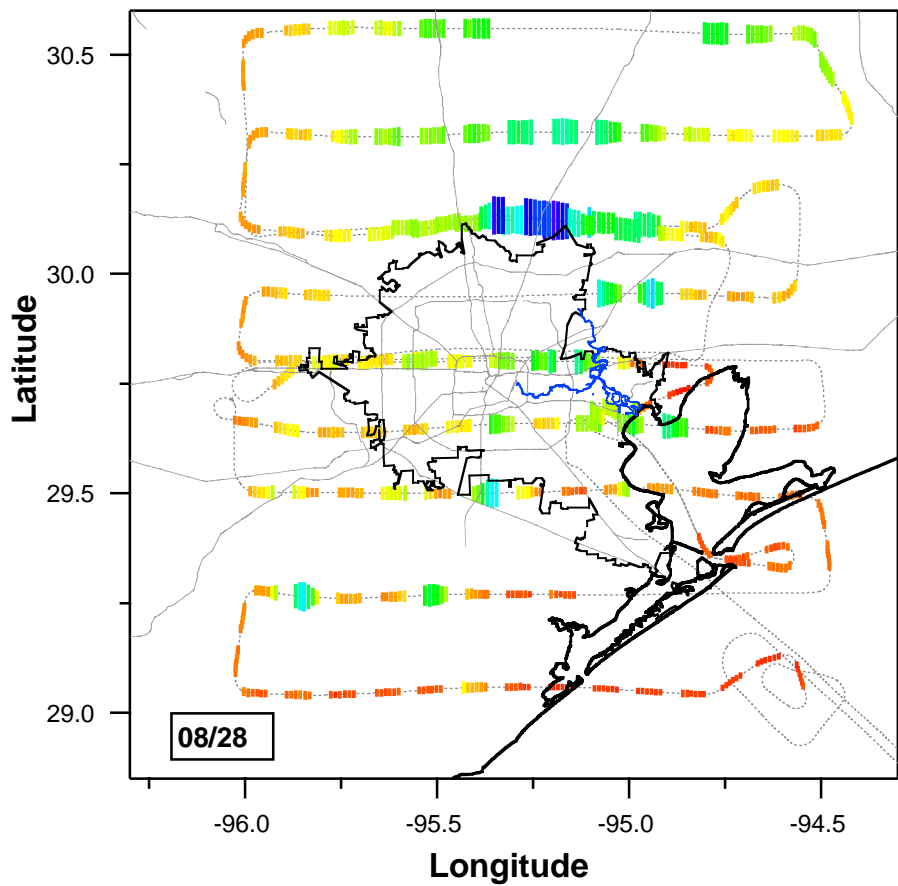
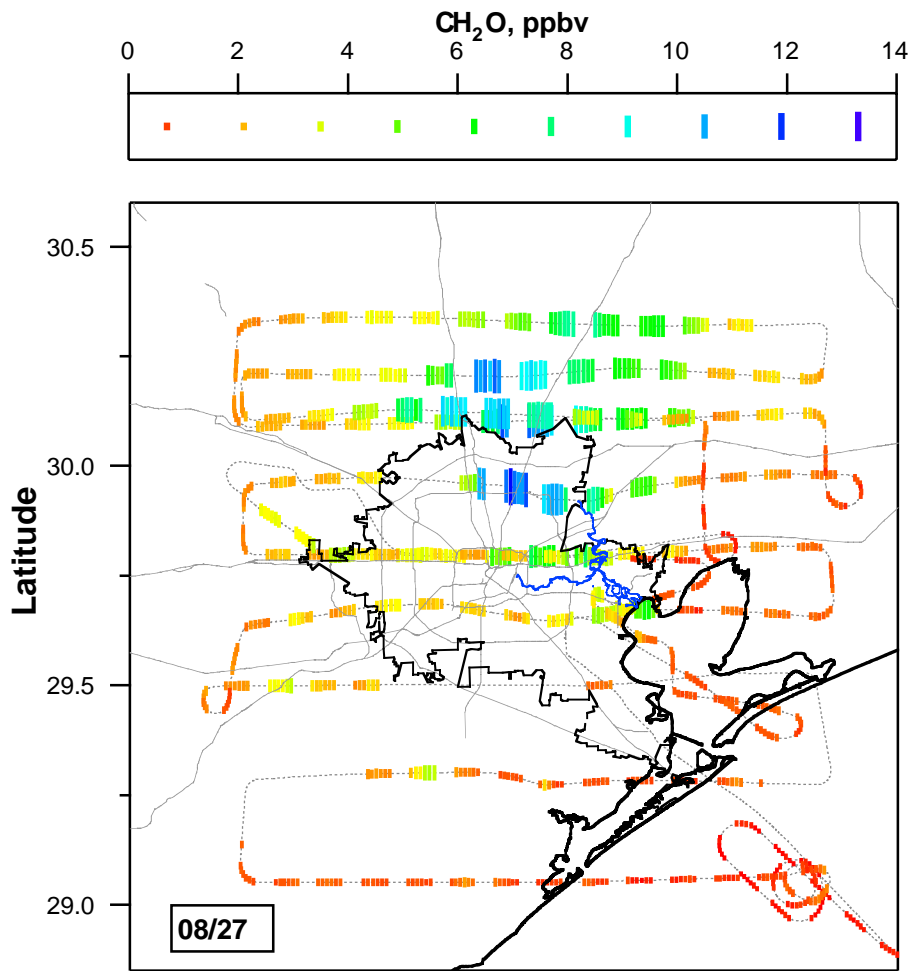


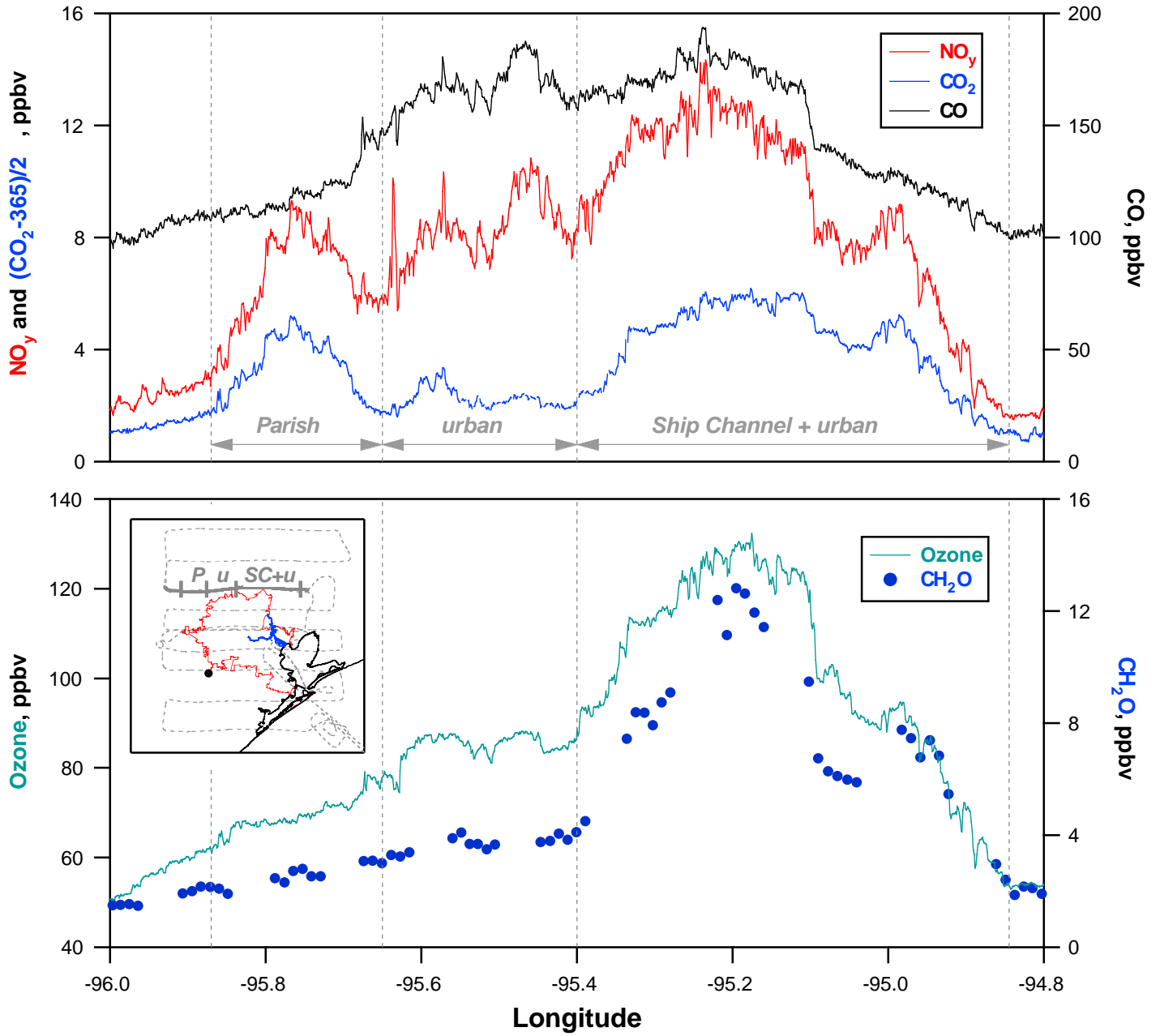


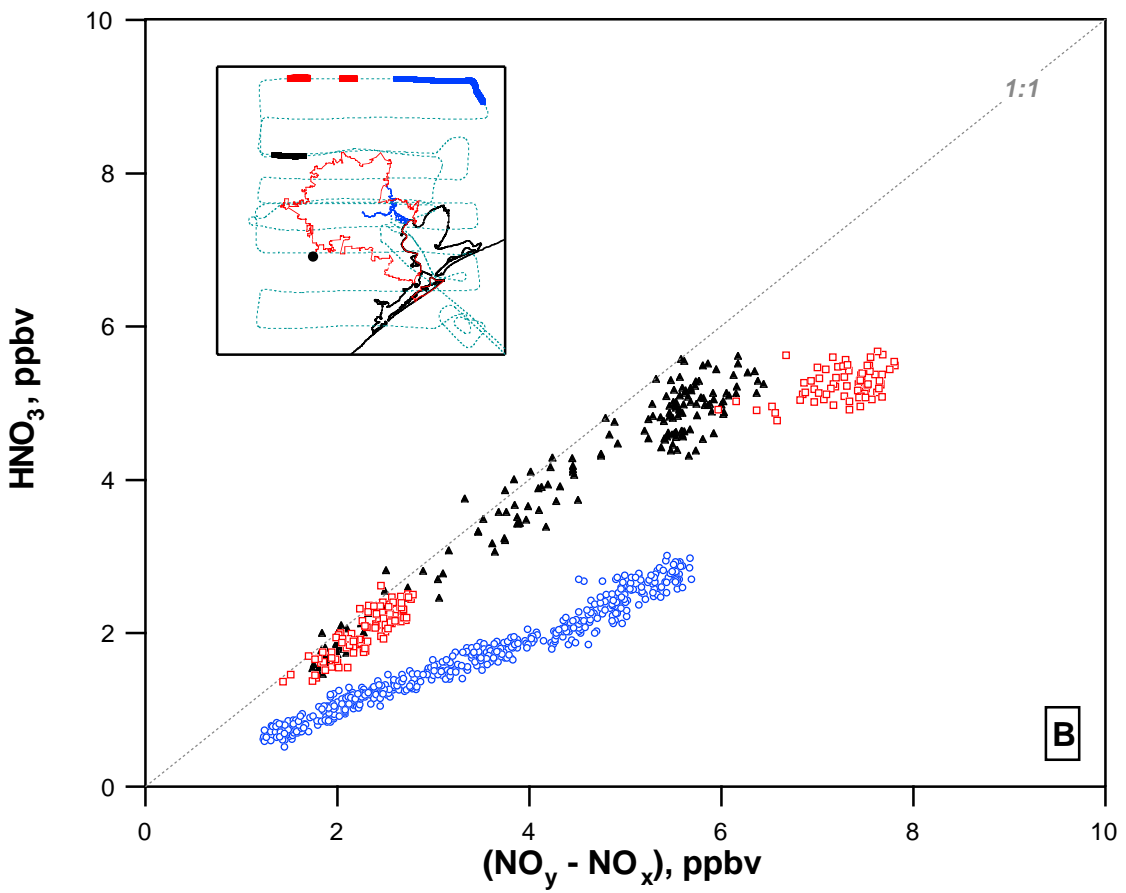
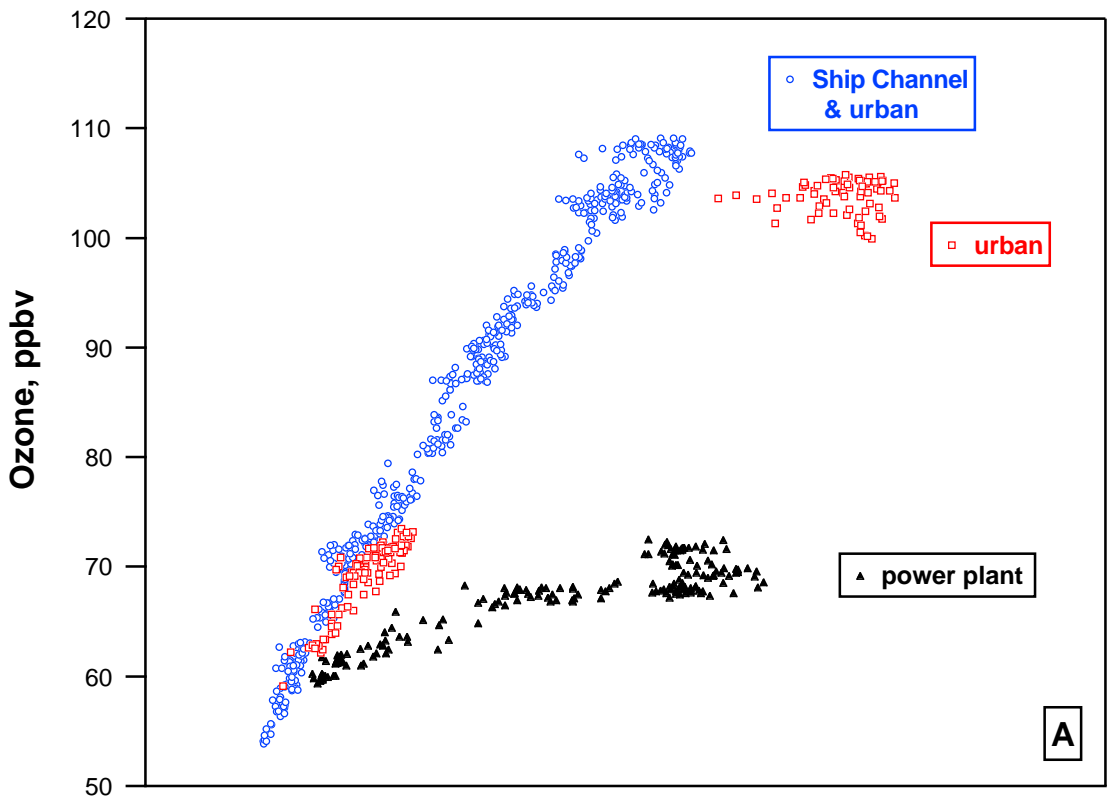












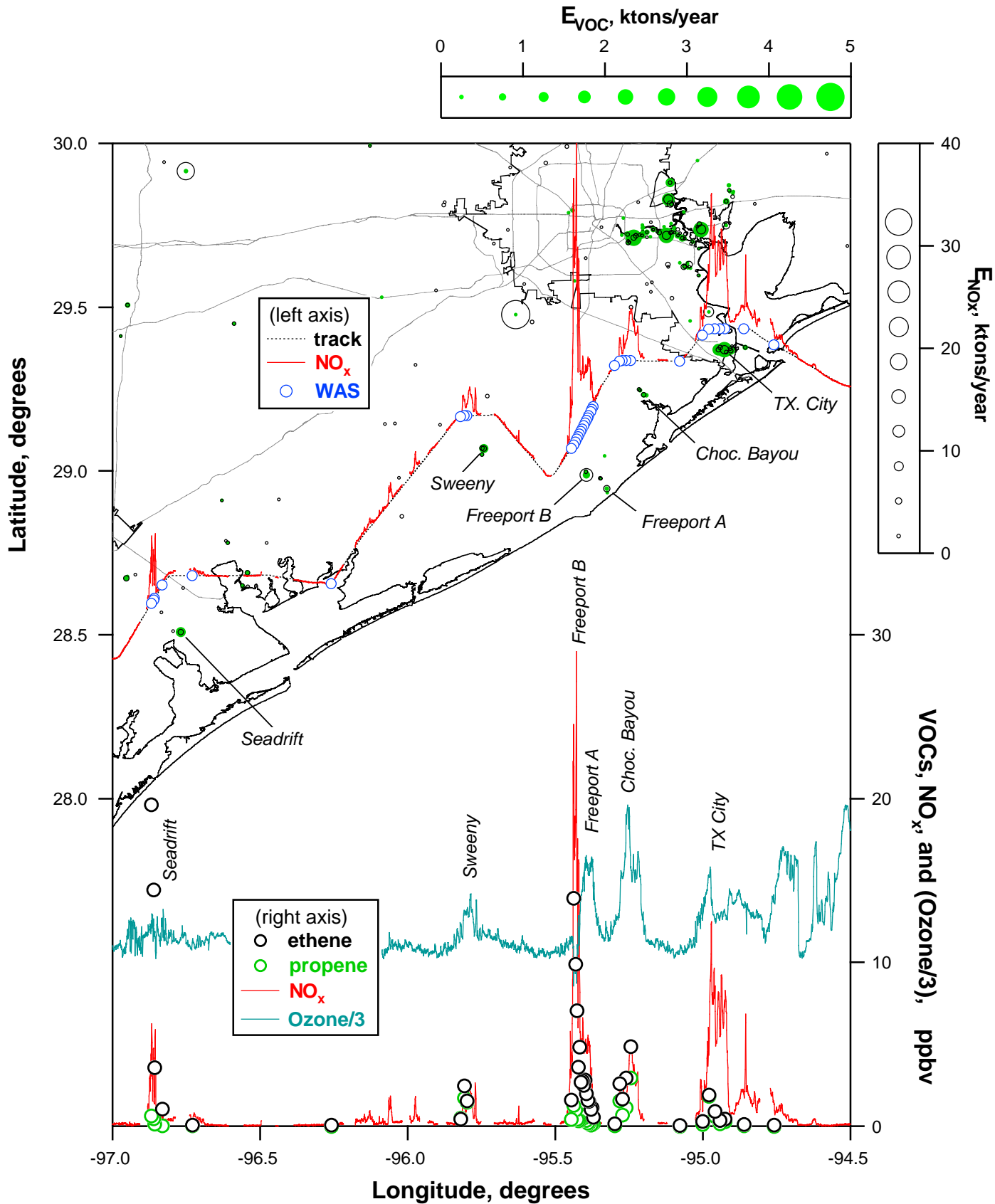


Figure 1

